ROLES OF MICROTUBULES AND MICROTUBULE REGULATORS IN COLLECTIVE INVASIVE MIGRATION OF *DROSOPHILA* BORDER CELLS

NACHEN YANG

B.Sc. (Hons.), Nanyang Technological University

A THESIS SUBMITTED FOR THE DEGREE OF DOCTOR OF PHILOSOPHY

INSTITUTE OF MOLECULAR AND CELL BIOLOGY

DEPARTMENT OF BIOLOGICAL SCIENCES

NATIONAL UNIVERSITY OF SINGAPORE

2012

DECLARATION

I hereby declare that this thesis is my original work and it has been written by me in its entirety.
I have duly acknowledged all the sources of information which have been used in the thesis.

This thesis has also not been submitted for any degree in any university previously.

_____

Nachen Yang

August 2012

Acknowledgements

I am indebted to my supervisor Prof. Pernille Rorth, without whom this work cannot be done at all. I started my Ph.D rotation in Pernille's lab in EMBL in Spring 2007 and was immediately fascinated by cell migration. I was extremely lucky to become her Ph.D student later on, despite my limited knowledge and productivity at that time. Her broad knowledge of biology, critical thinking and analysis, persistence in attacking challenging questions, inspire me all the way through my Ph.D studies. She sets a role model of a true scientist.

I am fortunate to have Dr. Adam Cliffe as my mentor in the lab. Adam taught me everything from the beginning, from fly genetics to confocal microscopy imaging and analysis. He never hesitates to discuss ideas and share information, give people advice whenever he is approached. His generosity in science as well as in many other things, is an invaluable virtue for nowadays scientists.

I would like to express my sincere thanks to my thesis advisory committee members Prof. Steve Cohen, Prof. Xiaohang Yang and Assoc. Prof. Snezhka Oliferenko for their useful advice and suggestions on the project throughout my thesis.

I would like to thank Dr. Adam Cliffe and Dr. Minna Poukkula for teaching me how to dissect ovaries and image border cells; I made my

first border cell migration movie with them. Also, thanks to Dr Mikiko Inaki for the collaboration in the Lis-1 project, without her, the characterization of border cell initiation could not have been possible. Thanks to Dr. Zhang Rui for his generous help in writing a Perl script to aid the EB1-GFP tracking and providing useful suggestions on statistics tests used in the study; Issac Yang for the help in the intial RNAi screen; Dr. Graham Wright, Mar KarJunn, Dr. Xiao Yong, Dr. Axel K Preuss and Dr. WeiMiao Yu for their assistance and useful advice in imaging and data analysis; Eva Looser, Dr. Zhang Wei, SingFee Lim and Xin Hong for teaching and help me in the S2 cell tissue culture assay and protein work.

I would also like to thank my dearest lab members from past to present for the friendship and support throughout the studies: Adam Cliffe, Minna Poukkula, Smitha Vishnu, Hsinho Sung, Oguz Kanca, Ambra Bianco, Georgina Fletcher, Isaac Yang, Rishita Changede, Mikiko Inaki, Ruifeng Lu, Isaac Lim, David Doupe, Maxine Lam and Lara Salvany Martin. Despite of the limited microscopy time and resources, they are always very considerate and help each other to create a smooth and friendly working environment in the lab. Thanks to Pernille Rorth, Adam Cliffe, Isaac Lim, Hsinho Sung and Xin Hong for reading my thesis and giving critical comments.

Finally, I would like to thank my parents and close family members. They constantly support me, care for my studies as they were me, and

encourage me all the way through my life. Without them, I could not have gone this far.

Table of Contents

Summary

Unlike actin, which is required for almost all eukaryotic cell migrations, the roles of another cytoskeleton component, the microtubule, are less clear. Much of our understanding of how cells migrate has largely come from studies in tissue culture assays, raising the concern that it may not always be applied in vivo. Border cells are a group of somatic follicle cells that perform a stereotypic migration between the nurse cells of the *Drosphila* ovary during oogenesis. During this migration the nurse cells act as the substrate over which the border cells migrate. This reproducible migration serves as a convenient model to study collective migration in vivo. Through imaging of both stable and dynamic microtubules, we found differential microtubule organization and dynamics within the cluster: microtubules are highly organized in the polar cells and form a microtubule organization center (MTOC)-like structure that is polarized towards the leading edge prior to migration. The outer border cells, in contrast, have some cortical microtubules, but are less organized. Tracking of the plus end marker EB1-GFP showed microtubules grow preferentially towards the center of the cluster.

We started investigations of general effects of microtubules in the border cell migration system by drugs. Net cluster movement was affected by both nocodazole and taxol which disrupt microtubules and

microtubule dynamics. The specific microtubule depolymerization factor Stathmin had a subtle role in migration, and was found to be largely required in the substrate nurse cells. To find additional regulators, we conducted a RNAi screen against genes encoding known or potential microtubule regulators in the fly genome. Among about 70 genes screened, the *dynein* interactors *Lissencephaly-1* (*Lis-1*) and *nudE*, together with *dynein* were found to be required both in the polar cells (in agreement with previous published results) and outer border cells. These genes have important roles in regulating the forward extensions that may generate traction force for cluster movement. In addition, compromising their activities severely disrupted the organization of the border cell cluster, as visualized by the abnormal distribution of adhesion molecules. In summary, we found microtubules do play roles in both migratory border cells as well as their interacting cells. Specifically, the Lis-1-NudE-Dynein complex was required, possibly through regulating front extensions and the reorganization of the follicular epithelium to ensure a properly organized migratory cluster.

List of Tables

List of Figures

List of Abbreviations

ADA	Adenosine Deaainase
AFG	Actin-Gal4 driver with a flipout cassette
APC	Anaphase promoting complex
C/EBP	CCAAT/enhancer-binding protein
CAMs	cell adhesion molecules
Chb	Chromosome bows
CLIP	Cytoplasmic Linker Proteins
CytoD	Cytochalasin D
DAPI	4',6-diamidino-2-phenylindole
Dhc	Dynein heavy chain
DMSO	Dimethyl sulfoxide
EB1	End binding protein 1
ECM	Extracellular matrix
EcR	Ecdysone Receptor
EGFR	Epidermal Growth Factor Receptor
ELMO	Engulfment and cell motility
EMT	Epithelium to Mesenchymal Transition
FAK	Focal Adhesion Kinase
FasII	Fasciclin II
FasIII	Fasciclin III
FCS	Fetal Calf Serum
GFP	Green fluorescence protein

JAK	Janus kinase
Lis-1	Lissencephaly-1
MAP	Microtubule associated protein
Mbc	Myoblast city
MTOC	Microtubule organization center
NCAM	neural cell adhesion molecule
neur	neuralized
PGC	Primordial Germ Cell
PVR	PDGF/VEGF Receptor
RFP	Red fluorescence protein
RGD	Arg-Gly-Asp
RTK	Receptor Tyrosine Kinases
Shg	Shotgun
Slbo	Slow border cell
STAT	Signal Transducer and Activator of Transcription
Tai	Taimen
Upd	Unpaired

1. Introduction

1.1 Cell Migration

1.1.1 Importance of cell migration

Cell migration was first witnessed by the Dutch microscopist and microbiologist Antonie van Leeuwenhoek in 1675 when he observed the movements of bacteria under his microscope (Porter 1976). Since then, cell migration has been found to be involved in a wide variety of biological processes. For example, in developmental morphogenesis, cell migration is important for gastrulation, when extensive cell movements take place to form the proper three-layered embryo. In the inflammatory response, leukocytes migrate to the sites of infection to mount proper immunity; and migration of fibroblasts and vascular endothelial cells is essential for wound healing. Cell migration is therefore a fundamental process for the normal physiology of living animals and requires strict regulation. Mis-regulation of cell migration can result in severe consequences and contribute to a variety of pathological conditions such as cancer metastasis and autoimmune diseases. Therefore, studying the molecular mechanism of cell migration and its regulation is important for both human physiology and pathology.

1.1.2 Different types of cell migration

Eukaryotic cells often display solitary migration, such as the migrating neutrophils that are well adapted to quickly respond and move to an infection site upon stimulation. Many other cells, however, migrate together, either in loosely or closely associated groups. Collective cell migrations usually occur in developmental contexts with spatial and temporal regulation. A few classical examples of collective cell migration include the branching and sprouting movement of endothelial cells to form vasculature in vertebrates and trachea in the fruit fly *Drosophila* (Adams and Alitalo 2007; Affolter and Caussinus 2008); the slug type of movement of the *zebrafish* lateral line primordium cells; the moving sheets of cells in *Drosophila* dorsal closure (similar to wound healing) as well as *Drosophila* border cells that migrate as a free group.

Finally, cell migration can be random or directed. Directional migration is achieved by detection and interpretation of guidance cues provided by the target.

1.1.3 Basic processes of cell migration

Eukaryotic cell migration has been studied extensively in simplied cultured models in the past decades and constitutes much of our knowledge in understanding the basic cellular and molecular machinery for cell motility. The general description of cell migration is taken from observations of a single migrating cell moving on a cover

slip. For example, the process of a migrating fibroblast in cultured dish can be conceptually described as a cyclic process that includes 1) initial polarization, 2) protrusion formation and establishment of adhesions, 3) translocation of the cell body and 4) retraction of the rear (Lauffenburger and Horwitz 1996; Sheetz et al. 1999). These steps are integrated by extensive signaling network regulations to ensure a coordinated process. For example, protrusions and retractions need to be coordinated with the formation and disassembly of adhesions between the migrating cells and the substrate as the migrating cell moves forward while remaining attached to the substrate (Lauffenburger and Horwitz 1996; Ridley et al. 2003).

1.1.3.1 Polarization

A migrating cell usually has a distinct front and back, oriented in the direction of migration. Polarization refers to the process of generating this cell asymmetry. Cell polarity can arise from asymmetric subcellular distribution of intrinsic factors such as proteins, mRNAs, and/or organelles, ultimately leading to cell type-specific morphological polarity. Cell polarity can also be externally imposed by signals from the environment, for example the presence of directional cues such as chemoattractants and morphogens.

1.1.3.2 Protrusion formation

A polarized migrating cell has a distinct leading edge with extended membrane structures named protrusions. The protrusions are usually driven by actin polymerization, which provides the driving force for cell motility. In fibroblast type cells, there are two types of protrusions: lamellipodia and filopodia, depending on the shape and the structure of the underlying actin network. Lamellipodia have large, flat and fan-like structures enriched in branched actin structures. They provide wide surfaces for generation of traction for forward movement (Small et al. 2002). Filopodia are spike-like protrusions comprised of long parallel actin bundles. They are thought to be the mechanosensory and chemosensing device for helping the migrating cells to explore the local environment (Mattila and Lappalainen 2008). Other cell types use somewhat different protrusions such as “blebs” of locally extruded cytoplasm and membrane; the blebs are also actin-based, however they are regulated differently (Insall and Machesky 2009).

1.1.3.3 Establishment of adhesions

Cell migration requires dynamic interactions between the migrating cells and the substrate to which it is attached and over which it migrates. The substrate can be extracellular matrix (ECM) or adjacent cells. Establishment of adhesions stabilizes protrusions and provides traction as the cell advances. Adhesion assembly and disassembly are highly dynamic and coordinated during migration.

Adhering of migrating cells to the substratum occurs via cell adhesion molecules (CAMs), which are typical transmembrane receptors that have an extracellular domain that binds directly to ECM or to other CAMs present on neighboring cells. CAMs have an intracellular domain that links the substratum intercellularly to the actin cytoskeleton via various adaptors and regulatory proteins. Cell-ECM adhesion is usually mediated by integrins, which are heterodimeric receptors that bind to extracellular matrix components such as Arg-Gly-Asp (RGD) peptides (Ruoslahti 1996; Juliano 2002). For cell-cell adhesions, they are usually mediated by cadherins, which comprise a family of calcium-dependent cell adhesion molecules that mediate homophilic adhesions between cells (Juliano 2002).

1.1.3.4 Translocation of cell body

Adhesions serve as traction sites for cell translocation, which happens immediately after the formation of protrusions of cellular body. Translocation of cell is driven by a coordinated contraction of the actomyosin cytoskeleton, which depends on myosin II activity (Svitkina et al. 1997). Beside actomyosin contraction, the microtubule cytoskeleton is implicated in nuclear translocation (Gomes et al. 2005; Levy and Holzbaur 2008).

1.1.3.5 Retraction of the rear

In order for a migrating cell to advance, protrusion of the front and translocation of the cell body must be followed by retraction of the rear. The rear retraction requires the coordinated contraction of the actin cytoskeleton and disassembly of the adhesions at the trailing edge (Crowley and Horwitz 1995; Chrzanowska-Wodnicka and Burridge 1996).

These basic steps of cell migration may happen sequentially as described here or can be overlapping and concurrent, but each type of function is required for cell migration in general.

1.2 Microtubules in cell migration

While actin and the actin cytoskeleton have a central role in essentially all types of eukaryotic cell migration, the roles of the other major cytoskeleton components, namely the microtubules, are less clear and can be variable in cell types.

1.2.1 Basic properties of the microtubule cytoskeleton

1.2.1.1 Microtubule structure and polarity

Microtubules are stiff hollow cylindrical structures assembled from 13 linear protofilaments side by side; each is composed of head-to-tail arrays of parallel $\alpha\beta$ Tubulin heterodimers (Figure 1.1). Because of the aligned arrangement of α and β Tubulin, microtubules themselves are

intrinsicically polar with α Tubulin facing at one end and β Tubulin at the other (Nogales 2000). In this polar filament, the rate of polymerization and depolymerization is also different between the two ends: the fast end is called the plus end that is exposed to β Tubulin whilst the slow end is called the minus end that is exposed to α Tubulin (Desai and Mitchison 1997).

Microtubule motor proteins such as Kinesin and Dynein can transduce chemical energy from ATP hydrolysis into mechanical force used for movement of cargos on microtubules (Vale 2003). The conventional Kinesin (Kinesin I) moves predominantly to the plus end, whilst Dynein is a large protein complex that primarily moves to the minus end of microtubules.

Microtubule polarity is important for directed motor-driven transport of cargos along microtubules. These motors move cargos such as membrane bound vesicles, protein-RNA complex, or even organelles around in interphase cells, for example, up and down a very long axon of a differentiated neuron.

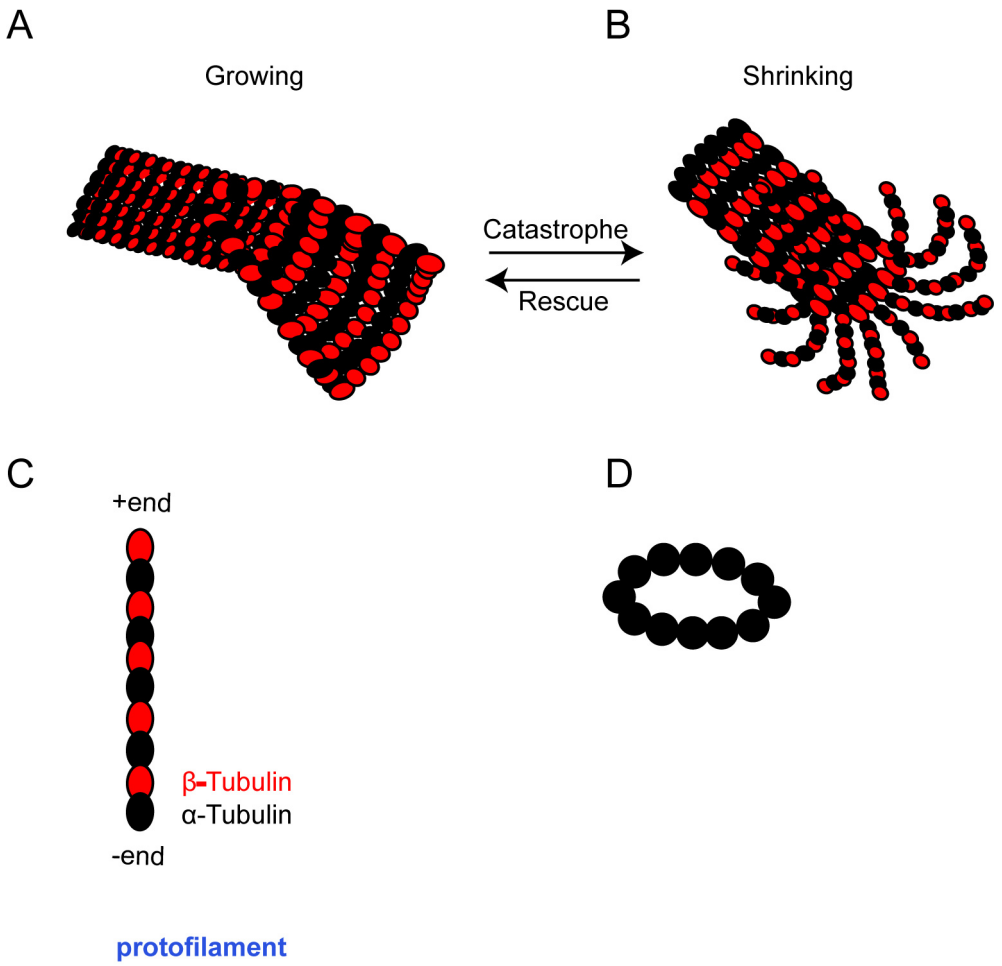

Figure 1. 1 Schematic representation of microtubule compositions

(A-B) Microtubules composed of head-to-tail arrangement of α (black) and β (red) Tubulin heterodimers. The plus end of microtubules is undergoing constant growing (A) and shrinkage (B). The growing microtubules are thought to form an open sheet of Tubulin polymer containing GTP β-Tubulin at the tips (A). During shrinking, microtubule plus ends have curved protofilaments (demonstrated in C) that peel away from the microtubule wall (B). The cross section at the minus end with 13 α Tubulin is shown in (D).

1.2.1.2 Microtubule dynamic instability and organization

Another important function of microtubules is to couple and move cellular structures around the cell, such as chromosomes during mitosis. This movement does not rely exclusively on motor proteins that move along microtubules, but the microtubules themselves can generate force to move those structures around. This is attributed to the dynamic instability of microtubules, a phenomenon of microtubules undergoing constant growth and shrinkage, mostly at the plus end (Figure 1.1, (Mitchison and Kirschner 1984). In most eukaryotic cells, microtubules are anchored at so called Microtubule Organization Center (MTOC) at their minus end. The main MTOC is built around pairs of centrioles within the centrosome. As the microtubules grow and shrink, the structures that are attached to the plus end of the microtubules get pushed or pulled around the cell, away or towards the centrosomes that remain attached. During mitosis, the two centrosomes emanate microtubules from spindle poles, and the microtubules capture chromosomes at the kinetochores and form the mitotic spindle, which provide the force for the separation of chromosomes in mitosis.

While many microtubule minus ends are focused at the centrosomes, a variety of differentiated cell types contain a substantial number of microtubules with free minus ends (Keating and Borisy 1999). The non-centrosomal microtubules perform specialized function in these cells.

For example, a polarized epithelial cells display a non-radial, apical to basal aligned microtubule array that plays a fundamental role in the establishment of apical-basal cell polarity.

1.2.1.3 Regulation of microtubules dynamics

Microtubule dynamics are modulated by various factors, and depending on the effect, these factors are classified as either microtubule stabilizing factors or microtubule destabilizing factors. Structural microtubule associated proteins (MAPs) such as the Tau protein, decorate the microtubule lattice and stabilize it (Mandelkow and Mandelkow 1995). Another class of MAPs is the plus-end tracking proteins (+TIPs), which can bind specifically to the plus end of growing microtubules and influence its dynamics, for example, the end binding protein 1 (EB1). Many +TIPs promote microtubule stabilizing by binding and connecting the plus end of microtubules to the cell cortex (Akhmanova and Steinmetz 2010).

Microtubule de-stabilizing factors can directly promote microtubule disassembly or inhibit its polymerization. The microtubule severing protein spastin or katanin can directly break microtubules. Stathmin, on the other hand, can bind and sequester $\alpha\beta$ Tubulin heterodimers to reduce free $\alpha\beta$ Tubulin subunits available for microtubule polymerization.

1.2.2 Microtubules and cell migration

Microtubules are important regulators of cell polarity and thus are important for the polarization of many migrating cells, such as neurons, fibroblasts and macrophages. In most cells microtubules are important for cell polarity and migration is altered when microtubules are disrupted (Vasiliev et al. 1970; Goldman 1971; Bershadsky et al. 1991). However, migration of fish keratocytes is not perturbed when microtubules are depolymerized (Euteneuer and Schliwa 1984) and neutrophil motility is even increased in the absence of microtubules (Keller et al. 1984). Unlike actin that provides the protrusive and contractive forces necessary for migration, microtubules appear to act to regulate and coordinate these actin-based activities (Vasiliev et al. 1970; Rinnerthaler et al. 1988; Danowski 1989; Bershadsky et al. 1991; Waterman-Storer et al. 1999). In addition, microtubules might modify adhesions by promoting adhesion turn-over (Danowski 1989; Bershadsky et al. 1996; Kaverina et al. 1998; Kaverina et al. 1999). Overall the roles of the microtubule cytoskeleton in migration appear quite variable and the molecular mechanisms are often not clearly defined. Below I summarized a few of the more well-studied functions of microtubules in regulating directional migration.

1.2.3 Microtubule dependent regulation of cell migration

1.2.3.1 Centrosomal repositioning and polarization of microtubules in migrating cells

Although not for all cell types, many migrating cells reposition their centrosomes ahead of the cell nucleus in the direction of migration (Kupfer et al. 1982; Kupfer et al. 1983; Ueda et al. 1997). It is not clear why cells do this, and whether centrosome repositioning is the cause or the consequence of cell polarization has been a matter of debate (Wittmann and Waterman-Storer 2001). Nevertheless, it was speculated that centrosomal repositioning may polarize the microtubules, which in turn provides a polarized membrane trafficking towards the leading edge (Kupfer et al. 1982; Kupfer et al. 1983). Concomitantly with centrosome repositioning, microtubules are selectively stabilized at the leading edge and this may count as an early event of generation of cell asymmetry (Gundersen and Bulinski 1988). Centrosomal repositioning is thought to be responsive to signaling molecules in migration such as the Rho GTPase Cdc42. The actual movement of centrosomes depends on the microtubules themselves as well as the microtubule motor Dynein (Palazzo et al. 2001).

1.2.3.2 Cross-talk between the microtubule network and the actin cytoskeleton

As the centrosome repositions towards the leading edge, microtubules emanate and grow towards the periphery, where they interact with the cortical actin network. In migrating fibroblasts, it has been shown that microtubule growth towards the leading edge per se can locally activate the Rho GTPase Rac1, leading to the increased

polymerization of actin in lamellipodial protrusions (Waterman-Storer et al. 1999). Therefore, microtubules can regulate the actin cytoskeleton via modulation of Rho GTPases. Rho GTPases, in turn, can influence microtubule activities (Wittmann and Waterman-Storer 2001). IQGAP1, an effector of Rac1 and Cdc42, can interact with several microtubules +TIPs such as the Cytoplasmic Linker Proteins (CLIP)-170 and the anaphase promoting complex (APC), leading to stabilization of microtubules in the leading edge. Such interactions represent an important aspect of the cross-talk between the actin and microtubule cytoskeletons, and are expected to be qualitatively different in the protrusions at the cell front compared to the retracting rear.

1.2.3.3 Microtubules promote adhesion turn-over

Microtubules can also target adhesions and promote their disassembly (Kaverina et al. 1999), particularly at the trailing edge, which is important for the rear retraction. The exact molecular mechanism is not quite clear. It has been speculated that microtubules may directly deliver some unknown relaxation signals to adhesion sites to promote adhesion disassembly (Kaverina et al. 1999). Alternatively, microtubules may mediate endocytosis of adhesion complex components for adhesion turn-over. The endocytosis component dynamin, together with the focal adhesion kinase (FAK), have been shown to have a role in microtubule-induced adhesion disassembly (Ezratty et al. 2005).

1.3 Cell migration in development

Although it shares many common features in terms of the actual machinery of motility, cell migration in a developmental context is more complex than cell migration in tissue culture both in terms of spatial and temporal regulation. Some of the best-studied examples of cell migration in developmental context include the movement of mesodermal cells during gastrulation, neuronal cell migration, germ cells migration (in different organisms), *Drosophila* dorsal closure whereby an eye-shaped gap in the dorsal epithelium is closed by coordinated actions of different cell types; and finally *Drosophila* border cell migration that is discussed in this study.

1.3.1 Spatial and temporal regulation

For most types of migration that occur during development, the first essential step is the initiation, during which an originally immotile cell becomes migratory. This involves multiple changes at a cellular level: a cell that is going to migrate remodels its adhesions to delaminate from previous attachment sites, reorganizes its cytoskeleton to assume a polarized shape and makes actin-rich protrusions at the leading edge. During the actual migration, the cell must adhere to and dynamically interact with the substrate on which it migrates to generate traction for movement. If it is a guided migration, the cell must also interpret guidance cues to establish a directional migration towards the target.

In physiological conditions, many cells migrate collectively, as part of a group. In addition to the basic migratory features seen in solitary cells, collective migrating cells also interact and influence each other while migrating. For example, neural crest cells migrate directionally in ‘‘streams’’ in vivo, with frequent dynamic interactions between the cells. This cell-cell interaction is regulatory and can generate non-cell-autonomous pushing and pulling forces to affect the overall movement. In addition, the collectively migrating cells have the potential to provide spatial information with each other when they occupy different locations in the substrate space (Rorth 2011).

1.3.2 Microtubules in cell migration during development

One in vivo system where the role of microtubules is quite clear from genetic evidence is the neuronal cell migration. Mammalian *Lis-1* was originally identified as a dosage sensitive gene that can cause lissencephaly, a defect in the migration of differentiating neurons in the developing brain (Reiner et al. 1993). Lis-1 participates in microtubule-based behavior. It was later found that both Lis-1 and its interacting proteins including the microtubule motor Dynein have an established role in neuronal migration, where they control the translocation of the nucleus in neurons (Vallee and Tsai 2006).

1.4 *Drosophila* border cell migration as a model to study collective cell migration in development

1.4.1 Physiology of border cells

Border cells are a group of somatic cells that perform a simple, stereotypic migration during *Drosophila* oogenesis. An early *Drosophila* egg chamber consists of germ-line derived cells, the oocyte and nurse cells, surrounded by a layer of follicular epithelium, with a pair of specialized polar follicular cells sitting at each end (Figure 1.2). At stage 8 of oogenesis, the two anterior polar cells signal to 4-8 neighboring follicle cells, inducing them to become border cells. The border cells form a tight cluster and delaminate from the epithelium as the cells become migratory. At early stage 9, the motile outer border cells invade between the giant nurse cells and migrate to the oocyte, carrying the two central non-motile polar cells along with them (Figure 1.2). By stage 10, the border cells have reached the oocyte, and then migrate a short distance dorsally toward the oocyte nucleus. There, they are important for making a hole in the micropyle through which sperm enters to fertilize the egg (Rorth 2002).

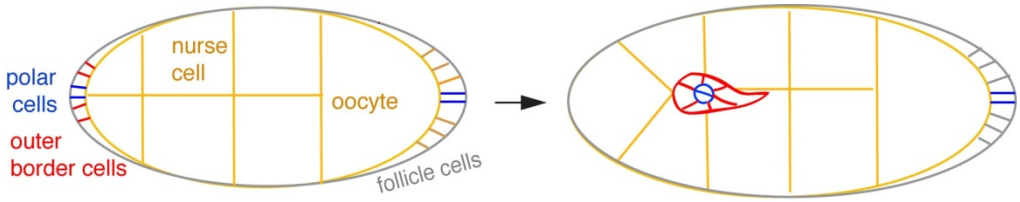

Figure 1. 2 Schematic representation of border cell migration

Schematic of egg chambers before (left) and after (right) initiation of border cells migration. In this and all other figures, anterior is to the left and cells migrate to the right. Border cells (red) and polar cells (blue) are indicated.

1.4.2 Specification of border cells

The process by which the epithelium-originated border cells become migratory and initiate invasive migration is under tight control both spatially and temporally. Spatially, the polar cells secret a ligand Unpaired (Upd), which acts non-cell antonomously through Domeless receptor (Ghiglione et al. 2002) and turns on Janus kinase (JAK)/Signal Transducer and Activator of Transcription (STAT) pathway in adjacent cells (Beccari et al. 2002). The JAK/STAT signaling is active at high levels in immediately surrounding follicle cells and activates the expression of another transcription factor named slbo border cell (Slbo). Both STAT and Slbo are important for border cells to become migratory.

The timing of border cell migration is regulated by both the ecdysone and Notch signaling pathways. Ecdysone is a fly steroid hormone that is expressed exactly at the stage when border cell migration occurs. Border cells express the ecdysone receptor (EcR) and its coactivators Taimen (Tai), and activated ecdysone signaling is essential for border cell motiity, possibly through regulating the turnover of adhesion complexes (Bai et al. 2000).

The transmembrane receptor Notch is activated in many follicle cells in stage 6 of oogenesis, however, later on at stage 9, its activation is exclusively restricted to migrating border cells, despite uniform expression of Delta. Like JAK/STAT, Notch signaling is required for the

expression of Slbo and therefore it is essential for border cell specification and migration (Gonzalez-Reyes and St Johnston 1998).

Slbo is the *Drosophila* homolog of vertebrate CCAAT/enhancer-binding protein (C/EBP), and is a transcriptional activator. It is expressed specifically in border cells and later in centripetal cells, another group of follicle cells that become motile later. Slbo expression is essential for border cell migration (Montell et al. 1992). Without Slbo, border cells are formed but do not migrate. One of the key target genes that is upregulated in border cells by Slbo is the gene encoding the *Drosophila* homolog of the cell-cell adhesion molecule *E-Cadherin* (*DE-cadherin*), which is essential for promoting border cell motility (Niewiadomska et al. 1999), see also in 1.4.4).

To find additional Slbo targets, comparative whole-genome expression profiling on wild-type and Slbo mutant border cells as well as non-migratory follicle cells have been performed to understand at a molecular level how a transcriptional switch induces migration (Borghese et al. 2006; Wang et al. 2006). A number of the border cell-enriched genes were found to be involved in adhesions, cytoskeletal regulation and the secretory pathway (Borghese et al. 2006; Wang et al. 2006) and these may affect cell shape changes and adhesion turnover during border cell migration.

Of the genes that require Slbo for their upregulation were a number of actin regulators and one microtubule regulator namely *stathmin*. *Stathmin* is quite robustly upregulated by Slbo in border cells.

1.4.3 Actin-dependent protrusions

The actin cytoskeleton is essential in border cells to make dynamic protrusions and together with myosin II, to generate contractile force to move the cell forward (Edwards and Kiehart 1996; Fulga and Rorth 2002; Rorth 2003). Many actin binding proteins control the rate and organization of actin polymerization and have a role in border cell migration. For example, the Arp2/3 complex which is essential for making branched actin structures in lamellipodium, is an essential regulator in border cell migration (Lu 2011) In addition, the minus-end directed actin motor Myosin VI can bind to DE-cadherin and β-catenin, stabilizing the adhesion complex and linking it to the cytoskeleton. This may provide additional force to facilitate the protrusion formation (Geisbrecht and Montell 2002).

1.4.4 DE-cadherin mediated adhesion and traction

The *Drosophila* homolog of the cell-cell adhesion molecule E-cadherin (DE-cadherin) is essential both in the migrating border cells and in the substrate nurse cells for migration to occur (Niewiadomska et al. 1999). It is expressed highly in border cells and accumulates prominently in cell contacts between individual border cells and to a less extent

between border cell and nurse cells. Such DE-cadherin mediated homophilic cell-cell adhesion is required and regulated to generate traction for border cell migration (Niewiadomska et al. 1999; Pacquelet and Rorth 2005). This is different as compared to some epithelial cells that undergo epithelial to mesenchymal transition (EMT) in becoming migratory both during normal development and tumor metastasis (Thiery et al. 2009). EMT involves multiple changes including the loss of cell-cell adhesion by downregulation of *E-cadherin*, the loss of cell polarity, and the acquisition of migratory and invasive properties (Thiery et al. 2009). Border cells instead upregulate *DE-cadherin* for becoming migratory, suggesting *E-cadherin* does not exclusively function as an invasion suppressor; it may contribute to the dynamic adhesions that can positively promote motility and invasiveness in this cell type, just as the *neural cell adhesion molecule* (*N-cadherin*) does as a invasion promoter in neuronal migration (Derycke and Bracke 2004).

1.4.5 Guidance signaling during border cell migration

Directional migration (guidance) of the border cells to the oocyte is controlled by two receptor tyrosine kinases (RTKs), the epidermal growth factor receptor (EGFR) and PDGF/VEGF Receptor (PVR). The ligands for these receptors, principally PVF1 and Gurken respectively, are expressed in the target, the oocyte (Duchek and Rorth 2001; Duchek et al. 2001). Border cells migrate in two distinct phases with different modes of guidance signaling: an initial rapid migration with

polarized cell behavior followed by a slower migration that depends on collective processing of guidance signals as a whole cluster (Bianco et al. 2007). Both PVR and EGFR act in both phases but use different downstream effectors to direct border cell migration with differential behavior effects: PVR dominantly induces large persistent front extensions and signals to Rac dependent atypical Rac exchange factor Myoblast city (Mbc) and engulfment and cell motility (ELMO) pathway (Bianco et al. 2007; Poukkula et al. 2011). EGFR is absolutely required for the migration in the late phase, till to the dorsal side towards the oocyte nucleus (Duchek and Rorth 2001).

1.4.6 Advantage of using border cell as a model

Border cell migration is spatially and temporally regulated and represents an excellent model to study collective migration in vivo (Rorth 2002; Montell 2003). They migrate in a physically constrained three-dimensional environment, squeezing between nurse cells. This type of cell-on-cell migration is best known from the neuronal migration in the brain and they may share some common features. Though detailed biochemical characterization is not as advanced as in tissue culture, powerful genetic approaches have allowed the identification of important molecules for migration, such as the guidance signaling. In addition, the ability to perform live imaging with this system has allowed the appreciation of this dynamic process ex in situ (Bianco et al. 2007; Prasad and Montell 2007; Tekotte et al. 2007; Poukkula et al. 2011; Inaki et al. 2012). Further studies are actively on-going to understand

the dynamic regulation of the cytoskeleton organization and adhesions, as well as how the guidance signaling regulate those downstream effectors in border cell migration.

1.5 Aim of the project

The aim of the Ph.D project was to understand how microtubules affects border cell migration and how microtubule dynamics are regulated; and in addition, to find out the roles of individual microtubule regulators including the previously identified gene *stathmin* in border cell migration.

2. Results

2.1 Microtubules in the border cells

2.1.1 Microtubule organizations

To investigate the functions of microtubules in border cell migration, I first tried to characterize the organization of microtubules in the border cell cluster. Anti-Tubulin staining of fixed samples showed that microtubules were present in the border cells cluster throughout migration: in early stage when border cells were specified (Figure 2.1 A) and formed a border cell cluster (Figure 2.1 B); this resembles the staining in follicle cells, the epithelium that border cells are derived from. Prior to migration, the two anterior polar cells contained a strong MTOC like structure that was oriented towards the front of the cluster, in the future migration direction (arrow in Figure 2.1 B). During migration, the two polar cells are assumed to be immobile (Niewiadomska et al. 1999) and not actively contributing to migration. They are thought to be carried along by the outer border cells as they migrate. Because the outer border cells are actively rotating and shuffling (Bianco et al. 2007), the polar cells also get rotated and the relative MTOC position in the cluster changes during migration (arrow in Figure 2.1 D). In contrast to the polar cells, the outer border cells displayed loosely organized bundles of microtubules enriched at the cell cortex, both when they initiating migration and during their active migration (arrow head, Figure 2.1 B and 2.1 D).

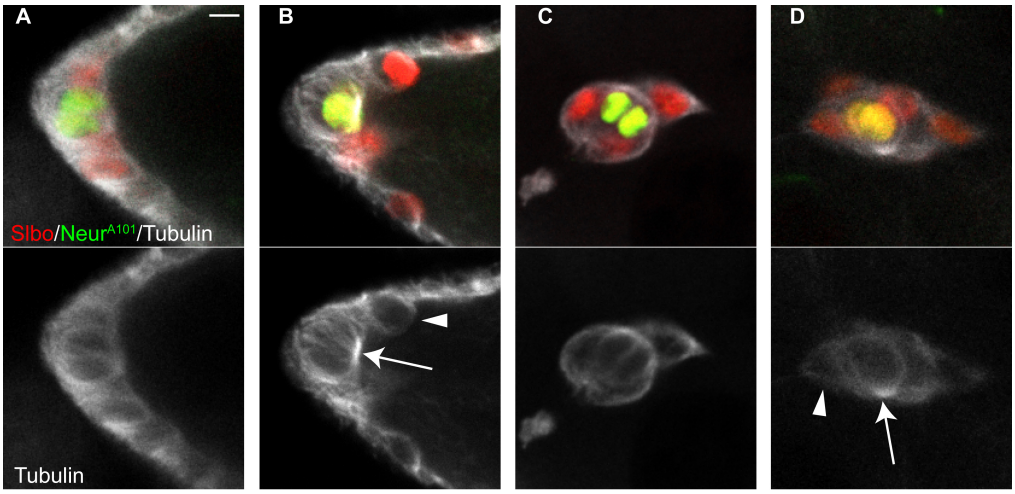

Figure 2. 1 Organization of microtubules in border cell clusters at different stages of migration

(A) late stage 8 when border cells are specified
(B) early stage 9 when border cells form a cluster
(C) middle stage 9 when border cell cluster have detached from epithelium and migrating
(D) late stage 9 when border cells are migrating
Border cells are marked with the transcriptional factor Slbo (red); polar cells are marked with Neur^{A101} (green); microtubules are stained by anti-Tubulin (white). Arrow indicates MTOC-like structure in polar cells; arrowhead indicates cortical microtubules in outer border cells. Genotype of egg chambers is *w1118/+; neur^{A101} /+* (Scale bar: 10μm).

Microtubules can be post-translationally modified and acetylation of α-Tubulin marks stable microtubules (Piperno et al. 1987). Anti-acetylated Tubulin staining in border cells showed a similar pattern to anti-Tubulin staining (Figure 2.2), possibility because fixation preferentially captured the stable but not the dynamic microtubules.

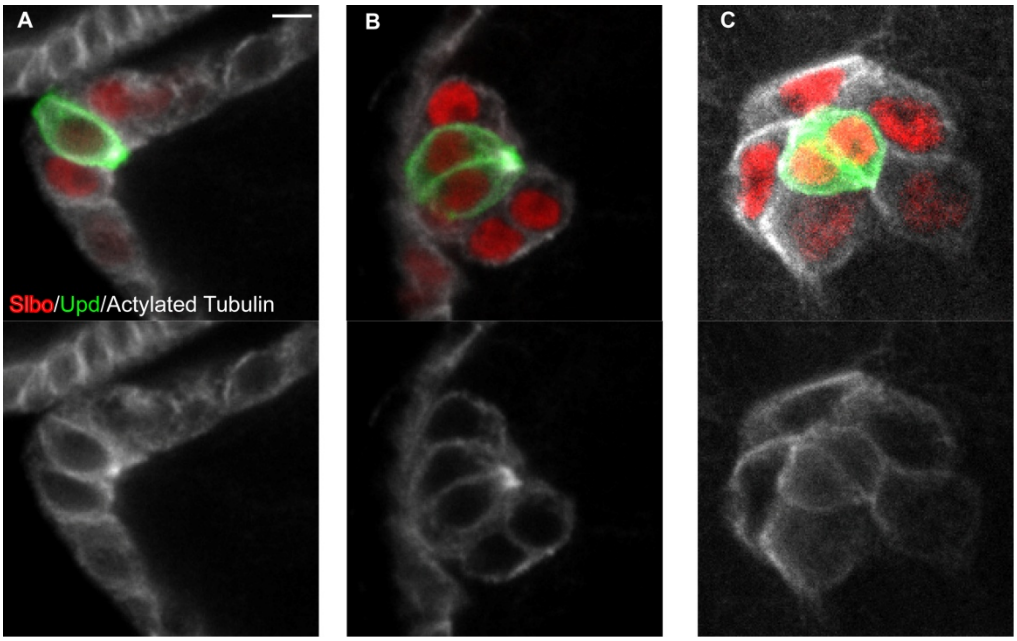

Figure 2. 2 Organization of stable microtubules in border cell clusters at different stages.

(A) late stage 8 when border cells are specified
(B) early stage 9 when border cells form a cluster
(C) middle stage 9 when border cells are migrating.
Border cells are marked with the transcriptional factor Slbo (red); polar cells are marked with Upd-GFP (green); stable microtubules are stained by anti-actylated Tubulin (white). Genotype of egg chambers is *UpdGal4/+;UAS-PH-GFP/+* (Scale bar: 10μm).

As microtubules are often not fixed very well, to confirm the observed staining pattern, I performed live imaging analysis of a green fluorescence protein (GFP) tagged Tubulin (tubulin-GFP). Tubulin-GFP showed similar results (Figure 2.3), indicating that both anti-Tubulin and anti-actylated Tubulin staining in fixed sample can both be used to examine microtubule organizations in border cells.

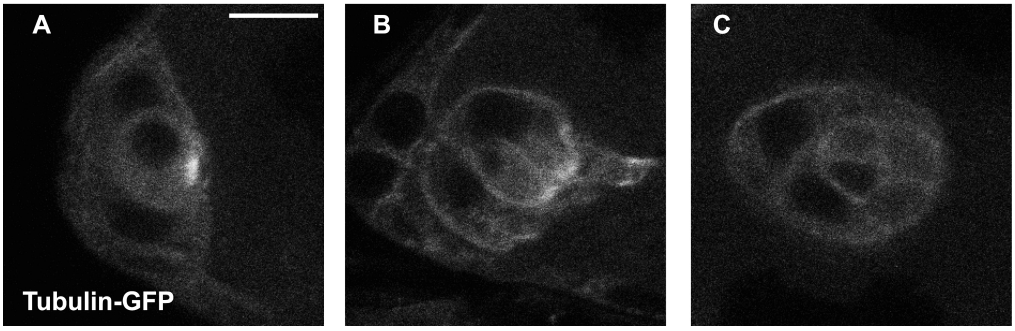

Figure 2. 3 Visualization of microtubules in border cells at different stages by live imaging of *tubulin-GFP* transgene.

(A) border cell cluster has just been formed
(B) border cell cluster is initiating migration
(C) border cell cluster is migrating
The genotype of egg chamber is *w1118/tubulin-GFP* (Scale bar:10 μm)

2.1.2 Microtubule dynamics

To visualize dynamic microtubules and check the dynamics of microtubules, I tracked the movements of the GFP tagged EB1 expressed in egg chambers by live imaging. EB1 associates with the plus end of growing microtubules, and therefore its direction reflects the direction of microtubule growth. As border cell migration occurs deep inside the tissue, I used confocal microscopy for live imaging. Live imaging was done at one confocal optical section of a delaminating or early migrating border cell cluster to allow reasonable detections of fast-moving EB1-GFP dots. In follicle cells, which have well-defined apical-basal polarity, all EB1-GFP dots were highly dynamic and most of the tracks moved exclusively from the apical side towards the basal side (Figure 2.4 B). The polar cells are the only cells with a visible MTOC like structure. As expected, most of the EB1-GFP tracks emanate from the MTOC like region and move towards the periphery (data not shown).

For the outer border cells, the highly dynamic EB1-GFP dots were found to move in multiple directions and therefore a quantitative analysis of the overall bias of all EB1-GFP tracks detected were needed. In the front cell within the border cell cluster, the overall bias of EB1-GFP comets was to move away from the leading edge (Figure 2.4 C). In the back cell of the border cell cluster, more EB1-GFP tracks moved away from the back (Figure 2.4 C).

The outer border cells are orientated with respective to each other. They have outer membrane touching the germline nurse cells and inner membrane facing inward, towards the center polar cells (Figure 2.4 E). If we consider the border cells as one cluster, the microtubules in the front and back cells are both organized inwards, towards the cluter center. Therefore, there is a subtle bias for EB1-GFP comets to move more towards the center of the cluster (Figure 2.4 D).

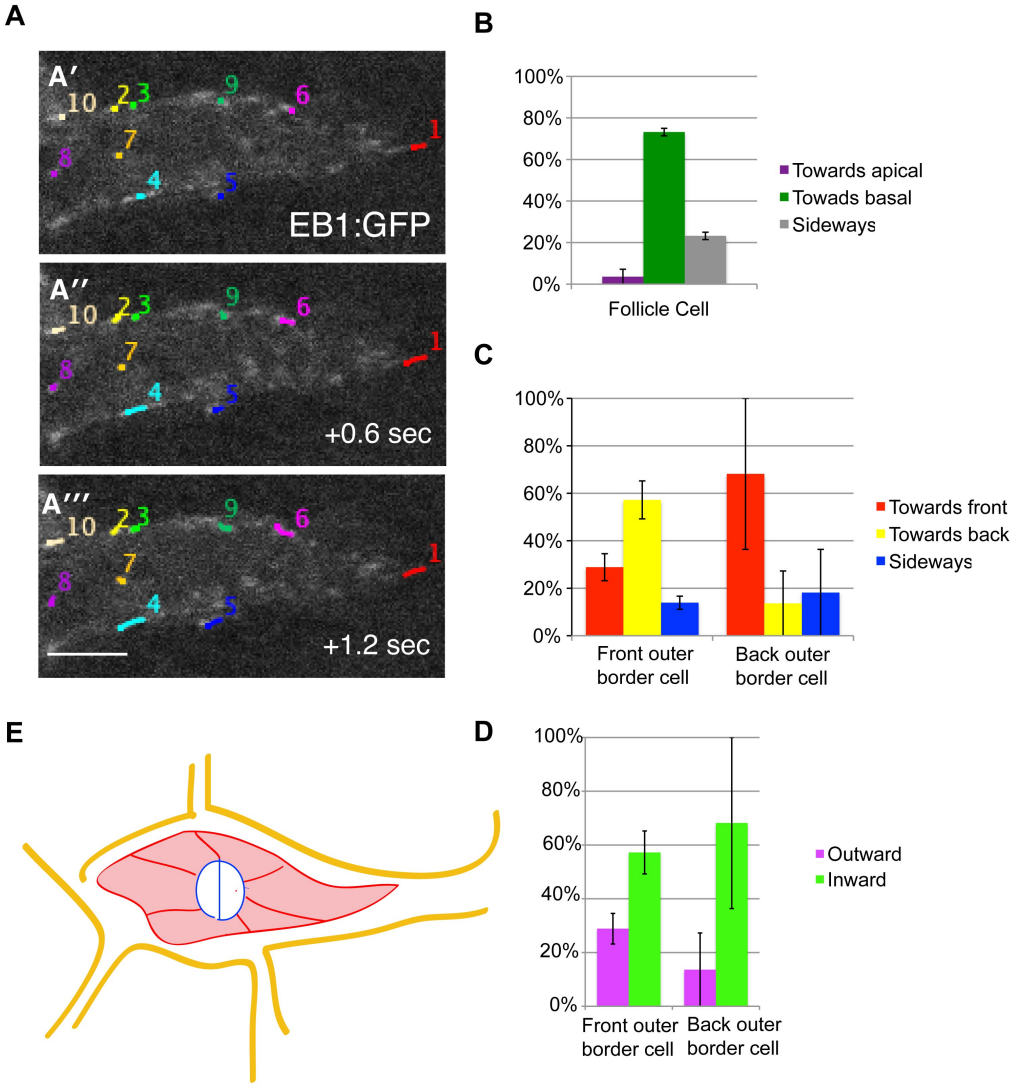

Figure 2. 4 EB1-GFP track directions in follicle cells and outer border cells

(A) Three cut-out frames from EB1-GFP movies illustrating tracking of EB1-GFP dots in the front part of the front border cell (Scale bar: 4μm).

(B) Quantificaiton of EB1-GFP directions in follicle cells
Measured EB1-GFP tracks are catagorized into three catogories according to apical-basal axis and the percentage of EB1-GFP tracks in each category is presented. 22 tracks from 2 movies were analyzed, SEM indicated; $P<0.05$ (two-tailed student t-test) for towards apical versus towards basal movement.

(C-D) Quantification of EB1-GFP directions in outer border cells according to (B) migration direction axis and (C) direction towards polar cells.131 tracks from 7 movies were analyzed, SEM indicated; $P<0.05$ (two-tailed student t-test) for outwards versus inwards movement.

(E) Schematic representation of the orientation of outer border cells (red) with respect to polar cells (blue) in a border cell cluster. The outer membranes are facing the germline (yellow).

It has been shown that the outer border cells retain some apical characteristics (Niewiadomska et al. 1999), so this modest bias of EB1-GFP comets moving away from the apical-like region (outer-membrane) is similar to that of the follicle cells, in which the EB1-GFP comets move more exclusively away from the apical region (Figure 2.5). However, the bias is less strong, consistent with border cells being less strictly apical-basal polarized, or rather, partially polarized. The less dominent presence of EB1-GFP tracks moving to the opposite direction indicates some reorganization of microtubules occurs upon formation of the motile cluster.

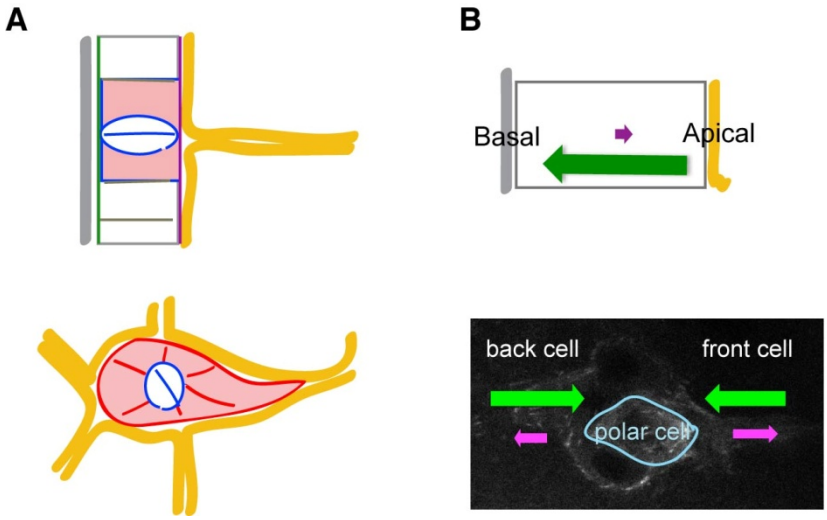

Figure 2. 5 Schematics illustration of cell organization and EB1-GFP directions in border cell cluster at different stages

(A) Cell organization and (B) EB1-GFP directionality before (upper panel) and after (lower panel) the formation of a migrating cluster (see Figure 1.2). Apical (purple line) surface is towards the germ line (yellow). The outer membrane (red) of migratory border cells (lower panel) is facing the germline (see also in Figure 2.4E). Polar cells (blue) are in the center. Arrows in B are colour coded and illustrate the directional bias of EB1-GFP tracks as shown in Figure 2.4 B and 2.4 D.

2.2 Effects of microtubule disruption drugs on border cells

2.2.1 Effects on microtubules in border cells

The immediate effects of perturbing microtubules can be determined by using specific drugs that interfere with microtubules and microtubule dynamics. Nocodazole is an anti-neoplastic agent that interferes with polymerization of microtubules. First, different concentrations of nocodazole were applied to egg chambers and the concentration was titrated to 2μM, which did not cause perturbations of the overal development of egg chambers and nurse cell nuclear dynamics, yet had a effect on the net cluster movement (Figure 2.6 A). I then checked whether this concentration had an effect on microtubules in the border cells. Treatment of 2μM nocodazole in egg chambers caused some attenuation of the strong foci of microtubules in polar cells (Figure 2.6 C) and a marked reduction of the cortical microtubules in border cells (Figure 2.6 C). Treatment with 2μM taxol, which stabilizes microtubules, caused microtubules in the border cells to become denser throughout the cytoplasm (Figure 2.6 D). More dramatically, the normally very dynamic microtubules in the surrounding germ line cells were stabilized and can be clearly visualized upon taxol treatment (see arrow in Figure 2.6 D). These changes were observed within minutes of drug addition, allowing immediate live assessment of effects of perturbing the microtubule cytoskeleton.

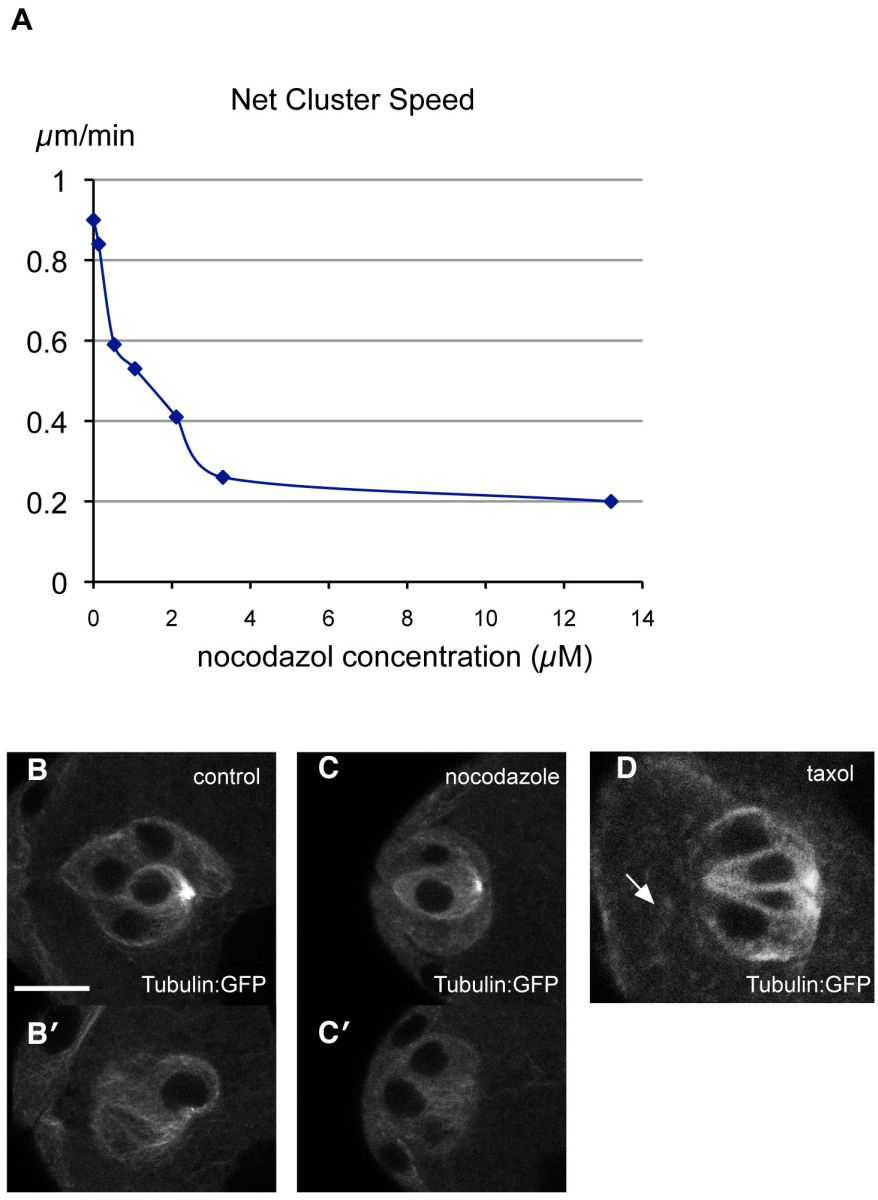

Figure 2. 6 Effects of drugs on microtubules in border cells

(A) Relationship between net cluster speed and nocodazole concentration.

(B-D) Microtubules visualized by live imaging of border cell clusters expressing *tubulin-GFP* transgene.
Top panel: One confocal section image including polar cells from Z-stack movies of (B) dimethyl sulfoxide (DMSO), (C) nocodazole and (D) taxol treated egg chambers. Arrow points to the germline.
Bottle panel: Another confocal section image including only outer border cells from Z-stack movies of (B) DMSO and (C) nocodazole treated egg chambers. The genotype of egg chamber is *w1118/tubulin-GFP* (Scale bar:10 μm)

2.2.2 Effects on initiation of border cell migration

To assess the effects of disrupting microtubules in border cell migration, live imaging was performed to analyze the behavior of border cell clusters upon drug treatment. Egg chambers were dissected from female ovaries and treated with microtubule disrupting drugs. Live imaging was set up immediately after the addition of the drug with a few minutes lag time to allow the assessment of immediate effects of microtubule disruption on border cells migration. Images were acquired for up to two hours, which allowed the healthy development of egg chambers ex in-situ (Bianco et al. 2007).

I first checked whether drug treatment could affect the initiation of border cell migration. Prior to the onset of imaging and addition of the drug, early stage 9 egg chambers in which border cells had not initiated migration but are likely to start migration soon were chosen, as judged by their stage and size. The competency of migration initiation was analyzed. This was done by monitoring the ability of clusters to start migration within a set period of time, in this case, in the two hours during which the egg chamber were imaged for (Figure 2.7). Nocodazole-treated border cell clusters showed reduced competency of initiating migration, indicating this particular stage is sensitive to microtubule disruption. Taxol treatment produced slightly opposite effect, but it was not statistically significant different to control.

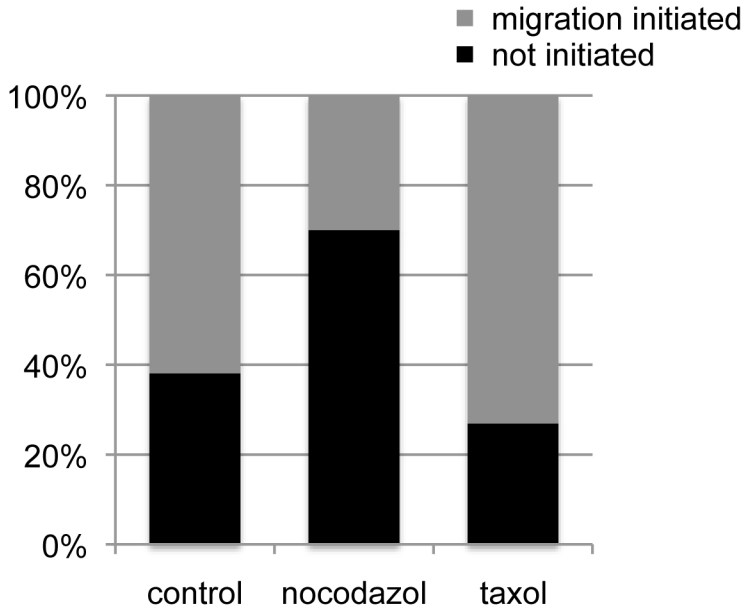

Figure 2. 7 Effects of microtubules drugs on initiation of migration

Quantification of percentage of border cell clusters from early stage 9 egg chambers that succeed in initiating migration during 2-hour movies. $P<0.05$ for comparison between nocodazole versus control (DMSO) treatment using two-tailed Fisher's exact test. Number of movies analyzed is between 6 (control sample) to 50 (drug treated sample). Genotypes are *slboGal4,10xGFP/+*

2.2.3 Effect of drugs on border cell migration

To assess whether drugs could have an effect on the process of migration, live imaging was done for clusters that had already initiated migration (cluster had detached from the anterior epithelium). The net speed of migrating border cell clusters in the early phase was analyzed. Both nocodazole and taxol treatment significantly reduced the net cluster speed by 50% (Figure 2.8 A), indicating microtubule and microtubule dynamics are important for border cell migration.

The defect in net cluster speed could be due to several possibilities. A reduction of basic motility of border cells in the cluster or a lack of proper directionality. In addition, net forward cluster movement requires invasiveness as border cells invade into the germ-line tissue. Disruption of the guidance cues would be expected to reduce net cluster speed but not the basic cell motility (Poukkula et al. 2011).

To determine whether drug treatment caused a change in cell motility, I estimated the movement of individual border cells by manually tracking the nuclei movement in 3D (Figure 2.8 C). The apparent cell movement speed in nocodazole and taxol treated border cells was reduced by about 30% and 20% respectively (Figure 2.8 B). Very recent data from the lab on 3D reconstruction of border cell clusters has revealed individual nucleus does move considerably within the cell and nuclei tracking overestimates the actual cell movement by 25%, and does so systematically (W Yu, et al, unpublished results). Therefore, this

reduction on the apparent cell movement could be caused by a subtle defect on cell movement, or could be caused by the disruption of nuclei movement within a cell. This was not surprising as microtubules are important for nuclei movement (Reinsch 2001; Dujardin and Vallee 2002).

Therefore, both microtubule drugs affect cell or nuclei movement and have an added effect on the net cluster movement. The additional defect in cluster movement could be due to disruption of guidance, but is unlikely, as explained in the next section (2.2.4). The defect could also be due to a lack of progressiveness, as border cells move and invade into the dense cellular environment and require proper invasiveness for progression.

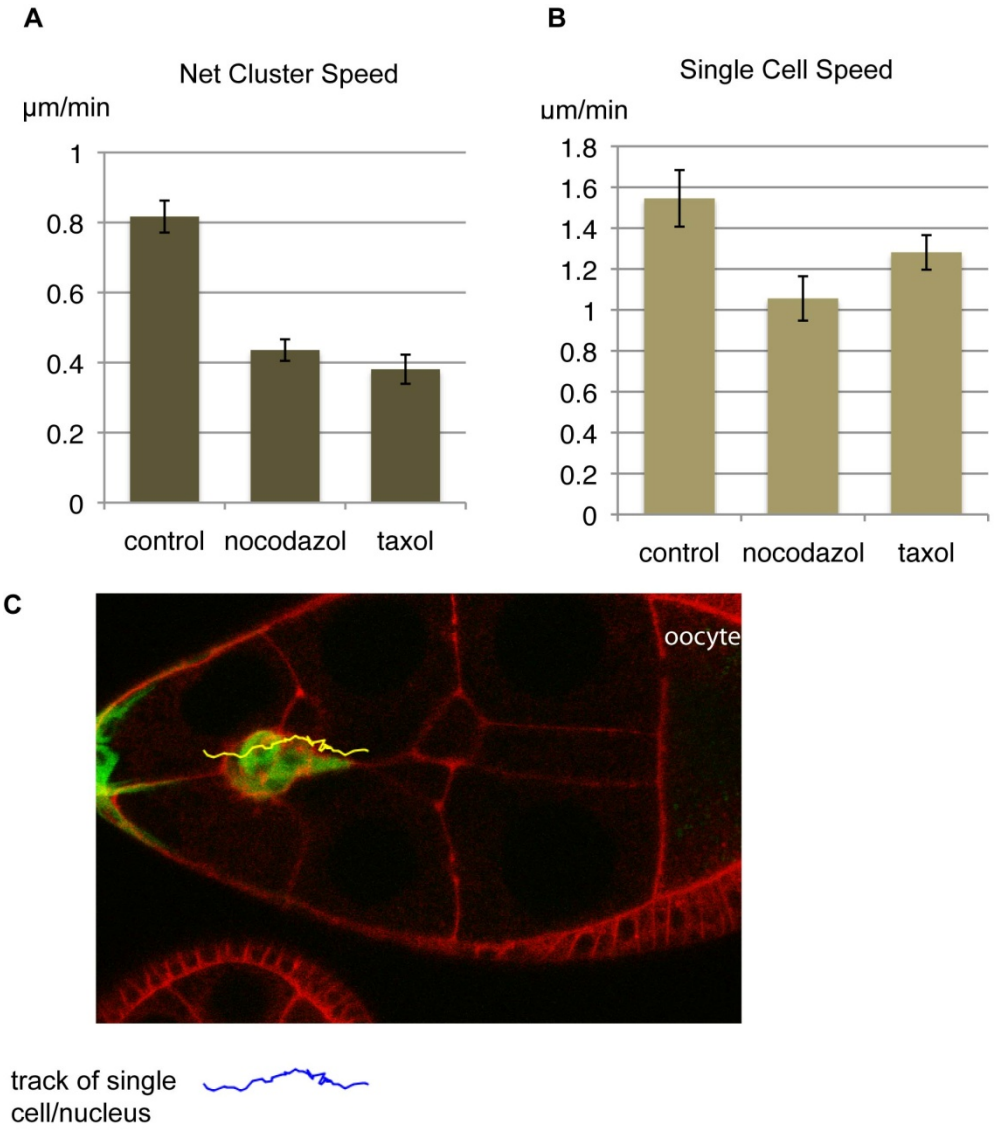
A
Net Cluster Speed
µm/min
1
0.8
0.6
0.4
0.2
0
control
nocodazol
taxol
B
Single Cell Speed
um/min
1.8
1.6
1.4
1.2
1
0.8
0.6
0.4
0.2
0
control
nocodazol
taxol
C
oocyte
track of single
cell/nucleus

Figure 2. 8 Effects of drugs on border cell migration

(A) Quantification of net cluster speed from migrating border cell clusters. P<0.001 for both comparisons between drug treatments versus control. Two-tailed student t-test was used. Number of movies analyzed is between 8 (control sample) to 21 (drug treated sample). Genotypes are *slboGal4,10xGFP/+*.

(B) Quantification of apparent single cell speed from migrating border cell clusters. Single cell nuclei were tracked between 1-2 minutes interval. P<0.05 for comparison between nocodazole treatment versus control using two-tailed student t-test. Number of movies analyzed is between 7 (control sample) to 17 (drug treated sample). Genotypes are *slboGal4,10xGFP/+.*

(C) Illustration of single cell nuclei tracking.
Image from a wild-type video (*slboGal4,10xGFP/+*) showing the border cell cluster migration and the track of one nucleus (cell) in the early phase (yellow in overlay; blue below). All cells are outlined by FM 4–64 (red).

2.2.4 Effect on extension profiles of border cells

To gain more insights into the alterations of behavior of border cell clusters in which microtubule cytoskeleton was perturbed by drugs, I analyzed their protrusion (extension) profiles. Extensions were identified by an automated method (Poukkula et al. 2011) and classified into one of the three categories according to their direction with respect to the direction of migration, front being toward the oocyte, back in the opposite direction and side covers the rest (Figure 2.9 A). In a border cell cluster, forward extensions grow from the front cell; backward extensions grow outward from the back cell and they are active extensions, not simply non-retracted tails (Poukkula et al. 2011). In wild type, extensions were observed in all the three directions, but front extensions were predominant (Figure 2.9 B). The front extension has a large size and generates traction for movement (Poukkula et al. 2011). Both drug treatments led to a reduction in front extension size (Figure 2.9 C), however, the clear bias for front extension was still retained (Figure 2.9 B), implying appropriate perception of the guidance cues and overall cluster polarity is maintained. Nocodazole treatment also led to a significant increase of both the abundance and size of back extensions (Figure 2.9 B and Figure 2.9 C). Therefore back extensions could have been stabilized or stimulated for increased growth upon microtubule disruption, indicating microtubules may negatively regulate or destabilise back extensions. Future higher time resolution movies would be needed to distinguish between the two possibilities.

A

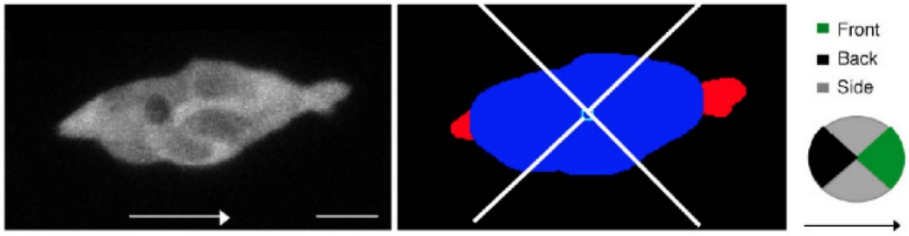
Front
Back
Side

B

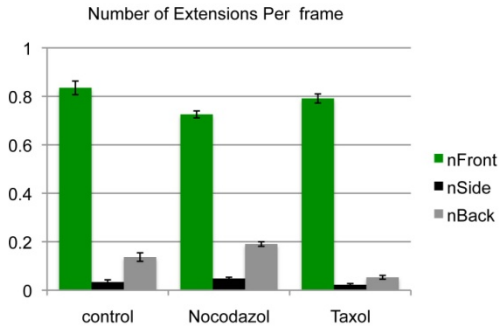
Number of Extensions Per frame
1
0.8
0.6
0.4
0.2
0
control
Nocodazol
Taxol
nFront
nSide
nBack

C

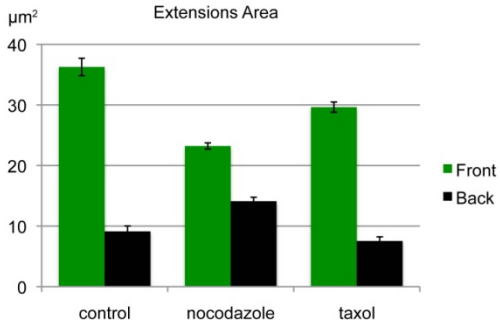
Extensions Area
μm²
40
30
20
10
0
control
nocodazole
taxol
Front
Back

Figure 2. 9 Drug's effect on extension profiles of border cells

(A) Illustration of identifying and classifying extensions.
Left: Projected GFP image of a wild-type border cell cluster (*slboGal4, UAS-10xGFP/+*); arrows indicate direction to the oocyte
Right: same as left, but after segmentation and automatic definition of the cluster body (blue) and extensions (red). Extensions are classified as front (0-45° and 315-360°), side (255-315°+45-135°), and back (135–225°). Scale bar, 10 μm. Image courtesy of Adam Cliffe.

(B) Quantification of number of extensions as presence per frame from migrating clusters. For nocodazol, front and back are significant ($P<0.001$). For taxol, only back is significant ($P<0.001$). Two-tailed student t-test was used. At least 388 frames were analyzed. Genotypes are *slboGal4,10xGFP/+*.

(C) Quantification of the area of front and back extensions from migrating cluster. For nocodazole, comparison with control in both the front and the back category is statistically significant ($P<0.001$). Taxol treatment only induced a significant decrease of front extension ($P<0.001$). Two-tailed student t-test were used. For front extensions, at least 289 extensions were analyzed. For back extensions, at last 42 back extensions (in control) were analyzed. Genotypes are *slboGal4,10xGFP/+*.

2.2.5 Autonomous and non cell-autonomous effect of disrupting microtubules in border cell migration

The above-mentioned experiments with drugs do not distinguish between border cell dependent/autonomous effect and effects due to changes in nurse cells, that is, non-autonomous effect. To disrupt microtubules generally but in a cell-specific way, I induced expression of the microtubule severing protein spastin (Roll-Mecak and Vale 2008) in migratory border cells using a specific expression inducer (slbo-Gal4). Slbo-Gal4 expression starts at late stage 8 and increases later on (Rorth et al. 1998). Prior to migration, the Slbo-Gal4 expression in outer border cells had not yet be fully turned on in all cells, leading to a variable and insufficient reduction of microtubules in outer border cells (Figure 2.10 A).

Later in migration, Slbo driven expression of spastin in migrating border cells led to a clear reduction of microtubule density in the migratory border cells but not in the polar cells (Figure 2.10 B). However, the net cluster speed in spastin-expressing border cells was similar to that of control (Figure 2.10 C). Therefore, the reduction of net cluster speed in nocodazole treated egg chambers could be due to a non cell-autonomously effect either on the polar cells or/and on the substrate nurse cells. Microtubules in the polar cells are required for the polarized localization of the cytokine Upd (Van de Bor et al. 2011), and therefore could in principle have a non-autonomous effect on border cell movement.

Although there was no reduction in the cluster speed in spastin over-expressing border cell clusters, I did observe some clear changes in extension dynamics, especially for the back extensions. Wild type border cells produce predominantly front extensions with a large size; reduction of microtubules in the border cells by over-expressing spastin resulted in some reduced frequency of front extensions but an increased frequency of both side and back extensions (Figure 2.10 D). The size of the back extensions also increased dramatically (Figure 2. 10 E), making the front and back extensions more similar to each other. This was similar to the effect from nocodazole-treated clusters; implying that microtubules are required in border cells and that they may negatively regulate the stability and/or growth of extensions, in particular in the back cell.

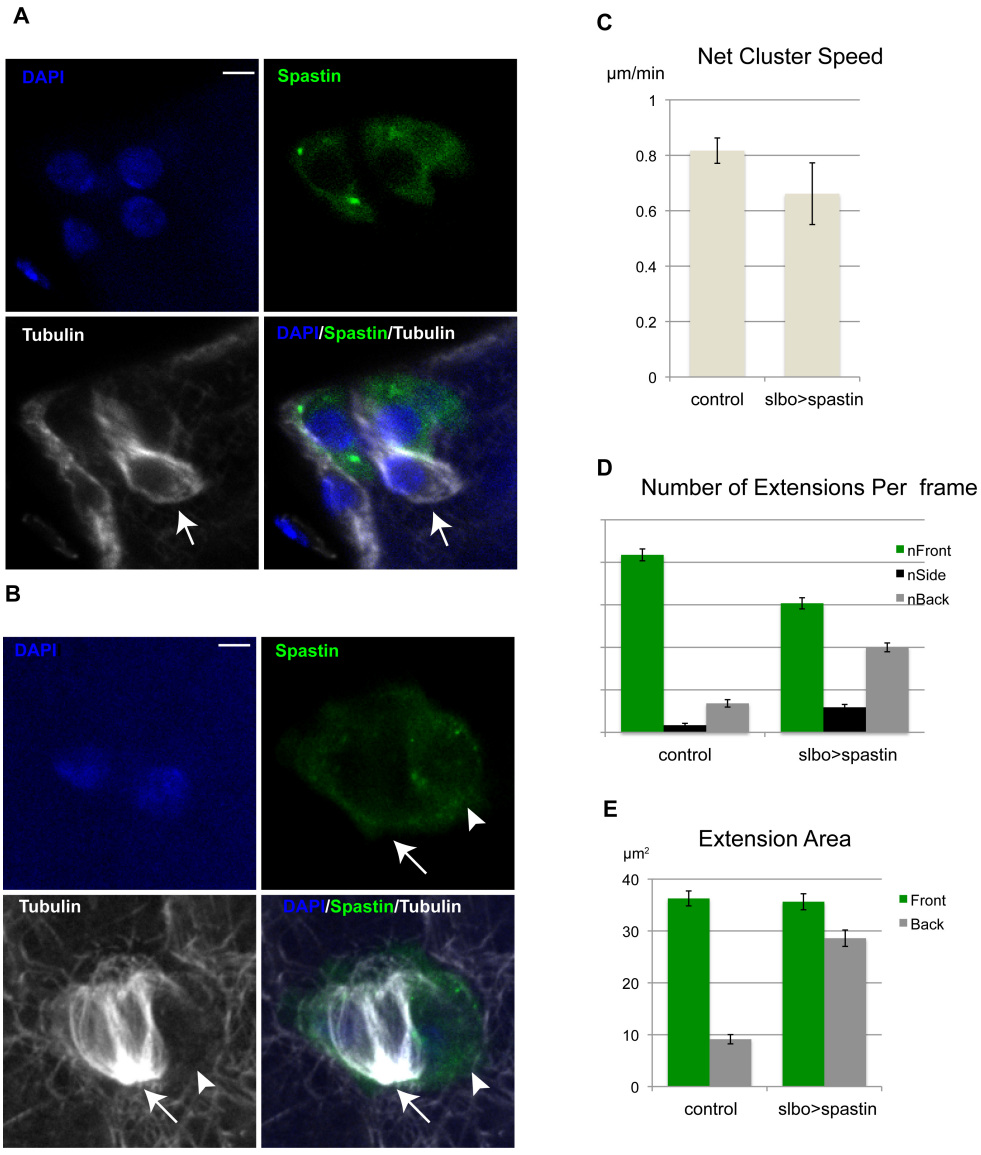
A
DAPI
Spastin
Tubulin
DAPI/Spastin/Tubulin
B
DAPI
Spastin
Tubulin
DAPI/Spastin/Tubulin
C
Net Cluster Speed
μm/min
1
0.8
0.6
0.4
0.2
0
control
slbo>spastin
D
Number of Extensions Per frame
nFront
nSide
nBack
control
slbo>spastin
E
Extension Area
μm²
40
30
20
10
0
Front
Back
control
slbo>spastin

Figure 2. 10 Non cell-autonomous effect of disrupting microtubules in border cell migration

(A-B) Effects of expressing spastin by SlboGal4 driver on microtubules in border cell clusters at (A) early stage prior to migration and (B) at late stage during migration. Microtubules are stained with anti-Tubulin (white). Spastin-expressing borer cells are marked with GFP. Border cell nuclei are marked with 4',6-diamidino-2-phenylindole (DAPI; blue).Genotype of egg chambers is *w1118/UAS-spastin-EGFP; slboGal4 /+* (Scale bar: 10μm).
Arrow in (A) indicates a non-expressing border cell.
Arrowhead in (B) indicates an expressing border cell with clear reduction of tubulin as compared to the non-expressing polar cells in the cluster (arrow in B).

(C) Quantification of net cluster speed from border cell clusters. Two-tailed student t-test was used. Number of movies analyzes is between 6 (control) to 10 (slbo>spastin). Genotype of egg chambers is *w1118/+;slboGal4,10xGFP/+* for control and *w1118/UAS-spastin-EGFP; slboGal4,10xGFP/+* for slbo>spastin.

(D) Quantification of number of extensions as presence per frame from migrating clusters. Comparisons between control and slbo>spastin in all the three categories are statistically significant ($P<0.001$). Two-tailed student t-test was used. At least 388 frames were analyzed for each category. Genotype of egg chambers is *w1118/+;slboGal4,10xGFP/+* for control and *w1118/UAS-spastin-EGFP; slboGal4,10xGFP/+* for slbo>spastin.

(E) Quantification of the area of front and back extensions from migrating cluster. For front extensions, at least 289 extensions were analyzed. For back extensions, at last 42 back extensions (in control) were analyzed. Genotype of egg chambers is *w1118/+;slboGal4,10xGFP/+* for control and *w1118/UAS-spastin-EGFP; slboGal4,10xGFP/+* for slbo>spastin.

2.2.6 Genetic interactions between microtubules and *DE-cadherin*

We know Cadherin-mediated adhesion is essential for border cell migration; border cells migrate more slowly when *DE-cadherin* activity is reduced. Because microtubules normally decrease the adhesive strength of Cadherin (amount and turn-over), I decided to check whether there was any interaction between microtubules and *DE-cadherin* in border cells. Shg^{R69} is a null allele for *DE-cadherin/shotgun*(*shg*); shg^{R69} heterozygous flies have reduced level of DE-cadherins in border cells and nurse cells yet show normal border cells migration (Figure 2.11 A). Interestingly, the reduction of net cluster speed upon nocodazole treatment can be suppressed in border cells from Shg^{R69} heterozygous flies (Figure 2.11 A), indicating a negative genetic interaction between *cadherin* and microtubules.

Shg^{PB4354} is an shg allele that efficiently reduces DE-cadherin levels specifically in border cells (Mathieu et al. 2007). The reduction of net cluster migration speed caused by nocodazole was not repressed but became worse in border cells from shg^{PB4353} heterozygous flies (Figure 2.11 B), indicating the rescue of nocodazole's effect on net cluster speed by shg^{PB4354} is via the reduction of DE-cadherins in the nurse cells. This further supported the previous idea that the immediate effect of nocodazole on border cell movement could be due to perturbations of microtubules in the substrate nurse cells.

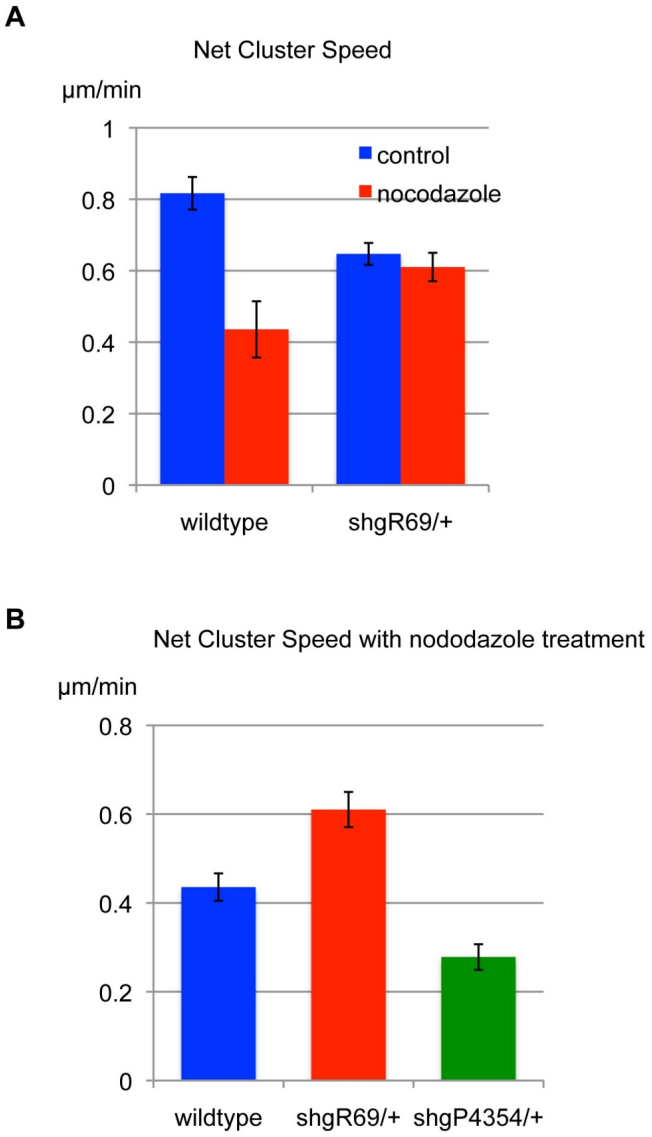

Figure 2. 11 Genetic interactions between microtubules and *DE-cadherin*

(A) Quantification of net cluster speed from wildtype and *cadherin* heterozygous mutant (shg^{R69}/+) border cell clusters. P<0.05 for wildtype cluster between control versus nocodazole treatment. Two-tailed student t-test was used. Number of movies analyzes is between 8 (control treated) to 26 (nocodazole treated). Genotype of egg chambers is *w1118/+;slboGal4,10xGFP/+* for control and *w1118/+;shgR69/+;slboGal4,10xGFP/+ for shgR69/+*

(B) Quantification of net cluster speed from nocodazole-treated wildtype, *cadherin* heterozygous mutant (shgR69/+), and *cadherin* piggyback allele heterozygous mutant (shgPB4354/+) border cell clusters. shgPB4354 is a *cadherin* allele that specifically disrupts its expression in border cells. Number of movies as indicated in Figure (A) except n=8 for *shgPB4354/+*.

2.3 Stathmin is a subtle regulator of border cell migration

Stathmin is a ubiquitous cytosolic phosphoprotein that can bind to αβ Tubulin heterodimer and promote microtubule depolymerization (Sobel 1991). Stathmin is a conserved protein and *Drosophila* Stathmin appeared to have similar function and regulation to the more studied mammalian protein (Ozon et al. 2002). The lab has previously identified Stathmin is highly expressed in border cells and it is also expressed in the substrate nurse cells (Borghese et al. 2006). More interestingly, *stathmin* is a slbo target, (Borghese et al. 2006), implying its possible roles in border cell migration.

2.3.1 Generating of the *stathmin^{KO}* allele

The initial characterization of Stathmin's function in border cells was incorrect (Borghese et al. 2009). The severe non-migrating phenotype displayed by the imprecise excision allele of *stathmin^{L27}* was later found to be contributed by the disruption of the neighboring gene *Arcp-20*, which encodes an important regulator of actin polymerization. To determine the correct function of Stathmin in border cells, I generated a knock-out allele of the *stathmin* (*stai^{KO}*) by homologous recombination (details in Material and Methods 4.1). This *stai^{KO}* allele removes three out of the four exons that are present in all Stathmin isoforms (Figure 2.12 A), resulting in a truncated protein with about 80% coding sequences being removed (Figure 2.12 B). In addition, the three removed exons encode peptide sequences covering two predicted

alpha helical structures (Ozon et al. 2002), which are conserved in mammalian Stathmin and essential for Tubulin binding (Gigant et al. 2000; Redeker et al. 2000). Therefore, the resulting truncated protein product encoded by *stai*^{KO} is expected to be non-functional.

A

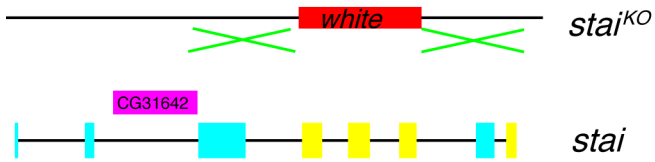
white
stai^KO
CG31642
stai

B

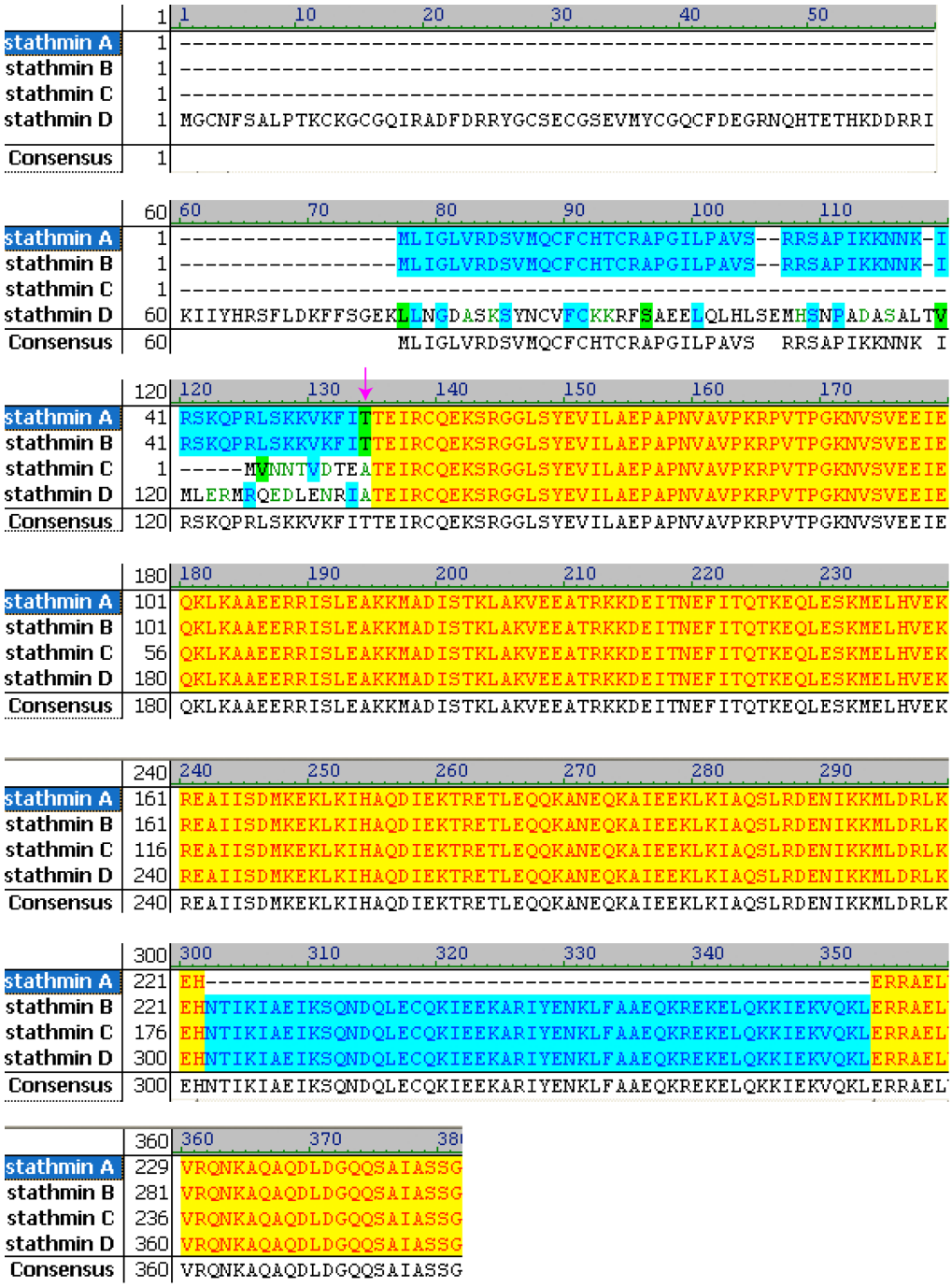
stathmin A
stathmin B
stathmin C
stathmin D
Consensus
MGCNFSALPTKCKGCGQIRADFDRRYGCSECGSEVMYCGQCFDEGRNQHTETHKDDRRI
MLIGLVRDSVMQCFCHTCRAPGILPAVS
KIIYHRSFLDKFFSGEKLLNGDASKSYNCVFCKKRFSAEELQLHLSEMHSNPADASALTV
RSKQPRLSKKVKFITTEIRCQEKSRGGLSYEVILAEPAPNVAVPKRPVTPGKNVSVEEIE
QKLKAAEERRISLEAKKMADISTKLAKVEEATRKKDEITNEFITQTKEQLESKMELHVEK
REAIISDMKEKLKIHAQDIEKTRETLEQQKANEQKAIEEKLKIAQSLRDENIKKMLDRLK
EHNTIKIAEIKSQNDQLECQKIEEKARIYENKLFAAEQKREKELQKKIEKVQKLERRAEL
VRQNKAQAQDLDGQQSAIASSG

Figure 2. 12 Schematics showing the coding exons of *stai* and the protein sequences of four isoforms

(A): Construction of *stai*^{KO}. Conserved coding exons between all four Stathmin isoforms are shown in yellow. Alternative coding exons are shown in light blue. A neighboring gene CG31642 locates within *stathmin* genomic region is marked in megenta. Targeted knockout region is replaced by *white* gene after homologous recombination, resulting in the disruption of translation since Thr^{55} as in Stathmin A (see magenta arrow in B, which contains 251 amino acids in total (refer to sequences of Stathmin A (with label shaded in dark blue) in B).

(B): Protein sequence alignment of four Stathmin isoforms. The conserved sequences are shaded in yellow. Megenta arrow indicates the start of the amino acid deletion in Stai^{KO}.

2.3.2 Overall phenotypes of *stathmin*^{KO} mutant animals

Homologous recombination can often lead to introduction of background mutations (personal communications with Cohen lab, also see Material and Methods 4.2.1.3), therefore I characterized the true loss of function phenotype of *Drosophila* Stathmin by examining transheterozygous flies carrying the *stai*^{KO} allele over the small *stathmin*^{L27} deficiency or transheterozygous flies of various *stai*^{KO} lines obtained (see Material and Methods 4.2.1.3). Similar to the viable *stathmin* null mice, flies without *stathmin* (*stai*^{KO}) are viable but display reduced survival rates (Figure 2.13 A), indicating the *Drosophila stathmin* is not an essential gene. In addition, these *stai*^{KO} flies do not move much as wildtype adults (Figure 2.13 C), suggesting the loss of Stathmin may cause neurological defects, just as in mammals (Schubart et al. 1996; Liedtke et al. 2002; Shumyatsky et al. 2005). Interestingly, *stai*^{KO} adult males display a high level of infertility (Figure 2.13 B), indicating Stathmin has a novel role in male germ cells.

To ensure the phenotypes observed were indeed due to loss of Stathmin, a rescue construct with the *stathmin* cDNA driven by a ubiquitous promoter was introduced back to *stai*^{KO} flies. The observed phenotypes were largely rescued, indicating they were due to loss of Stathmin, and the *stai*^{KO} allele generated is a true *stathmin* mutant.

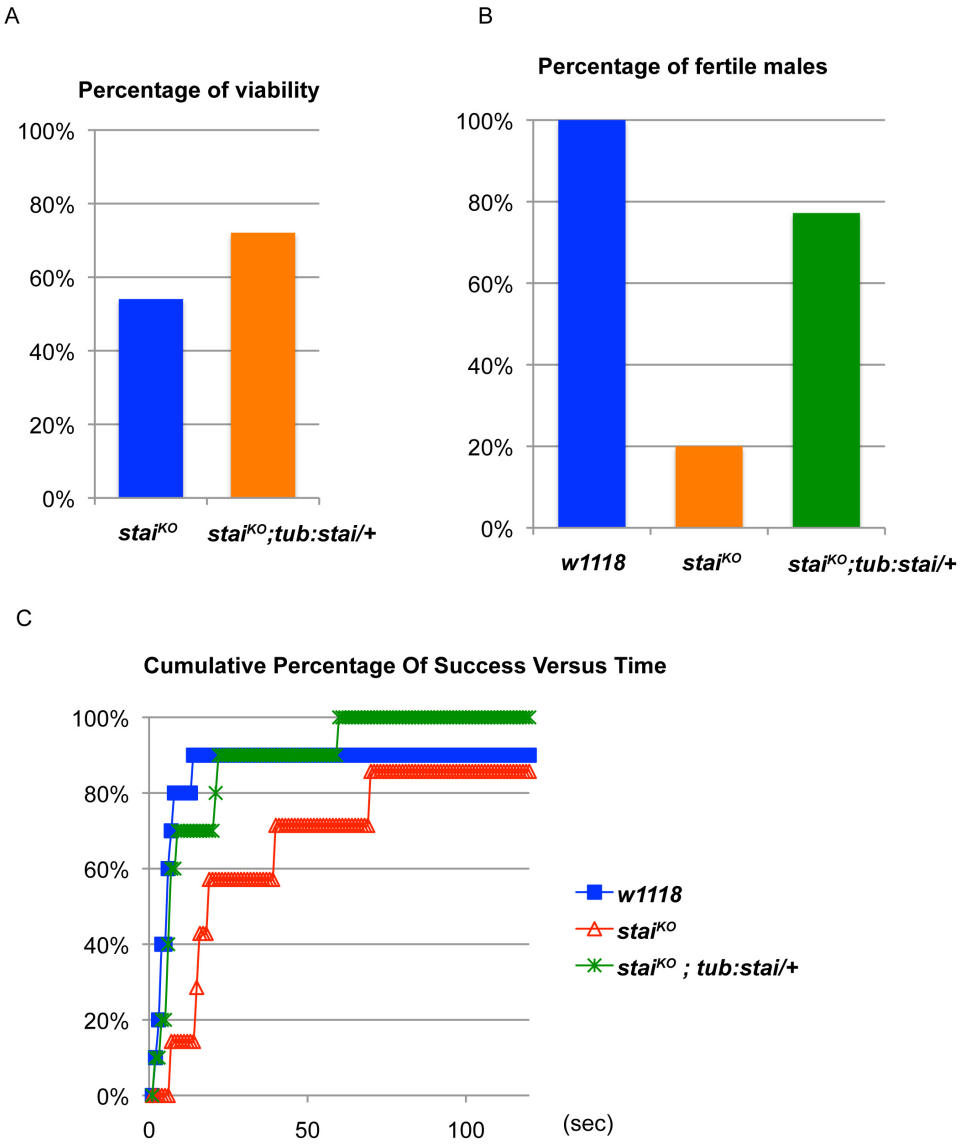

Figure 2. 13 Overall phenotypes of *stathmin*^{KO} mutant animals

(Details see in Material and Methods 4.3-4.5)

(A) Viability assay.
Shown is the quantification of percentage of viable flies. At least 82 F1 progenies were scored for each genotype as indicated.

(B) Fertility assay.
Shown is the quantification of percentage of fertile male flies. At least 10 male flies were analyzed for each genotype indicated.

(C) Climbing assay.
Shown is the cumulative success rate for each genotype as indicated; 7<n<10.

Ubiquitous-expression of *stai* in all tissues largely rescues the phenotype.

2.3.3 Roles of Stathmin in border cells

2.3.3.1 Effects of *stathmin*^{KO} on microtubules

As the *stai*^{KO} homozygous mutant flies are viable, I was able to directly dissect the mutant females' ovaries to analyze border cell migration. Note that in addition to the high expression level in border cells; Stathmin is also expressed in nurse cells, making it possible that it functions in both cell types.

I first checked whether microtubules in border cells are affected. The gross organization and level of microtubules in border cells from *stai*^{KO} homozygous mutant ovaries appeared to be normal both before and during migration (Figure 2.14). This indicates Stathmin does not play a major role in microtubule destabilization in border cells.

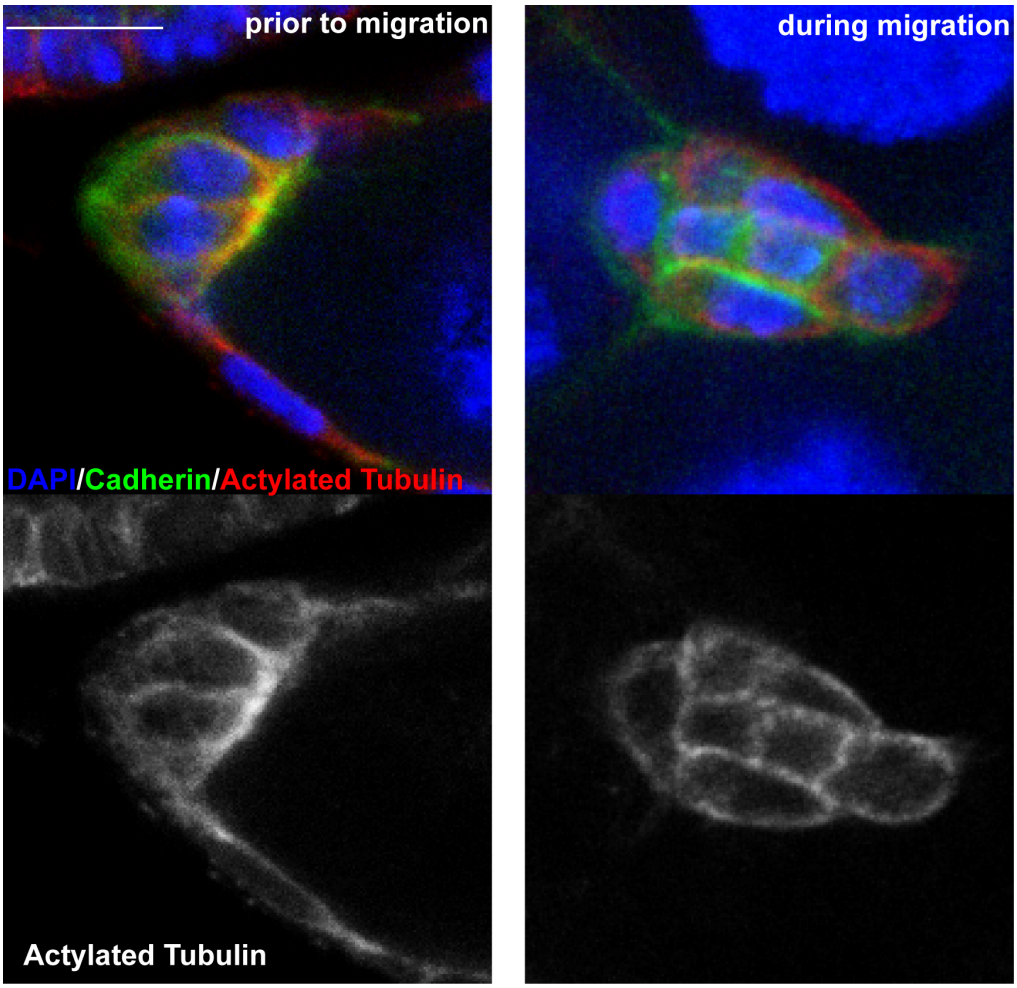

Figure 2. 14 Effects of *stathmin*^{KO} on microtubules

Organization of stable microtubules in *stathmin*^{KO} mutant border cell cluster prior to (left panel) and during migration (right panel). Cell nuclei are marked by DAPI (blue) and cell membrane is marked by DE-cadherin (green). Stable microtubules are marked by anti-acetylated Tubulin staining (red in top merge panel and white in bottom panel). (Scale bar: 10μm).

2.3.3.2 Effects of *stathmin*^{KO} on border cell migration

In addition to *stai*^{KO} mutant ovaries, I also generated *stai*^{KO} mutant border cell clones to analyze the autonomous effect. I first scored border cell migration phenotype from a number of fixed samples. At stage 10, when wild type border cells have finished migration, most of the *stai*^{KO} mutant border cells managed to reach the oocyte, indicating Stathmin is not essential for border cell migration (Figure 2.15 A). However, when I analyzed stage 9 egg chambers when border cells are still in the course of migration, I found a migration phenotype. In both *stai*^{KO} border cell clones and *stai*^{KO} border cells from *stai*^{KO} mutant tissue, there was a significant percentage of egg chambers showing border cell migration delays compared to that of control (Figure 2.15 B), indicating Stathmin does have a regulatory role in border cell migration. Therefore I decided to pursue further to characterize Stathmin's regulatory function in border cell migration.

To investigate the cause of the migration delay in stage 9, I performed live imaging experiments of *stai*^{KO} border cells and analyzed the movies as described. *Stai*^{KO} mutant egg chambers showed similar initiation competency as compared to wild type control (Figure 2.15 C), however after initiation, the mutant clusters migrate a bit slower with reduced net cluster speed (Figure 2.15 D). I confirmed that this effect was due to lack of Stathmin, as the reduction of cluster speed can be rescued by *tubulin-stathmin*, which restores the expression of the *stathmin* cDNA transgene in the mutant tissue (Figure 2.15 D).

Therefore the mild migration delay seen from the fixed sample analysis of *stai*^{KO} mutant ovaries at stage 9 (Figure 2.15 B) was at least partly due to the less efficient migration of the *stai*^{KO} mutant clusters rather than an initiation delay.

Stai^{KO} mutant border cell clones in *stai*^{KO} heterozygous mutant background display different phenotypes: the mutant border cell clusters did not initiate migration as efficiently as control (Figure 2.15 C), however, once the mutant cluster had initiated migration, they migrate as effectively as control (Figure 2.15 D). This is again due to lack of Stathmin, because the defect of inefficient initiation of migration can be rescued upon restoring the expression of Stathmin using a cDNA transgene in the border cells (Figure 2.15 C). The reduced rates of initiation of migration in *stai*^{KO} mutant border cell clones may contribute to the observed migration delay phenotype from fixed sample studies at stage 9 (Figure 2.15 B).

A

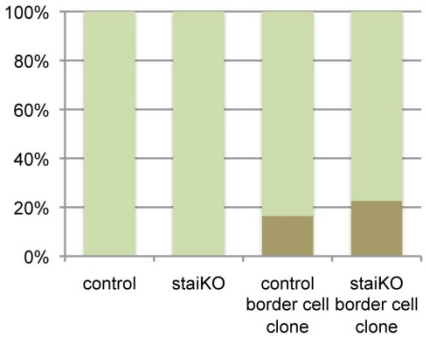
Border cell migration delay at stage 10
100%
80%
60%
40%
20%
0%
control
staiKO
control border cell clone
staiKO border cell clone

B

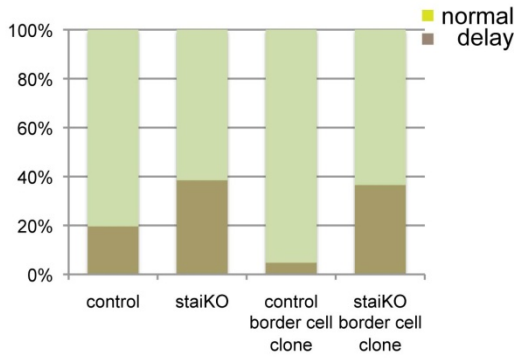
Border cell migration delay at stage 9
normal
delay
100%
80%
60%
40%
20%
0%
control
staiKO
control border cell clone
staiKO border cell clone

C

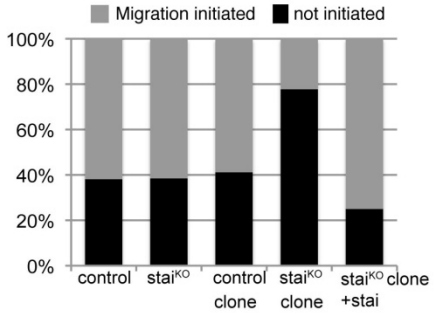
Migration initiated
not initiated
100%
80%
60%
40%
20%
0%
control
staiKO
control clone
staiKO clone
staiKO +stai clone

D

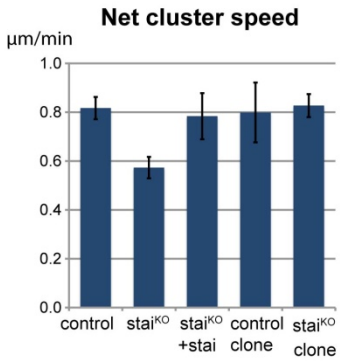
Net cluster speed
µm/min
1.0
0.8
0.6
0.4
0.2
0.0
control
staiKO
staiKO +stai
control clone
staiKO clone

Figure 2. 15 Effects of *stathmin*^{KO} on border cell migration

(A) Quantification of percentage of stage 10 egg chambers with migration delay. Stage 10 egg chambers were scored from fixed samples.
Genotypes are indicated below:
Control: border cells from egg chambers with genotype of *slboGal4,10xGFP/+*
stai^{KO}: border cells from egg chambers with genotype of *stai*^{KO}
control border cell clone: GFP negatively labelled border cell clones in egg chamber with genotype of
hsFLP/+;FRT40/FRT40,ubiqutin-GFP
stai^{KO} border cell clone: GFP negatively labelled border cell clones in egg chamber with genotype of
hsFLP/+;stai^{KO}*,FRT40,FRT42/FRT40,ubiquitin-GFP*
20<n<120

(B) Quantification of percentage of stage 9 egg chambers with migration delay. Mid-late stage 9 egg chambers were scored from fixed samples.
Genotypes for control and stai^{KO} as indicated in (A). Additional genotypes are indicated below:
Control: border cells from egg chambers with genotype of
control border cell clone: GFP positively labelled border cell clones in egg chamber with genotype of
hsFLP/+;FRT40,FRT42/FRT40,Gal80;slboGal4/10xGFP
stai^{KO} border cell clone: GFP posotively labelled border cell clones in egg chamber with genotype of
hsFLP/+;FRT40,stai^{KO}*,FRT42/FRT40,Gal80;slboGal4/10xGFP*
For stai^{KO}, 26 border cell clusters from stai^{KO} egg chambers and 219 stai^{KO} border cell clones were scored. For the control, 56 border cell cluster from control egg chambers and 105 control border cell clone clusters were scored. The comparison between control border cell clone versus stai^{KO} border cell clone was statistically significant with P<0.001 using Fisher's exact test.

(C) Quantification of percentage of border cells that succeed in initiation of migration as analyzed in Figure 2.7. Genotypes as indicated in B except for stai^{KO}+stai, of which the genotype of the egg chamber is *stai*^{KO}*; tub-stai/+*. The comparison between control clone versus stai^{KO} clone is statistically significant with P<0.05 using two-tailed Fisher's exact test. At least 13 movies were analyzed for each genotype.

(D) Quantification of net cluster speed from migrating border cell clusters. Genotypes as indicated in B. For stai^{KO}, 11 stai^{KO} egg chambers and 10 stai^{KO} border cell clones were analyzed. Only the comparison between control and stai^{KO} is statistically significant with P<0.05 using two-tailed student t-test.

Therefore, the delay in migration at a specific stage in both fully mutant egg chambers and border cell mutant clones appeared to reflect two roles, one at initiation of migration, where Stathmin acts in border cells, and another during migration where Stathmin likely functions in the nurse cell substrate. The defects in whole tissue could be due to disruption of Stathmin in nurse cells or a combined effect of loss of Stathmin in both nurse cells and border cells. This is similar to what was observed with severe disruption of microtubules as shown in previous session: differences in disrupting microtubules in whole tissue versus in border cells alone. However, as *stathmin* is a negative regulator of microtubules, knocking out this gene in border cells would take away a mode of negative regulation, causing a different effect as compared to nocodazole treatment. Interestingly, the unexpected absence of initiation delay in $stai^{KO}$ mutant tissue as compared to $stai^{KO}$ border cell clones indicates that effects on border cells and the substrate nurse cells are not simply additive, but may sometimes be compensatory.

2.3.3.3 Effect of *stathmin*^{KO} on extension profiles of border cells

During migration, *stai*^{KO} mutant border cell clusters from *stai*^{KO} mutant egg chambers (stai, in Figure 2.16 A) have increased number of back and side extensions, and this can be rescued by restoring the expression of a *stathmin* cDNA transgene in the whole tissue (Figure 2.16 A). However, this alteration of extensions was not observed in *sta*^{KO} mutant border cell clones (stai^{KO} clone, in Figure 2.16 A), indicating Stathmin may play a non-cell autonomous effect in the nurse cell substrate to regulate extensions. *Stai*^{KO} mutant border cell clones, however, display another phenotype: an increased frequency of non-resolved extensions from the back cell of the *stai*^{KO} mutant border cells clone during initiation of migration (Figure 2.16 B). About 25% of *stai*^{KO} mutant border cell clones retained an attachment to the anterior epithelium for a long period and this extension from the back cell was persistently present during the two-hour imaging period and did not get resolved (see Figure 2.16 B). This was rarely observed in wild type clusters (Figure 2.16 B). The attached clusters migrated slower than the free clusters, indicating the non-resolving extensions from the back cell exerted pulling force or drag that counteracted and interfered with the migrating cluster (Figure 2.16 C). The attached clusters were not included in the calculation of net cluster speed and the extension profiles (Figure 2.15 D and Figure 2.16 A). Therefore, the migration delay scored from fixed sample analysis in which whether back attachments were present or not was not considered (Figure 2.15 B),

could be due to a combined effect: the inefficient initiation of migration of *stai*^{KO} mutant border cell clusters and the attached clusters that migrate less effectively. Overall, Stathmin apparently functions in both border cells and nurse cells; in a way that affects border cell movement: at initiation, Stathmin is required in the border cell to promote effective detachment from anterior epithelium. During migration, the presence of Stathmin appears to have a non-autonomous effect to regulate extensions from border cells.

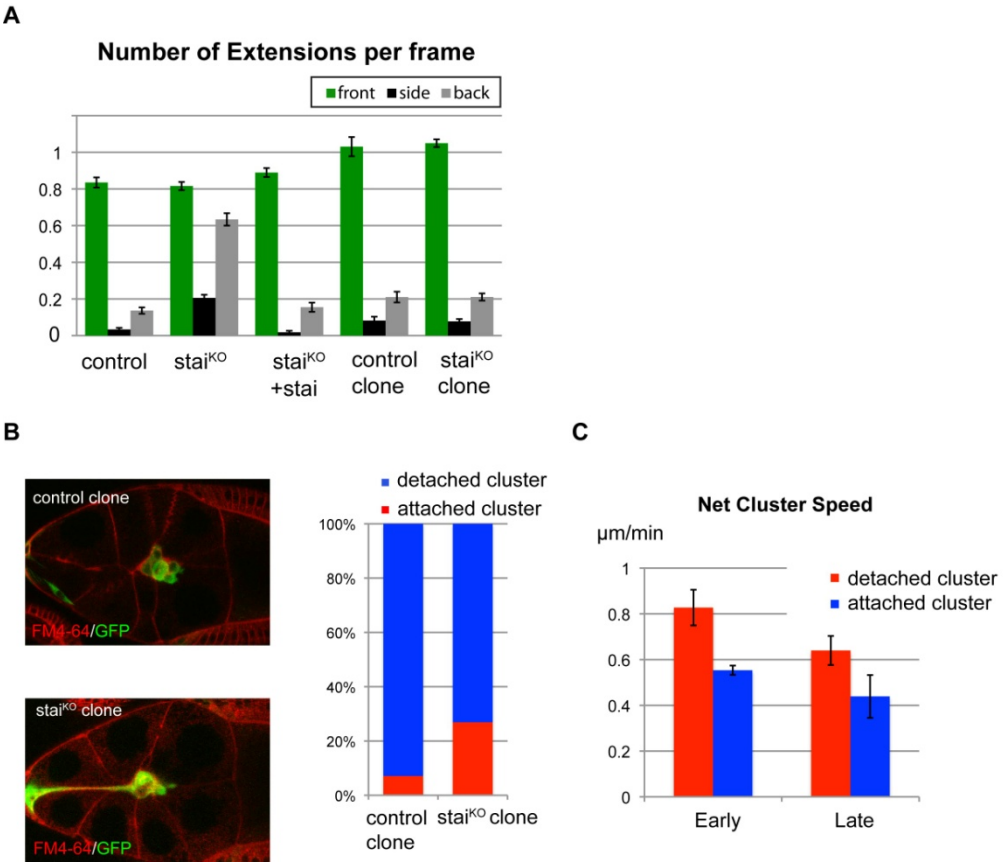

Figure 2. 16 Effect of *stathmin*^{KO} on extension profiles of border cells

(A) Quantification of number of extensions as presence per frame from migrating clusters.
For control, total number of extensions analyzed is 388 from control and 195 from control border cell clones. For stai^{KO}, 792 extensions from stai^{KO} and 465 from stai^{KO} border cell clones were analyzed. Only comparisons of back and side extensions between control and stai^{KO} are significant with $P<0.001$ using two-tailed student t test. Genotypes are as indicated in Figure 2.15 B.

(B) Non-resolved extension phenotypes in stai^{KO} border cell clones.
(Left panel) Selected images of control and stai^{KO} border cell clones at comparable migration path from live imaging movies. Border cells were marked with GFP (green) and membrane of the egg chamber was marked by a lipophilic marker FM4-64 (red). After two hours of imaging, the back cell from the stai^{KO} border cell cluster still retained an extension connected with anterior epithelium. The frequency of such attached cluster was quantified (right panel). Genotypes are as indicated in Figure 2.15 B.

(C) Quantification of net cluster speed from border cell clusters at both early and late phase of migration.
$P<0.05$ for detached cluster versus attached cluster in both phases. Two-tailed student t-test was used. A total of 26 movies were analyzed. Genotypes are as indicated in Figure 2.15 B.

2.4 Systematic screen of microtubule regulators and motors

Disrupting microtubules have clear consequences in border cell migration, yet the phenotype of *stai*^{KO} mutant border cells are quite subtle. As Stathmin is only one of many microtubule regulators, I decided to perform a systematic screen of a larger set of microtubule regulators for their potential roles in border cell migration. These 67 genes encode known or potential microtubule regulators, which include microtubule motors and their interacting proteins; regulators for microtubule organization; regulators of microtubule dynamics such as microtubule severing proteins and microtubule polymerization/depolymerization promoters. A full list is given in Table 2.1.

2.4.1 Screen schemes

For genes that have mutant alleles available, border cell migration was analyzed in either homozygous mutant ovaries (for viable mutations) or border cell mutant clones (for lethal mutations). For the genes which have no mutant alleles available, border cell migration was analyzed in clusters expressing transgenic RNAi constructs to knock down expression of the gene product. One or two RNAi lines were used per gene. RNAi expression was induced in all follicle cells using the actin-Gal4 driver with a flipout cassette (AFG) several days prior to analyzing of border cell migration. Past experiments done in the lab had shown that the border cell specific driver SlboGal4 only induced overt

phenotypes for a small subset of genes known to be important for border cell migration, with protein levels only decreased significantly after migration was well underway. This was also demonstrated by the inefficient depolymerization of microtubules by over-expressing spastin using SlboGal4 in early stage as shown in Figure 2.10 A. Therefore, to provide strong and robust expression of the RNAi transgene both prior and during migration, AFG was used.

2.4.2 Screen results

Border cell migration was scored by comparing the position of border cells with follicle cells at mid-late stage 9 or at stage 10. Generally, border cells lagging behind the anterior end of retracting follicle cells by at least one nurse cell is scored as a migration delay. For RNAi-mediated knockdown, at least100 egg chambers were scored for each genotype. From the total 67 genes screened, only 4 genes had a border cell migration phenotype upon generation of RNAi mediated knockdown or loss-of-function mutants (Figure 2.17 and Table 2.1).

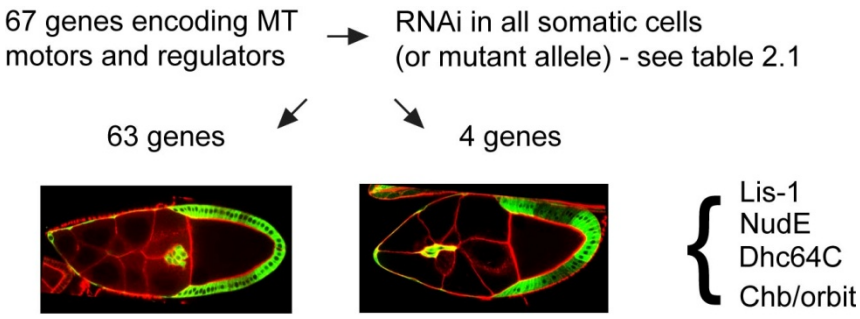

Figure 2. 17 Summary of the screen to identify microtubule regulators important for border cell migration

RNAi expressing cells are marked with GFP. The egg chamber membrane is marked with FM4-64 (red).

Table 2.1: Full list of genes included in the screen

Flybase ID	Gene	Function	Alleles	RNAi lines	Migration
FBgn0032390	*dgt2*	MT nucleator		Trip.HM04038	normal
FBgn0034569	*dgt3*	MT nucleator		v103624	normal
FBgn0026085	*dgt4*	MT nucleator		v108969	normal
FBgn0033740	*dgt5*	MT nucleator		v13788	normal
FBgn0039638	*dgt6*	MT nucleator		105330	normal
FBgn0026431	*Grip75*	MT nucleator		v106044	normal
FBgn0032705	*Grip71*	MT nucleator		v103377	normal
FBgn0026432	*Grip163*	MT nucleator		v108586	normal
FBgn0026430	*Grip84*	MT nucleator		v105640	normal
FBgn0001612	*Grip91*	MT nucleator		v2983	normal
FBgn0027500	*spd2*	MT nucleator		v101882	normal
FBgn0036059	*nudE*	MT minus end anchor		v29788	**delay**
FBgn0027066	*Eb1*	MT aseembly promoter		v106233	normal
FBgn0027948	*msps*	MT aseembly promoter		v21982	normal
FBgn0020503	*CLIP-190*	MT aseembly promoter		v107176	normal
FBgn0004379	*Klp67A*	MT disassembly promotor		v108852 Trip.JF02701	normal
FBgn0022085	*ssp4*	MT severing		v108927	normal
FBgn0039141	*spastin*	MT severing	*spas5*$^{.75}$	v108739	normal
FBgn0040208	*katanin 60*	MT severing		v106487	normal
FBgn0259108	*futsch*	MT stabilizing	*futsch*^{K68}	v6973	normal
FBgn0004378	*Klp61F*	MT bundling		v109280	normal
FBgn0021760	*chb*	MT stabilizing	*chb*^{S068607}	v108620 v26051	**delay**
FBgn0013733	*short stop*	MT stabilizing	*shot*^{3}		normal
FBgn0040232	*cmet*	MT stabilizing		v35081	normal
FBgn0005316	*mud*	MT stabilizing	*mud*^{4}		normal
FBgn0026620	*D-tacc*	MT stabilizing		v101439	normal
FBgn0015754	*Lis-1*	MT stabilizing	*Lis-1*$^{G10.14}$	v106777 v6216	**delay**
FBgn0028902	*tektin-A*	MT stabilizing		v101714	normal
FBgn0035638	*tektin-C*	MT stabilizing		v100094	normal
FBgn0029687	*Vap-33-1*	MT stabilizing	*Vap-33-1*^{47}	v100809	normal
FBgn0041174	*Vhl*	MT stabilizing		v108920	normal
FBgn0022959	*yps*	MT assembly promoter		v27473 v27472	normal normal
FBgn0000150	*awd*	MT binding		v33198	normal
FBgn0001108	*Glued*	Dynein binding		v3785	normal
FBgn0001308	*Khc*	MT plus-end motor	*Khc*^{27}	v44337	normal
FBgn0000140	*asp*	MT associated		v2911 v2910	normal
FBgn0040233	*cana*	MT plus-end motor		v107714	normal
FBgn0000352	*cos*	MT motor	*cos*^{5}	v108914	normal
FBgn0011606	*Klp3A*	MT plus-end	*Klp3A*$^{mei-352}$	v104682	normal

		motor			
FBgn0001612	*l(1)dd4*	MT minus-end binding		v104667 v2983 Trip.JF01719	normal
FBgn0002924	*ncd*	MT minus-end motor	*ncd*^{D}		normal
FBgn0004374	*neb*	MT motor		v108138	normal
FBgn0002948	*nod*	MT plus-end binding	*nod*^{a}	v48148	normal
FBgn0011692	*pav*	MT motor		v46134	normal
FBgn0003545	*sub*	MT motor		v18754	normal
FBgn0003654	*sw*	MT motor		v101559	normal
FBgn0034155	*unc-104*	MT motor		v23464 v47171 v23465	normal
FBgn0014133	*bif*	MT binding		v109722	normal
FBgn0000256	*capu*	MT binding	*capu*^{EE}	v34278	normal
FBgn0032210	*CYLD*	MT binding		v101414	normal
FBgn0004167	*kst*	MT binding		v37074	normal
				v37075	normal
FBgn0013726	*pnut*	MT binding		Trip.JF02792	normal
FBgn0003475	*spir*	MT binding		v107335	normal
FBgn0250788	*β Spectrin*	MT binding		v42054	normal
FBgn0004380	*Klp64D*	MT motor		v45373	normal
FBgn0086362	*spn-F*	MT minus-end motor		v103358 v107850	normal
FBgn0260991	*Incenp*	MT binding		v101123	normal
				v17044	normal
FBgn0033687	*CG8407*	MT motor		v100696	normal
FBgn0019968	*Khc-73*	MT motor		v105984	normal
FBgn0035800	*CG7716*	MT nucleation		v24225 v104217	normal
FBgn0004381	*Klp68D*	MT motor		v101058	normal
FBgn0038205	*Kif19A*	MT motor		v106569	normal
FBgn0030268	*Klp10A*	MT motor		v41534	normal
FBgn0026141	*Cdlc2*	MT motor		v42113	normal
FBgn0011760	*ctp*	MT motor		v109084	normal
FBgn0034824	*Klp59C*	MT motor		v109829	normal
FBgn0052371	*CG32371*	MT binding		v106233	normal
FBgn0261797	*Dhc64C*	MT minus end motor	*Dhc*$^{4-19}$	Trip.JF03177	**delay**
FBgn0001316	*klar*	MT attachment	*klar*^{1}		normal

Each gene is presented with its synonyms and functions. The unique Flybase identification number (ID) was shown on the left of each gene. Mutant alleles include characterized amorph and hypomorph alleles or based on mutant phenotypes associated with as reported in other system. RNAi lines starting with v are VDRC stock number; RNAi lines staring with Trip are TRiP line numbers from Trip Harvard Medical School. Mutants showing border cell migration delay are highlighted in bold.

2.4.2.1 *Chb*

Chromosome bows (*Chb*), also known as *Orbit/Mast*, is the *CLASP* orthologue of *Drosophila* (Lemos et al. 2000). CLASPs are conserved class of microtubule binding proteins that associate with microtubule plus-end and regulate its stability (Bratman and Chang 2008). *Drosophila* CLASP had been shown to regulate microtubule bundling which is important for persistent motility and contact repulsion in *Drosophila* macrophages in vivo (Stramer et al. 2010). Border cell clones for a hypomorphic allele of *Chb* showed some migration delay (Figure 2.18 A and B). I tried to further verify the migration delay phenotype in *Chb* null clones; however, I was not able to get generate any null clones, indicating *Chb* may be essentially required for cell viability and/or growth in follicle cell epithelium. I also tested the effects of two single RNAi lines by live imaging analysis, which had apparent no effects in the net cluster speed from an average of 10 movies analyzed. To push this further, I tried to combine the two RNAi lines together to achieve an increased knock down and found the net cluster speed was reduced slightly, but not statistically significant (Figure 2.18 C). Therefore, the function of this gene in border cell migration was not pursued further.

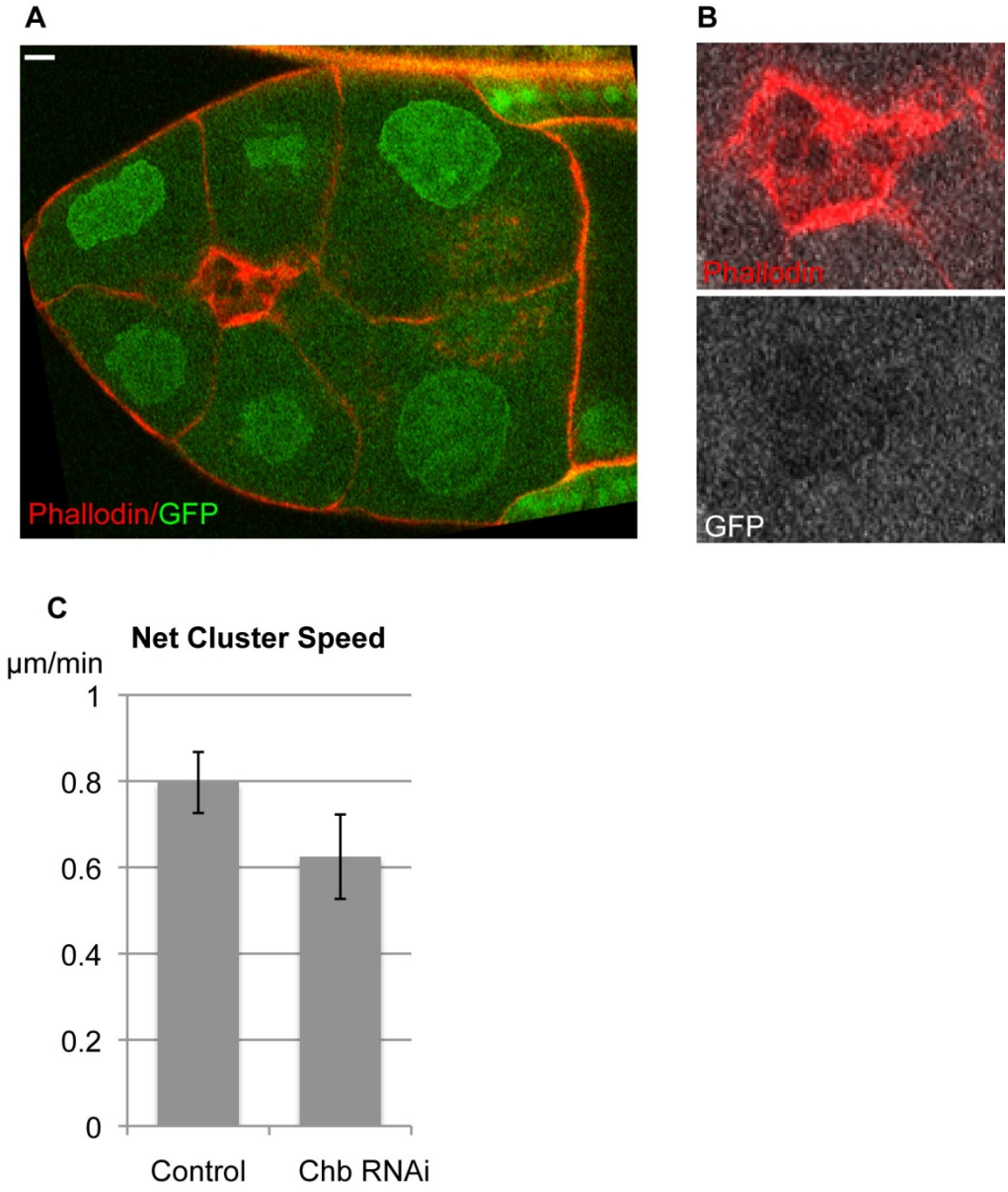

Figure 2. 18 Effects of *Chb* on border cell migration

(A) Border cell migration delay of *Chb* hypomorph clone. Phallodin stained actin (red) and mutant clones were marked by the absence of GFP (green). Border cell cluster with 2X zoom in was displayed in (B) and the GFP image was shown in white. Genotype of egg chamber is *hsFLP; chb*^{1}*, FRT80/ubiquitinGFP, FRT80*. In total 8 *Chb* hypomorph clones were scored and 6 displayed migration delay. Scale bar: 10µm.

(C) Quantification of net cluster speed. Genotypes are *hsFLP/w1118; AFG,10xGFP/+* for control and *hsflp/w1118; chb*^{v108620}*/chb*^{v26051}*; AFG,10xGFP/+* for *Chb* RNAi. n=14.

2.4.2.2 *Lis-1, nudE and Dhc64C*

Depletion of three other genes, namely the *Lis-1*, *nudE*, and *cytoplasmic Dynein heavy chain 64C* (*Dhc64C*) caused border cell migration delay (Figure 2.19). Lis-1 and NudE are Dynein interactors that form a complex. The Lis-1/NudE complex binds to cytoplasmic Dynein and help it to process large load cargos, such as nuclei, centrosomes or entire microtubules (McKenney et al. 2010). This high-load regulatory mode of cytoplasmic Dynein is important for nuclei movement, microtubule organization and cell migration (Dujardin et al. 2003; Vallee et al. 2012). Finding that all the three genes produced border cell migration delay, whereas downregulation of most other microtubule regulators had not effect (Table 2.1) suggests that this cooperating protein complex has an important role in border cell migration.

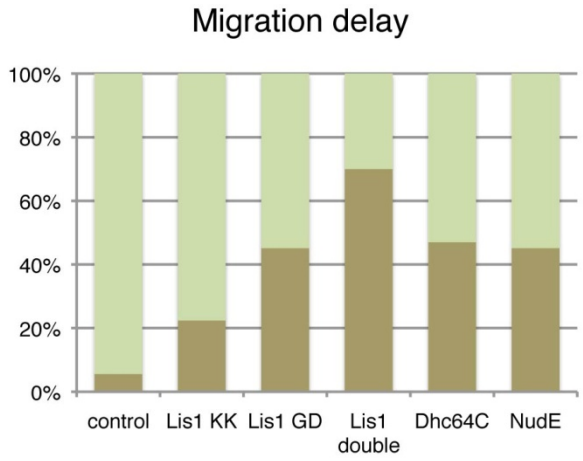

Figure 2. 19 Effects of *Lis-1*, *nudE* and *Dhc64C* RNAi on border cell migration

Quantification of percentage of mid-late stage 9 egg chambers with migration delay from fixed sample analysis. About 100 egg chambers were scored for each genotypes as indicated below:
Control: *hsFLP/w1118; AFG,10xGFP/+*
Lis-1KK: *hsFLP/w1118; Lis-1KK^{108813}/+;AFG,10xGFP/+*
Lis-1GD: *hsFLP/w1118;Lis-1GD^{1480}/AFG,10xGFP*
Lis-1 double: *hsFLP/w1118;Lis-1 RNAi (KK^{108813})/+;Lis-1 RNAi(GD^{1480})/10xGFP*
NudE: *hsFLP/w1118; nudE(GD^{29788})/AFG,10xGFP*
Dhc64C:*hsFLP/w1118,Dhc64C RNAi (TripJF^{03177})/AFG,10xGFP*
All comparisons of RNAi to control are statistically significant using two-tailed Fisher's exact test. P values were all below 0.001 with the exception of Lis-1KK that has a P value<0.05.

2.5 Probing the functions of the Lis-1/NudE/Dynein complex in border cell migration

2.5.1 The Lis-1/NudE/Dynein complex is required in both polar cells and outer border cells for border cell migration

While this work was underway, the other researchers reported that the Dynein complex functions in the polar cells for polarized localization of the cytokine Upd (Van de Bor et al. 2011). Upd in turn, is important for border cell fate specification through activation of the JAK/STAT pathway. This could in principle explain the observed border cell migration delay phenotypes because the RNAi is expressed in all the cells in the border cell cluster including the two polar cells. To investigate whether the observed migration delay phenotype was solely caused by a dysfunction of the complex in the polar cells, I checked border cell migration when the RNAi construct is expressed only in polar cells. Using a polar cell specific driver Upd-Gal4 that mediates the knockdown of *Lis-1* RNAi only in polar cells, a much milder border cell migration delay was observed (Figure 2.20 A). The two treatments caused apparently the same strength of defects in cell fate specification, as measured by the number of border cells expressing the cell fate marker Slbo (Figure 2.20 B).

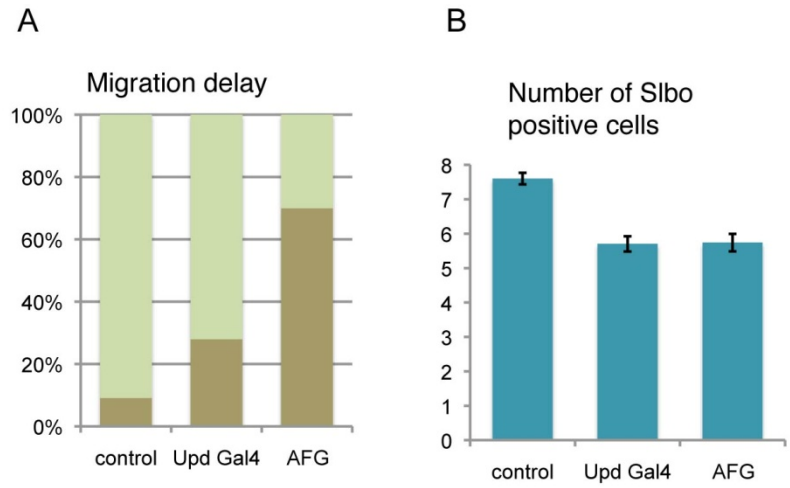

Figure 2. 20 The Lis-1/NudE/Dynein complex functions beyond polar cells

(A) Quantification of percentage of mid-late stage 9 egg chambers with migration delay. Genotypes of egg chambers are:
Control: *hsFLP/+; Lis-1 RNAi (KK^{108813})/+; Lis-1 RNAi (GD^{1480})/ $neur^{A101}$,UAS-RFP*
Upd Gal4: *UpdGal4/hsFLP; Lis-1 RNAi (KK^{108813})/+;Lis-1 RNAi (GD^{1480})/UAS-PHGFP*
AFG: *hsFLP/+; Lis-1 RNAi (KK^{108813})/+;Lis-1 RNAi (GD^{1480})/AFG,10xGFP*
Comparison between UpdGal4 and AFG are statistically significant with $P<0.0001$ using two-tailed Fisher's exact test. At least 91 mid-late stage 9 egg chambers were scored for both Upd and AFG.

(B) Quantification of numbers of slbo positive cells in border cell cluster from egg chambers with genotypes as indicated in (A). For Upd and AFG, at least 27 egg chambers were scored.

Therefore, the strong border cell migration delay phenotype observed in RNAi mediated knock down in all cells by AFG was not solely caused by the defect of cell fate specification, suggesting that Lis-1, NudE and Dynein play additional roles in the outer migratory border cells. To test this, SlboGal4, which drives RNAi expression in outer border cells but not in polar cells was used in a slightly sensitized genetic background with one copy of *slbo* hypomorph allele $slbo^{1310}$ and at 29 ºC to increase Gal4 expression. This led to significant delay of migration from *nudE* RNAi expressing border cell clusters (Figure 2.21). Mild migration delay was observed with *Lis-1* RNAi. Thus the migration defect of knocking down *nudE* and less so with *Lis-1* by SlboGal4 supports a role of the protein complex in outer border cells. The effect of *nudE* RNAi is stronger than that of *Lis-1* and *dynein* with this driver as compared to AFG suggests that NudE might be a more unstable protein or more sensitive to the short term downregulation by SlboGal4.

Nevertheless the migration delay phenotype seen in *nudE* and *dynein* RNAi knock down by SlboGal4 demonstrated the requirement of the two genes in outer border cells, further supporting the idea that the Lis-1/NudE/Dynein complex functions in outer border cells in addition to polar cells in regulating border cell migration.

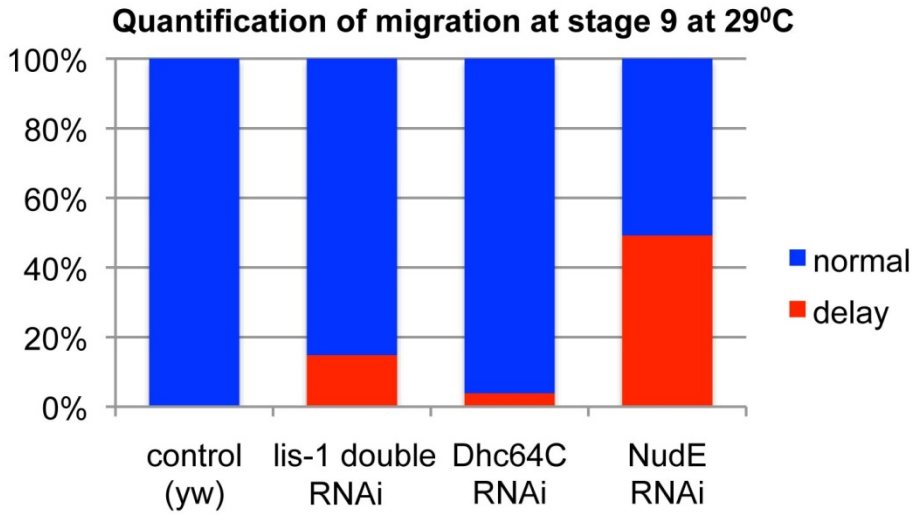

Figure 2. 21 NudE and Lis-1 are required in outer border cells for migration

Quantification of percentage of egg chambers with migration delay at *slbo*^{1310} heterozygous background. *slbo*^{1310} is a *slbo* hypomorph allele and heterozygous of *slbo*^{1310} provides a sensitized genetic background for border cell migration delay. Egg chambers has been kept for 29 degree for two days before analysis. About 100 stage 9 egg chambers were scored from fixed samples for each genotype as indicated below:
Control: *yw/+; SlboGal4,slbo*^{1310}*/+*
Lis-1 double RNAi: *Lis-1 RNAi* $^{(KK108813)}$*/SlboGal4,slbo*^{1310}*; Lis-1 RNAi* $^{(GD1480)}$*/+*
Dhc64C: *SlboGal4,slbo*^{1310}*/+; Dhc64C RNAi* $^{(TripJF03177)}$*/+*
NudE: *SlboGal4,slbo*^{1310}*/+; NudE RNAi* $^{(GD29788)}$*/+*

To test this idea more stringently, I analyzed genetic mosaic clones of complete loss-of-function (null) alleles of *Lis-1* and *Dhc64C*, where I looked for clones in which outer border cells were mutants but none of the polar cells were mutants. Such clones were rare: two were found for *Lis-1* and two were found for *Dhc64C*. In both cases severe border cell migration delay was observed (Figure 2.22). In addition, the few mutant border cells were found located at the back of the migrating cluster (see arrow in Figure 2.22 right panel), a hallmark of mutations that specifically affect migratory cells. Therefore, I conclude that Lis-1, NudE and Dynein together perform a critical function in outer border cells and that RNAi-mediated gene knock down can mimic the mutants' effects.

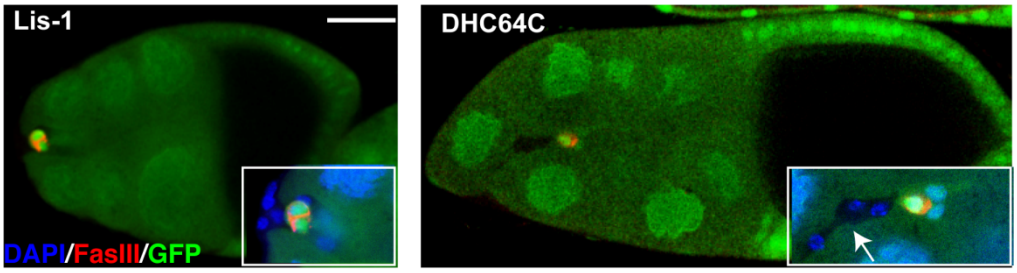

Figure 2. 22 Autonomous requirement of Lis-1 and Dynein in outer border cells for migration

Left panel: Image of a full *Lis-1*$^{G10.14}$ outer border cell clones from a late stage 9 egg chamber with genotype of *hsFLP/+; FRT*^{G13}*,Lis-1*$^{G10.14}$ */FRT*^{G13}*,ubiquitinGFP.*
Right panel: Images of a partial *Dhc64C*$^{4-19}$ outer border cell clones from a stage 10 egg chamber with genotype of *hsFLP/+; Dhc64C*$^{4-19}$*,FRT*^{2A}*/FRT*^{2A}*,ubiquitnGFP.*
Mutant clones are marked by the loss of GFP. Polar cells are marked by FasIII (red). DAPI marks cell nuclei (blue). Regions covering border cells are zoomed in 3X and shown as boxed region on top of the original image on the right hand side. (Scale bar: 30 μm)

2.5.2 Lis-1/NudE/Dynein is strongly required in border cells for initiating migration

From fixed sample analysis, *Lis-1* RNAi mediated knock down caused a strong border cell migration delay, where more than a half of the egg chambers showed no migration at all (Figure 2.23). This lack of migration phenotype was prevalent at a similar penetrance at both stage 9 and stage 10, indicating a complete block of initiation of migration. If knockdown only caused a delay in migration, more clusters would be expected to reach the oocyte by stage 10.

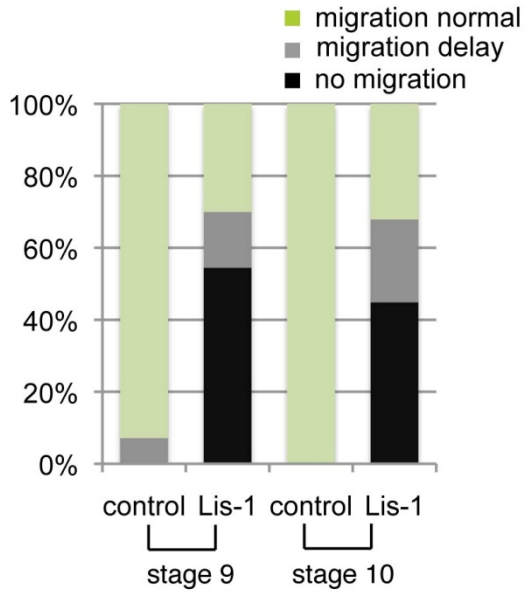

Figure 2. 23 Border cell migration defect upon Lis-1 disruption

Quantification of border cell migration from both stage 9 and stage 10 egg chambers. Genotypes are indicated as below:
Control: *hsFLP/w1118; AFG,10xGFP/+*
Lis-1: *hsFLP/w1118;Lis-1 RNAi (KK^{108813})/+;Lis-1 RNAi(GD^{1480})/AFG, 10xGFP*
13-42 egg chambers were scored for control and 90-133 egg chambers were scored for Lis-1.

To determine why some *Lis-1* knockdown border cell clusters did not initiate migration, I did live imaging analysis and focused on the stage when wild type border cell clusters normally initiate migration. For wild type control clusters, migration was well initiated at early stage 9. The competent cluster has a polarized cell shape with a large prominent forward extension in the leading edge (top panel in Figure 2.24 A). All wild type clusters analyzed showed this behavior. *Lis-1* RNAi knock-down border cell clusters were much more rounded and lacked large extensions at the leading edge (bottom panel in Figure 2.24 A).

The process of the initiation of migration in border cell clusters has been extensively analyzed by Dr. Mikiko Inaki in the lab and she found that invasion did not necessarily take place upon the formation of the first or longest forward extension, indicating this was not the sole determination for initiation. Instead, the initiation of migration was best correlated to the total forward reach of the cluster, which was defined to be the distance between the most anterior tip of the follicle cells and the most posterior tip of the extension (see illustrations in Figure 2.24 A). Initiation of migration occurred when the total reach was on average 49 μm and at least 36 μm (Figure 2.24 D). In *Lis-1* knock down situation, the forward extensions occurred much rarer (Figure 2.24 B) and they were shorter (Figure 2.24 C), making the total reach ranged from 15 μm to 36 μm (Figure 2.24 D). In agreement with the non-migrating phenotype observed from fixed samples, for a total number of 21 movies analyzed, only three *Lis-1* knock down border cell clusters

succeeded in initiation of migration. Those clusters that did initiate migration were three of the five most extended ones; further support the importance of this feature for the initiation of migration (Figure 2.24 D).

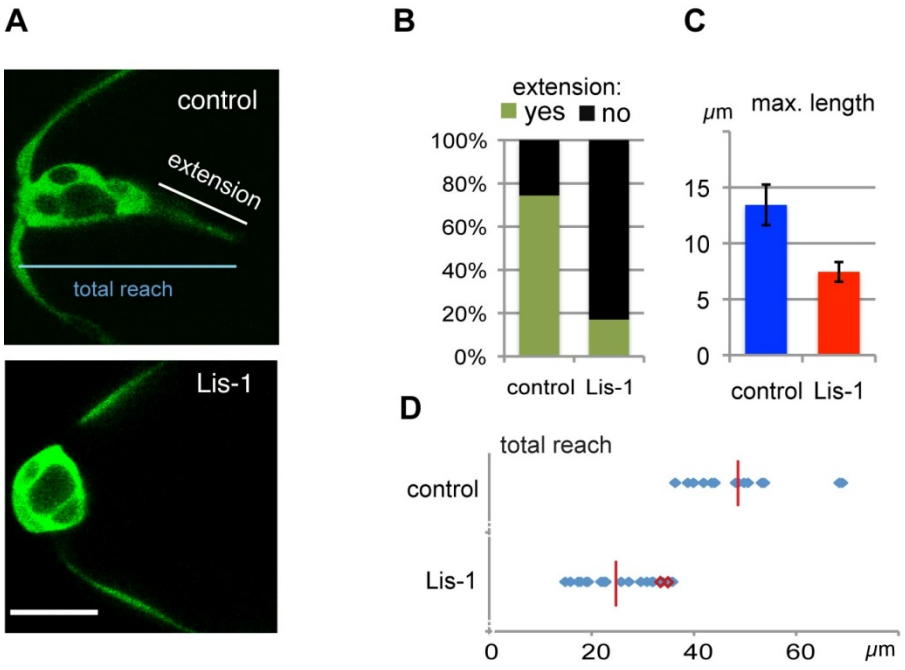

Figure 2. 24 Lis-1 has a strong effect on forward extension in initiation

(A) Still Images from live imaging movies of border cells of (top) control and (bottom) Lis-1 at initiation stage (early stage 9). Border cells are marked by GFP. Genotypes as in Figure 2.23. Scale bar: 20μm.

(B) Quantification of presence of forward extension from two-hour movies of control (n=15) and *Lis-1* RNAi border cells clusters (n=25) during the stage of initiating migration. Genotypes as in A.

(C) Maximum length of extensions were manually identified from movies of early stage 9 control clusters (n=15) and *Lis-1* RNAi clusters (n=25). The difference is statistically significant with $P<0.05$ using two tailed student t-test. Genotypes as in A.

(D) Total forward reach (see A) for control clusters at time of detachment from anterior end (n=15); for *Lis-1* RNAi clusters maximal forward reach in movie, only 3 (red) detach (n=21). Genotypes as in A.

2.5.3 The Lis-1/NudE/Dynein complex is required in border cells during migration

As there were three *Lis-1* knock down escapers that did initiate migration, it allowed me to analyze whether this strong reduction of Lis-1 affected the process of migration as well. As with the initiating clusters, the migrating *Lis-1* knock down clusters formed much fewer forward extensions and their sizes were much smaller (Figure 2.25 A). The number and size of back extensions were also reduced. Border cell specific knock down of *nudE* by RNAi using SlboGal4 showed similar effects (Figure 2.25 A), but not as severe. This indicates that the few *Lis-1* RNAi knock down escapers truly represented the effect of reducing Lis-1 complex. Therefore, the Lis-1/NudE/Dynein complex plays an important role in regulating extensions both for the initiation and the actual process of migration.

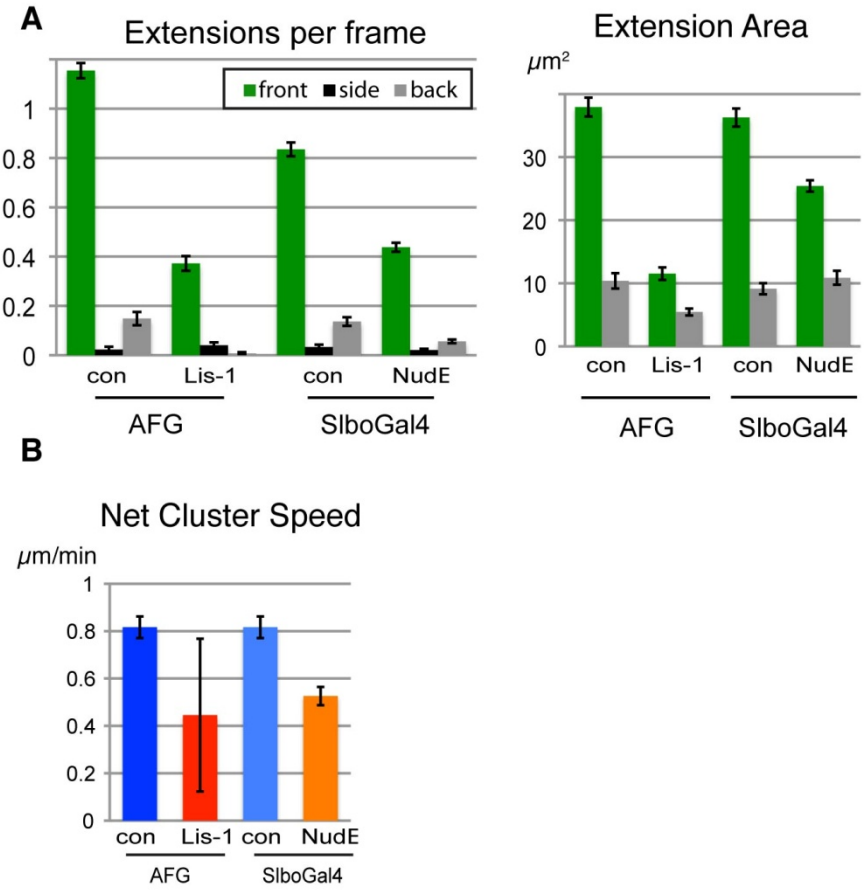

Figure 2. 25 The Lis-1/NudE/Dynein complex is required in border cells during migration

(A) Effects of disrupting Lis-1 and NudE in border cells on (left panel) number and (right panel) size of extensions from movies of migrating border cells. Genotypes for AFG are the same as Figure 2.23; for SlboGal4: *10xGFP/+* (con) and *slboGal4,10xGFP/nudE*^{GD15226} (NudE); n=3 for Lis-1 (escapers) and n=13 for NudE, differences to control are both significant (P<0.01) using two tailed student t-test.

(B) Effects of disrupting Lis-1 and NudE in border cell cluster speed. Quantification of net cluster speed of border cells from egg chambers with genotype as in A.

It has been shown previously that the net cluster speed of wild type border cell clusters was directly correlated with the ability of making and maintaining large forward extensions (Poukkula et al. 2011), thus the severe reduction of the size of forward extensions observed in *Lis-1* knock down border cell clusters would predict a pronounced defect in movement. Indeed, when analyzing the three *Lis-1* knock down escapers, despite a high variation due to the small sample size, the average net cluster speed was much reduced as compared to control (Figure 2.25 B). Border cell specific knock down of *nudE* showed similar effect of reducing the net cluster speed, further confirming that the phenotypes observed were indeed indicative of Lis-1/NudE complex function. Because the *nudE* knock down was only induced in migrating border cells and after their specification, it indicates the effects were within the border cells, i.e. not due to a potential non-autonomous effect from polar cells. In addition, the effects were not an indirect effect of long-term depletion, as could have been for the case with *Lis-1* knock down. Therefore, I conclude that the Lis-1/NudE/Dynein complex functions in border cells to allow the formation of big forward extensions, which in turn, are required for both the initiation of migration and effective cluster movement during migration.

2.5.4 The Lis-1/NudE/Dynein complex is required to maintain the proper organization of a migratory border cell cluster

2.5.4.1 Disrupting Lis-1/NudE/Dynein can affect cell polarity

To better understand the defects in cells with disrupted Lis-1/NudE/Dynein complex, I first checked the apical-basal cell polarity. Apical-basal cell polarity is important for maintaining the proper organization of the follicular epithelium (Tanentzapf et al. 2000) as well as border cell migration (Pinheiro and Montell 2004). It has been shown that strong loss of *dynein* function in follicle cells disrupts both molecular and morphological aspects of apical-basal polarity (Horne-Badovinac and Bilder 2008), however partial block of Dynein activity using combinations of hypomorph alleles or injecting anti-Dhc antibodies failed to produce epithelial polarity phenotypes (Harris and Peifer 2005). Those studies indicate the epithelium cells can tolerate a substantial reduction of Dynein activities (Horne-Badovinac and Bilder 2008). Similar to *dynein*, complete removal of *Lis-1* in follicle cells null mutants resulted in the loss of apical-basal polarity (Figure 2.26 A), whilst a reduction of *Lis-1* by RNAi mediated knockdown did not (Figure 2.26 B). Similarly, microtubule polarity in the *Lis-1* knockdown follicle cells was essentially normal, as revealed from live EB1-GFP tracing (Figure 2.26 C). These results further supported that Lis-1 acts with Dynein in follicle cells, and small amount of Lis-1/Dynein is sufficient to maintain the simple apical-basal epithelial polarity. Thus,

the strong border cell migration phenotype caused by *Lis-1* RNAi mediated knockdown was unlikely to be due to the loss of apical-basal polarity.

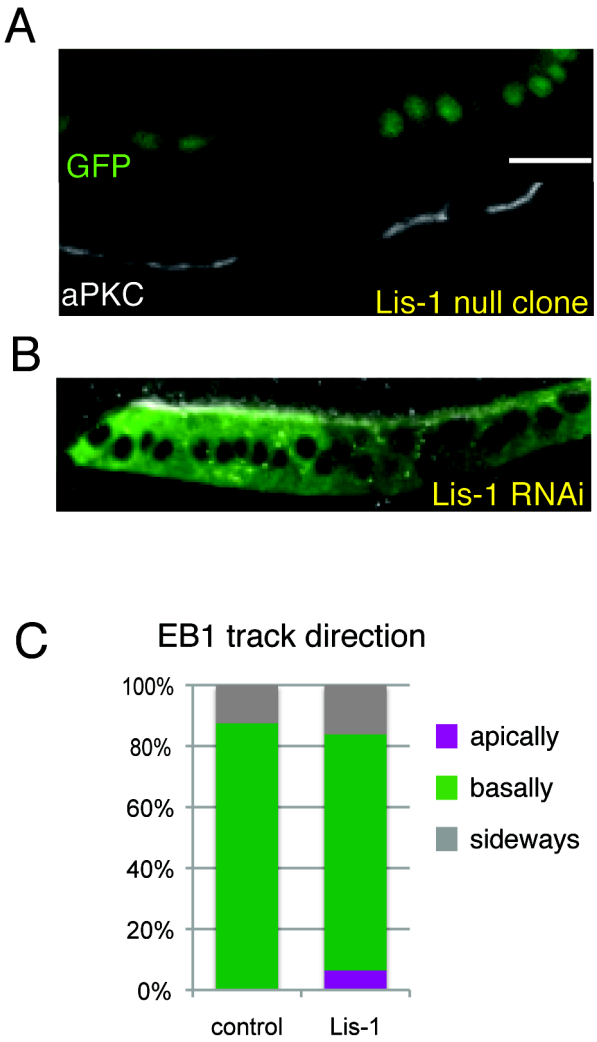

Figure 2. 26 Assaying apical-basal polarity upon Lis-1 disruption

(A-B) Follicle cells from stage 9 egg chambers stained with aPKC (white) in (A) *Lis-1*$^{G10.14}$ clones marked with absence of GFP (green) and (B) Lis-1 expressing cells marked positively with GFP. Scale bar: 5μm.

(C) Quantifications of directions of tracked EB1-GFP comets in control and *Lis-1* RNAi expressing follicle cells. Genotypes: *hsFLP/+; AFG/+, ubiqutin-EB1-GFP, UAS-RFP/+* (control) and *hsFLP/+;AFG/Lis-1*^{KK106777}*, ubiqutin-EB1-GFP,UAS-RFP/Lis-1*^{GD6212} (Lis-1). 16 tracks from control and 31 tracks from *Lis-1* RNAi were analyzed.

2.5.4.2 Disrupting Lis-1/NudE/Dynein affects microtubules and the organization of the border cell cluster

It has been shown that in neuronal cells, disrupting either Lis-1 or Dynein had a dramatic effect on the morphological reorganization of growth cone and interfered with microtubule behavior (Grabham et al. 2007). To determine the role of Lis-1 in microtubule organization in border cells, I first looked at fixed samples. In *Lis-1* knockdown border cells, I observed a mis-localization of microtubules (Figure 2.27 B, C and D). In wild type, prior to migration, all border cell clusters consist of two adjacent polar cells with an apically present MTOC-like structure. The two polar cells align closely with each other and position their MTOC-like structures towards the leading edge, such that they appear as one structure (see previous Figure 2.1 B and 2.2 B). During migration, the two MTOC-like structures get repositioned however they still remain together as the two polar cells are kept close with each other while they are carried along by the migrating outer border cells (see Figure 2.27 A, also refer to previous Figure 2.1 D and Figure 2.2 C).

This prominent type of MTOC-like structure was mostly lost or altered in *Lis-1* knockdown clusters. Instead of being close to each other, two separate foci can be observed in different positions, often far apart (Figure 2.27 B, C and D), they also appeared less focused and more diffuse, sometimes in a belt like structure (Figure 2.27 B, C).

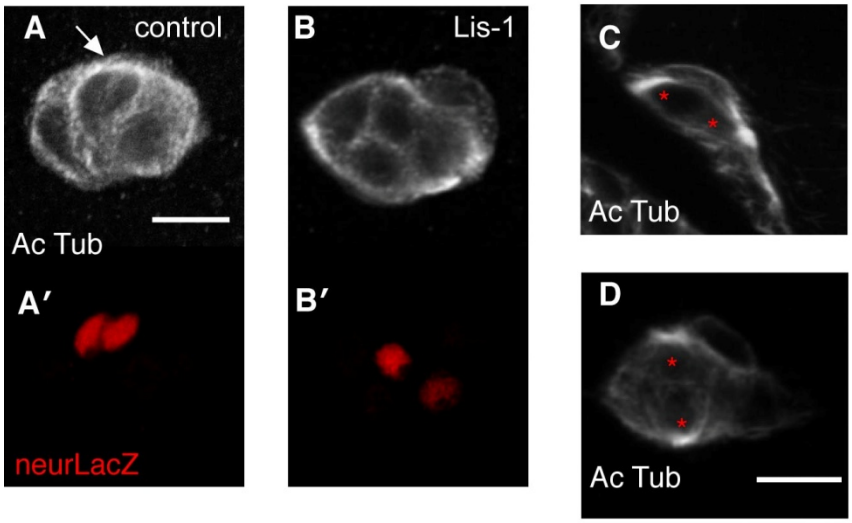

Figure 2. 27 Mislocalization of microtubules upon Lis-1 disruption

Migrating border cell clusters stained with anti-actylated Tubulin (white) and anti-βgal (red) from lacZ in *neur*^{A101} in (A) control and (B) *Lis-1* RNAi knockdown border cell clusters. Arrow points towards the MTOC like structure. Genotypes are *hsFLP/+;AFG/+;UAS-RFP,neur*^{A101} */+* (control) and *hsFLP/+; Lis-1*^{KK108813} */AFG;UAS-RFP, neur*^{A101} */ Lis-1*^{GD1480} (Lis-1). (C) Non-migrated and (D) migrating Lis-1 depleted clusters show similar polar cell displacement. Note also the rotated MTOC-like structure in both. Anti-actylated tubulin (white); red asterisks indicate center of polar cell nuclei, determined as in B; genotype as B. Scale Bars: 20μm.

Microtubule organization was also analyzed by imaging of EB1-GFP in *Lis-1* knockdown clusters. The MTOCs clearly localize abnormally (Figure 2.28 C-F). Prior to migration, there is one area in which the two MTOCs are present in the apical region in the two adjacent polar cells (Figure 2.28 A, Figure 2.29 A and B); these MTOCs later get repositioned when border cell clusters are migrating (Figure 2.28 B and Figure 2.29 C). In *Lis-1* knockdown cluster, however, the MTOCs are frequently mis-localized (Figure 2.28 C and D); in addition, the two polar cells often have their own MTOC independently positioned (Figure 2. 28 E and F).

These prominent defects of microtubule misorganization were observed both in clusters that were unable to initiate migration (Figure 2.27 C, Figure 2.28 C and E), as well as those that did (Figure 2.27 B and D, Figure 2.28 D and F), indicating this defect is not the simple consequence or cause of the lack of migration.

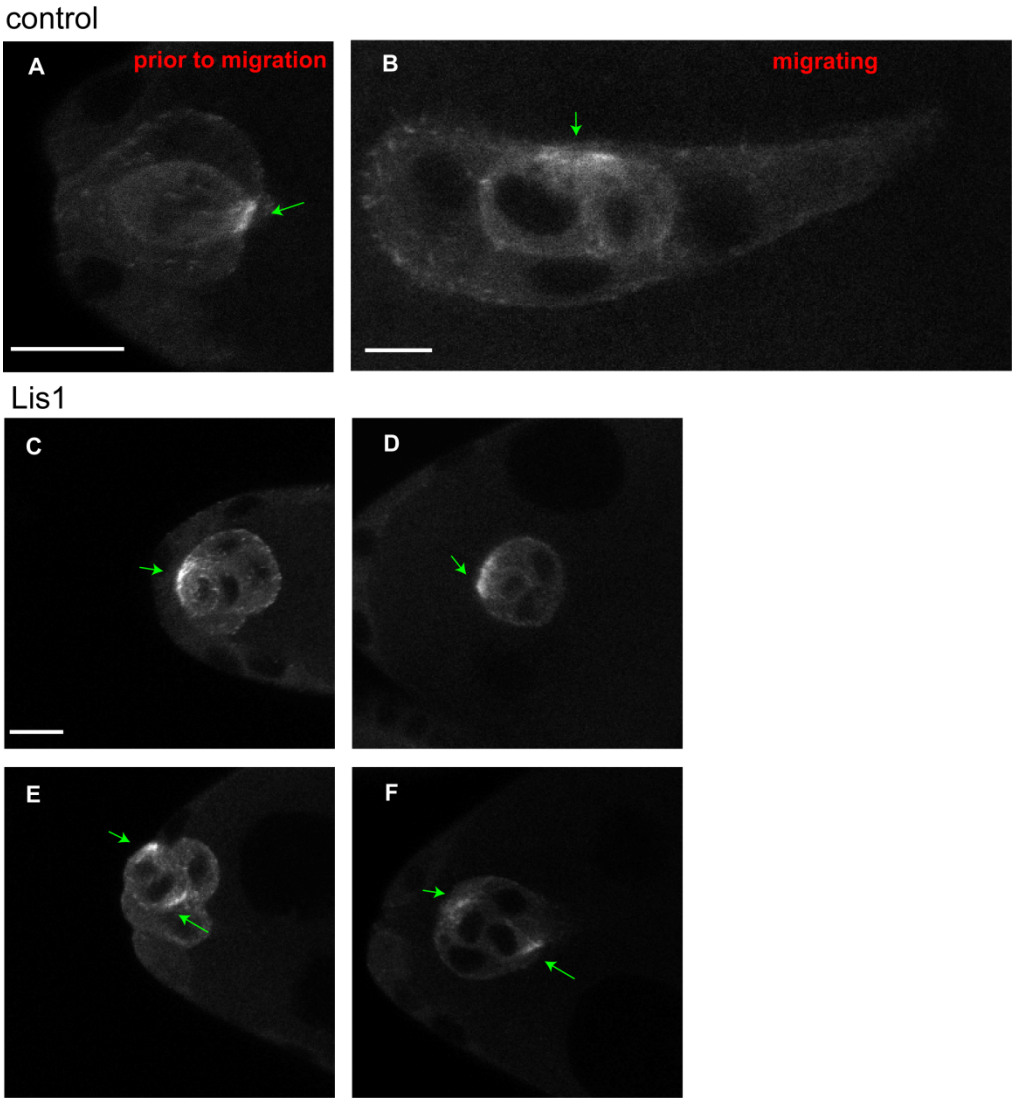

Figure 2. 28 Mislocalizaton of MTOC like structure upon Lis-1 disruption

Still Images of EB1-GFP from live imaging movies of non-migrating (left panel: A,C,E) and migrating (right panel: B,D,F) border cell clusters with genotypes as indicated in Figure 2.26. Green arrows indicate MTOC-like structure. Scale bars: 10μm.

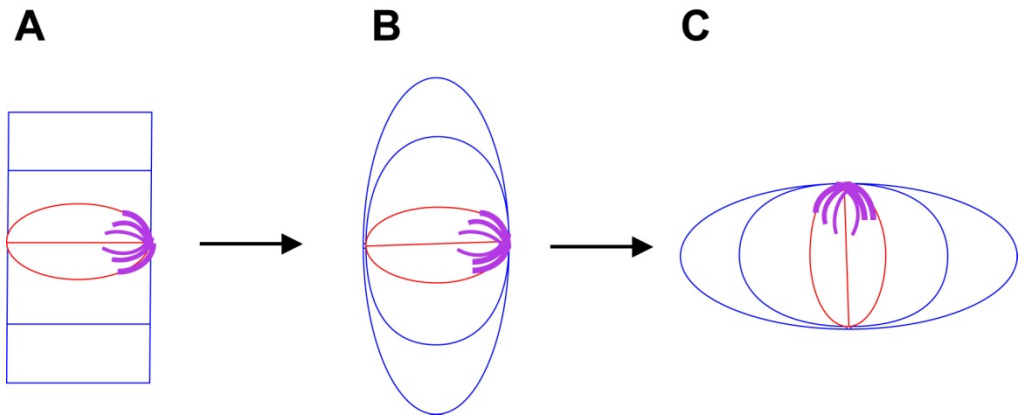

Figure 2. 29 Illustration of MTOC in polar cells at different stage of oogenesis

(A) prior to the formation of border cell cluster
(B) border cell cluster has just been formed
(C) border cell cluster is migrating

Microtubules (magenta) emanate from the two MTOCs in adjacent polar cells (red); outer border cells are marked with blue.

The abnormal localization of polar cell MTOCs in border cell cluster suggested that the polar cells were not correctly localized, i.e. a defect in overall cluster organization. To look at this more specifically, I used a nuclear marker Neuralized (Neur), which is specifically expressed in polar cells. Normally the distance between two polar cell nuclei is in average about 4.03 μm (Figure 2.30 B), close to the radii of two nuclei (4μm, Figure 2.30 A), indicating the two polar cells are kept close together. When *Lis-1* is knocked down, some clusters showed abnormal number of polar cells, in consistent with the reported functions of Lis-1 in mitosis (Faulkner et al. 2000). These mitosis defective clusters were excluded from furture quantification and phenotypic analysis. For the remaining *Lis-1* knockdown clusters, the two polar cells were no longer in close proximity; instead, they were apart and apparently detached (Figure 2.30 B). Polar cell displacement in *Lis-1* knockdown clusters was a progressive effect: it was visible prior to the formation of a motile border cell cluster (Figureg 2.30 C and 2.30 D) and became more severe later in migrating clusters (Figure 2.30 C and 2.30 D).

In conclusion, disrupting Lis-1 causes mis-organization of microtubules and that was most easily observed in polar cells but likely to also occur in outer border cells. In addition, Lis-1 is required to maintain the tight association between the two polar cells to ensure the proper positioning of polar cells within the border cell cluster. The question would be then are these two phenotypes related, and if so, how they

are related. As microtubules are known to regulate adhesions and cell-cell adhesions may be important for cluster organization (see next section, 2.5.4.3), I thus went on to test whether adhesions are affected in *Lis-1* knockdown border cell clusters.

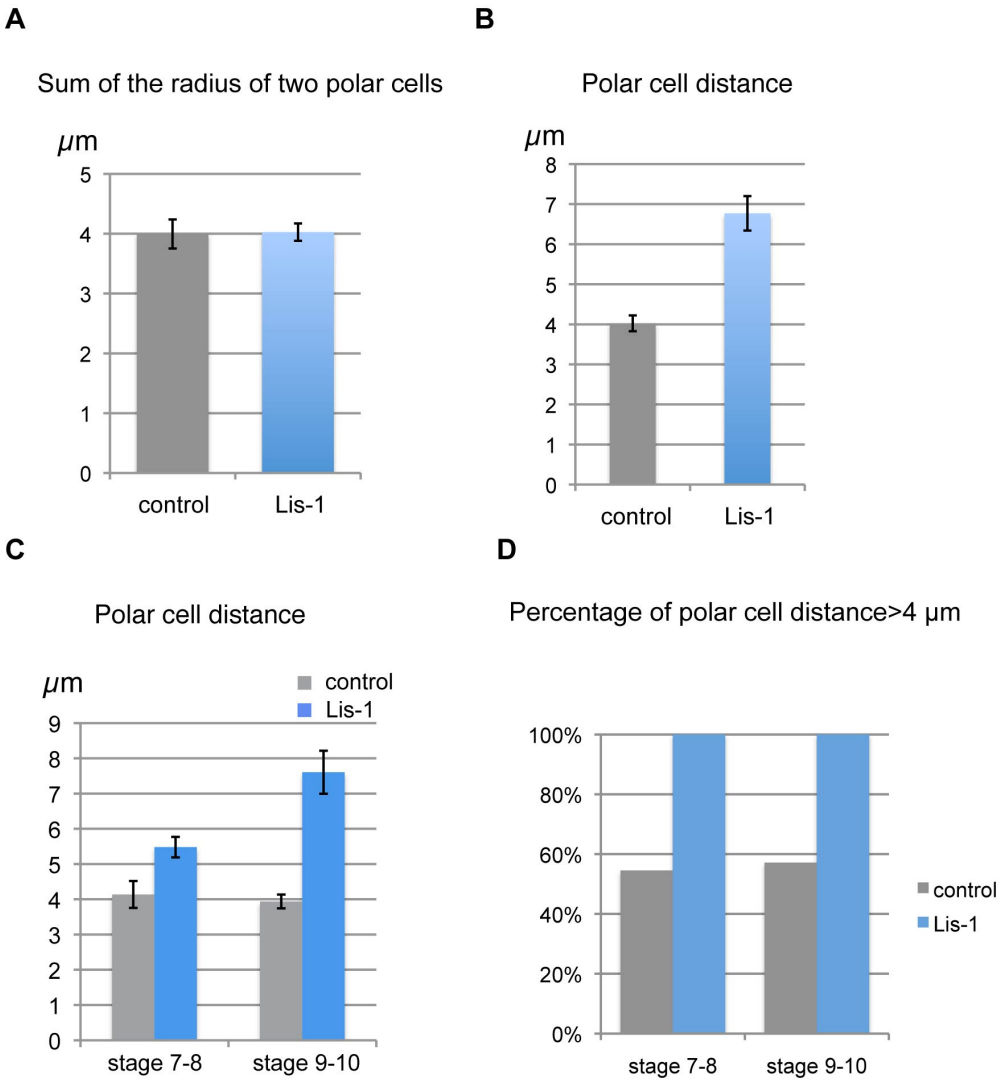

Figure 2. 30 Separation of polar cells in *Lis-1* RNAi clusters at both early and late stage.

(A) Sum of the radius of two polar cells in control (left) and *Lis-1* RNAi (right) border cell clusters.

(B) Distance between 2 polar cells in a cluster is measured between the centers of nuclei, in 3D, genotypes as in Figure 2.27.

(C) Distance between 2 polar cells as measured in (B) at different stages.

(D) Percentage of polar cell distance over 4 μm at different stages.

2.5.4.3 Disrupting Lis-1/NudE/Dynein affects the localization of adhesion molecules

Fasciclin II (FasII) is a transmembrane homophilic CAM that is the *Drosophila* ortholog of mammalian *neural cell adhesion molecule 2 (NCAM2)*. Similar to *NCAM2*, *Drosophila FasII* undergoes alternative splicing to generate multiple isoforms with differential expression pattern and intracellular binding partners: two transmembrane isoforms, one glycosylphosphatidylinositol (GPI) linked (Grenningloh et al. 1991; Lin et al. 1994) and another recently identified new variant $FasII^{PB}$ that expresses in glial cells (Silies and Klambt 2010). The glial $FasII^{PB}$ can mediate homophilic adhesions with transmembrane bound axonal FasII to regulate subcellular gradient of adhesiveness in glial migration in the *Drosophila* peripheral nervous system (Silies and Klambt 2010). The monoclonal antibody that is generally used to detect FasII recognizes an epitope in the intracellular domain of the two transmembrane FasII isoforms. This antibody (mAb 1D4) showed enriched expression in polar cells (Figure 2.31 A and A', see also (Szafranski and Goode 2004). Interestingly, the outer border cells have a non-autonomous role in FasII localization (Szafranski and Goode 2004), either through a putative border cell receptor as postulated by Szefranski and Goode, or more likely via homophilic binding to other FasII isoforms that are not recognized by the mAb 1D4 antibody. Fasciclin III (FasIII), another homophilic CAM, is exclusively localized to the interface between the two polar cells. The localization of these

two markers as well as DE-cadherin was analyzed in *Lis-1* knockdown cells and compared to control (Figure 2.31). FasII and FasIII were visibly abnormally localized in 30-50% of *Lis-1* knockdown clusters (Figure 2.31). The mislocalization of adhesion molecules could contribute to the final polar cell separation phenotype, or could be a consequence of polar cell separation. To distinguish between these two possibilities, FasII and FasIII localization were examined in earlier stages of *Lis-1* knockdown follicle cells, prior to the establishment of a cluster topology. The abnormal localization of FasII and FasIII were evident even before the onset of a rounded cluster (Figure 2.31), indicating mislocalization of adhesion molecules procedes polar cell displacement in *Lis-1* knockdown cells. In addition, some categories of mislocaliztion did not show obvious cell separation. Therefore, mislocalization of adhesion molecules could be a result of Lis-1 depletion, perhaps due to the abnormal microtubule cytoskeleton. This might cause subsequent polar cell separation during the epithelium to cluster transition stage.

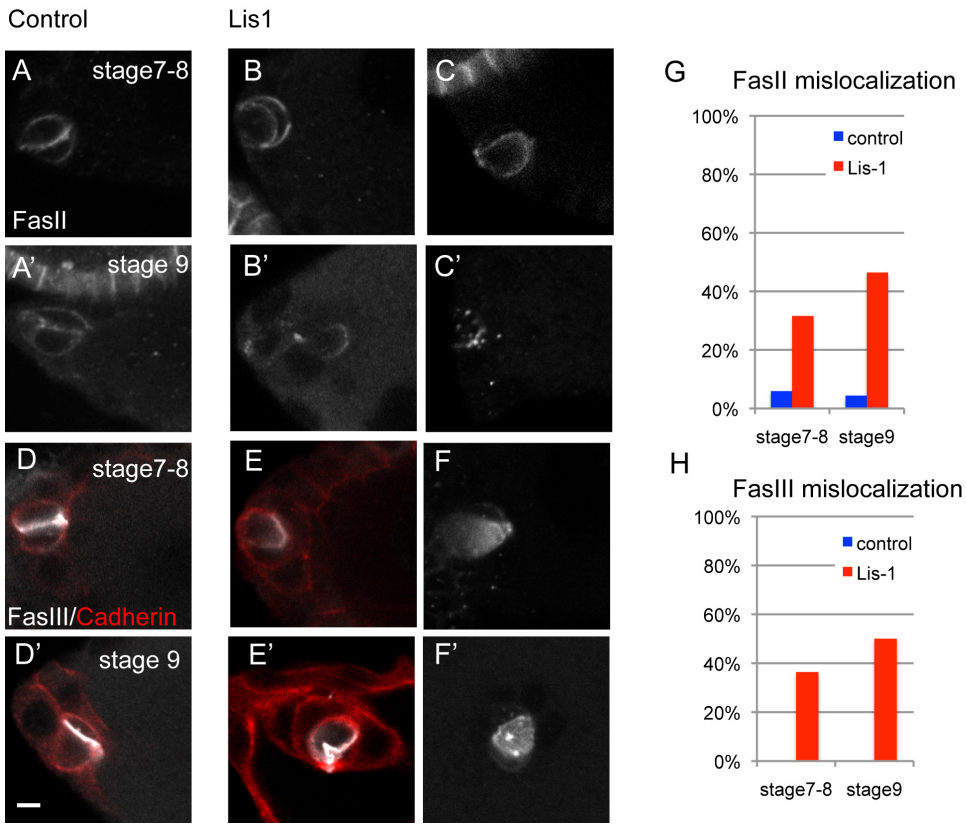

Figure 2. 31 Mislocalization of adhesion molecules in *Lis-1* knockdown border cells

(A and A') FasII staining patten in control border cells at early (A) and late (A') stage.

(B-C) Examples of abnormal FasII localization in Lis-1 depleted clusters at early (B, C) and late (B', C') stage. Quantification shown in G, n=17-28.

(D and D') FasIII (white) and Cadherin (red) staining patten in control border cells at early (D) and late (D') stage.

(E-F) Examples of abnormal FasIII localization in Lis-1 depleted clusters at early (E, F) and late (E', F') stage. (H) Quantification shown in H, n=8-14.

Genotypes are *hsFLP/+; AFG,10xGFP/+* (control) and *hsFLP/+;Lis-1^{KK108813} /+;AFG,10xGFP/ Lis-1^{GD1480}* (Lis-1). Scale bars: 10μm.

How would mislocalizaiton of adhesions cause polar cell separation during the epithelium to cluster transition stage? To understand how the cluster mis-organization may occur, I considered what normally happens during the formation of a migratory border cell cluster from their epithelial cell precursors. In order to initiate migration, the specified border cells must rearrange themselves to change from an epithelial to cluster topology. Mikiko has performed extensive live imaging analysis of wild type clusters at this stage and found actin-dependent rotational or jostling movement of border cells (Figure 2.32). The two central polar cells need to be displaced by adjacent motile outer border cells during this and subsequent phases, whether invasion takes place or not, and in a progressive manner (refer to previous Figure 2.29). As such, border cell and polar cell interactions and remodeling of adhesions at the junction between them are expected to allow this epithelial to cluster topology conversion. Defects in cell-cell adhesion at the cell contact would result the polar cells jossled out of position within the border cell cluster. Cell-cell interaction defects would be consistent with the overt cluster disorganization phenotype not being a purely polar cells autonomous defect.

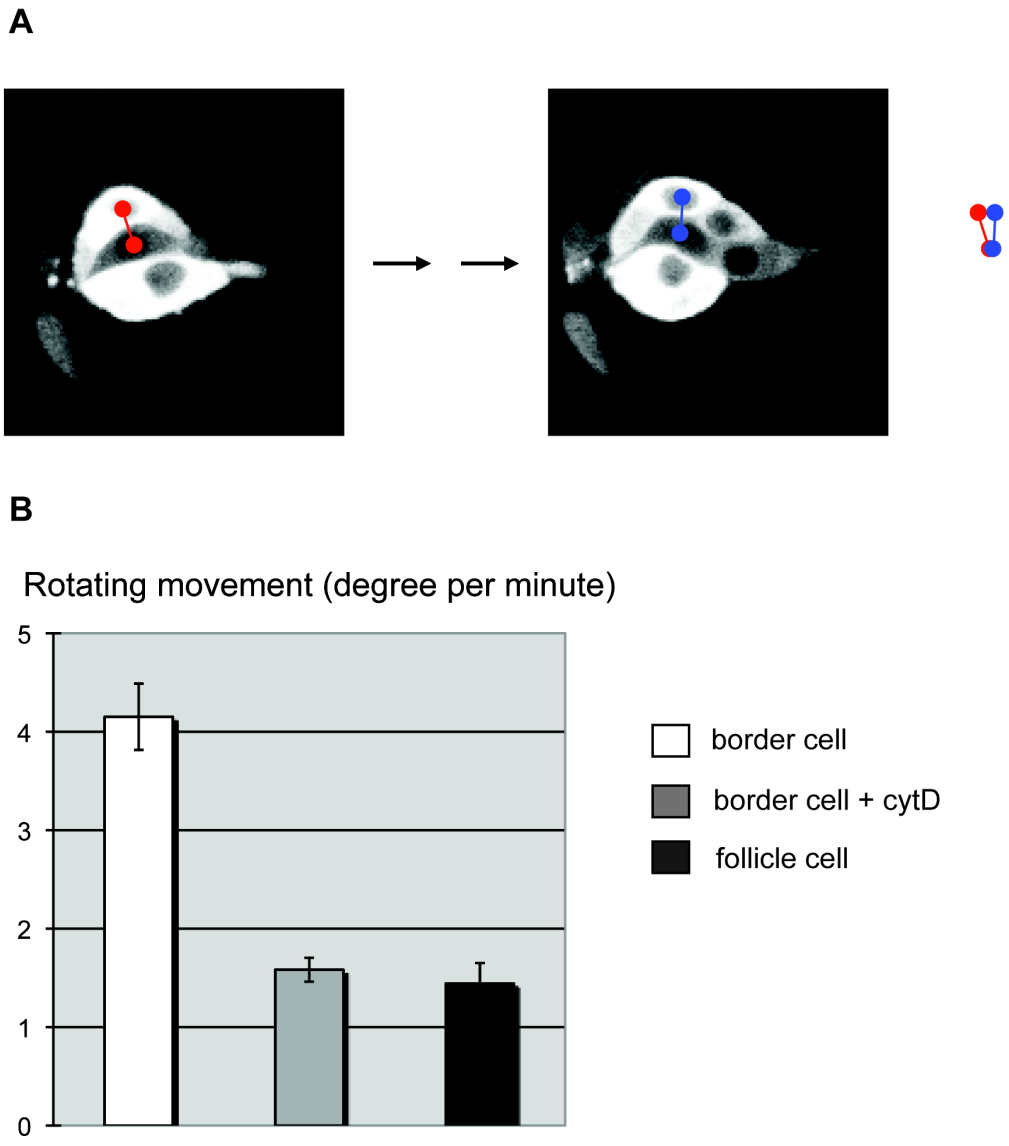

Figure 2. 32 Analysis of early rotating movement

Rotating movement in border cell clusters at initiation of migration (*slbo-Gal4,UAS-10xGFP/+*), compared to posterior follicle cells at the same stage and border cells in egg chambers treated with 1μM of cytochalasin D (n=7-9 clusters, two cells tracked per cluster). The angle from cluster center to nucleus is tracked (see illustrations in A). The baseline "movement" may mostly be intracellular nuclear movement and manual tracking inaccuracies.

3. Discussion

3.1 Microtubule polarity in border cells

Many migratory cells perform directional migration, and some of them require polarized microtubules to establish and/or maintain cell polarity. The polarity of microtubules and its function has largely been studied in single cell migration in tissue culture (Keller et al. 1984; Liao et al. 1995), such as the polarized migration of fibroblasts on ECM. Such cells have a prominent centrosome located in the middle of the cell, where microtubules minus ends are concentrated. During migration, the centrosomes are repositioned ahead of cell nucleus, and microtubules grow towards the leading edge. In these cells, there is a clear bias of microtubules to grow towards the front.

There are several differences between border cells and these well studied single cell migration in tissue culture system. Border cells migrate as a cohesive cluster contacting each other. On the outside of the cluster, border cells interact with the substrate, which are the neighboring nurse cells.

The border cell cluster forms an elongated shape when initiating and during early phase of migration. It is thus interesting to study the polarity of microtubules in such group of cells. If the whole cluster is considered as one unit, the microtubule polarity is essentially the

opposite to what has been found in most of the single migrating cells. In border cell cluster, the overall bias of microtubules is to grow away from the periphery, towards the middle of the cluster. It is thus interesting to consider how and why border cells have opposite microtubule polarity as compared to single migrating cells. One difference is that with the exception of the center polar cells that are specialized and have a MTOC like structure, the outer border cells do not have an obvious MTOC, and in those cells microtubule grow in a less biased way, only with a subtle bias towards the center (inward bias) as revealed from quantification. In other words, some microtubules grow towards the periphery as well.

The inward bias may reflect that these cells were polarized epithelial follicle cells before reorganizing into a migratory cluster, and some of the microtubule apical-basal polarity got retained with them later when they form a cluster. In follicle cells that with strict apical-basal polarity, the minus end is at the apical side and plus ends grow basally. Thus the outside membrane of border cells can be considered as modified apical membrane (Niewiadomska et al. 1999) with a subtle bias for the minus end.

Polar cells have a clearly polarized microtubule cytoskeleton with the minus end enriched at the apical side. The microtubule minus end motor Dynein together with its interacting proteins Lis-1 and NudE have an indispensable role in Upd RNA localizatioin to the apical site (Van

de Bor et al. 2011). I have found the same complex is required in the migrating border cell as well. Since the outer membrane of border cells can be considered as modified apical-like membrane that has a subtle inward bias, we would expect the bias for the minus end is outward, i.e, the minus end of microtubules would be located more towards the periphery. As Dynein is a minus end motor, it is interesting to speculate that the Lis-1/NudE/Dynein complex may be involved in transporting some putative cargos towards the periphery, raising the possibility that it might have a role in regulating extensions. We do see that both the forward and backward extensions are severely affected when the complex is disrupted in outer border cells.

If Lis-1/NudE/Dynein functions in minus end transport of some putative cargos in regulating extensions, we would expect this is microtubule dependent and disruption of microtubules may cause a similar effect. When microtubules were disrupted upon nocodazole treatment, we observed only a modest effect on extensions. One possible explaination of the subtle phenotype would be the low concentration of nocodazole only depolymerizes dynamic microtubules, leaving the stable microtubules largely unaffected. It will be interesting to find out if there is a difference in polarity of stable and dynamic microtubules in border cells.

3.2 Regulatory roles of microtubules in border cell migration

Roles of microtubules in cell migration are variable; they make different contributions to cell migration in different cell types. I have done both drug studies and mutants to investigate the roles of microtubules in border cell migration. Drug studies showed that both reducing microtubules and altering microtubule dynamics affect the process, indicating a requirement of microtubules in border cell migration. However, though drug treatments were effective to reduce the cluster speed, it neither completely nor severely block cluster movement, implying a modest effect of microtubules in regulating border cell migration. This is in contrast to the effects caused by actin depolymerisation using cytochalasin D (CytoD) treatment (data not shown), which completely blocks migration, showing that actin cytoskeleton is essential for movement (as expected). Thus microtubules appear to play more a supportive or regulatory role during border cell migration. The modest effect was also seen in the genetic perturbation of the specific microtubule depolymerization factor *stathmin*. Furthermore, systematic screen of a large set of genes encoding microtubule regulators only recovered few genes having a role in border cell migration. Although most of the results were obtained from RNAi mediated knockdown but not from complete loss of function studies, and so may have missed some of the genes in the list; I did observe detectable effects from knockdown each of the 3 genes that encode a cooperating protein complex, suggesting a reliable overall efficiency of the screen. This, in turn, supports the notion that only a

few microtubule regulators and motors have uniquely required functions in border cell migration.

3.3 Autonomous and non-autonomous requirement of microtubules in border cell migration

Another difference between border cells and many of the migrating cells studied is the migration substrate. For many well-studied migratory cells, the migration substrate is either the ECM or the culture dish surface. In contrast, border cells migrate between and on the giant nurse cells and we study the migration process within the tissue. Reduction of microtubules in the tissue using drug treatment caused a clear reduction of net cluster speed whilst autonomous reduction of microtubules in the border cells by over-expressing the severing protein spastin did not. One difference between drug treatment and genetic perturbation is the timing: drug treatment produces immediate acute effect whilst genetic perturbations depend on the timing when the transgene is well turned on by the driver; in addition, long term genetic pertubation may allow cells to build up compensatory mechanisms that eventually lead to adaptation. However, the non-autonomous effect was also seen in the genetic perterbation of loss of *stathmin* situation, implying the diffences in timing may not be the primary cause of the differences.

Drug treatment might also affect microtubules in the polar cells, which are important for the localization of Upd RNA. Therefore drug treatment

may in-principle affect border cell migration by affecting the specification of border cells. We cannot formally rule out this possibility, however, given the immediate acute effect of drugs on clusters that have been already specified prior to drug addition, any cell specification defect that might have slowly built up would not be the primary cause. In addition, loss of Stathmin activity in the whole border cell cluster (including polar cells) produces different effect to loss of Stathmin in the whole tissue, further demonstrating the importance of microtubules in both border cells and the substrate nurse cells.

3.4 Interactions between microtubules and adhesions

One possible explanation for both autonomous and non-autonomous effects of microtubule is that the cell-cell adhesions are affected when microtubules are disrupted. In the case of border cells migrating on nurse cells, this appears to be mediated by *DE-cadherin* mediated homophilic adhesion (Niewiadomska et al. 1999; Pacquelet and Rorth 2005). Microtubules have in other contexts been shown to regulate *cadherin*-dependent adhesion or adherens junctions, and vice-versa (Chausovsky et al. 2000; Stehbens et al. 2006) and we did observe a genetic interaction with *DE-cadherin*. Reducing DE-cadherin in the tissue but not in the border cells rescued the migration defect in nocodazole treated border cell clusters, suggesting a role of microtubules in negatively regulating *DE-cadherin* in the nurse cells. Nocodazole treatment may preferentially stabilize nurse cell adhesions

and thus increase the stickiness of the substrate, making them difficult for border cell to migrate on. Alternatively, as border cells use DE-cadherin mediated adhesions for migration in the crowded three-dimensional environment by squeezing between the nurse cells, there might be a competition for DE-cadherin mediated adhesions between border cells and nurse cells. This is relevent as DE-cadherin mediated adhesion is homophilic. Border cell-nurse cell adhesions need to “win” over nurse cell-nurse cell adhesions for invasaion and migration to progress in border cells. Our lab has previously observed that increasing the level of DE-cadherin in the nurse cell substrate can cause border cell migration delays (A. Pacquelet and P. Rorth, unpublished observations), highlighting the importance of proper balance of DE-cadherin between border cells and nurse cells. It would ultimately be ideal to characterize and compare DE-cadherin localization and dynamics in control and nocodazole treated condition to clarify the exact roles of microtubules in regulation of *DE-cadherin*.

In addition, when perturbing microtubule regulations, other phenotypes that may be related to defects in adhesions were observed, both in the modest regulator Stathmin and the strong regulator Lis-1. *Stathmin* mutant border cell clones have prolonged attachments with anterior epithelium cells and did not delaminate completely. This may be caused by inappropriate de-adhesions or lack of retraction of the mutant border cells, which could be due to an altered cell-cell adhesion, with neighboring somatic cells and substrate nurse cells,

respectively. *Lis-1* RNAi causes severe block in the initiation of border cell migration, with cluster reorganization and redistribution of adhesion molecules largely affected. Therefore, both microtubule regulator mutant phenotypes imply defects in adhesions, with neighboring cells and within the whole cluster, respectively. Therefore, it is tempting to speculate that spatial regulation of cell-cell adhesion is a key role of the microtubule cytoskeleton in border cell migration.

3.5 Regulatory roles of microtubules in cellular extensions

Cell migration is often associated with the formation of membrane protrusions, which contain an underlying dynamic cytoskeleton network to provide both the protrusive and contractile force essential for cell motility. In border cells, initiation of their invasive migration is linked to the formation of a robust forward-directed extension from the front cell most of the time. Such front extensions are stable and seem to generate the traction force needed for forward-directed movement (Poukkula et al. 2011). Border cells also have back extensions, which are active just as front extensions, but they are outward, non-trailing tails from the back cells. Back extensions are fewer, smaller, and short-lived; they do not seem to generate traction force. It has been shown that in normal situation, back extensions are non-productive and do not interfere with clusters' movement, and their non-productivity is regulated by the guidance signaling through the RTKs PVR and EGFR (Poukkula et al. 2011). Interference of the guidance signaling by over-

expressing double dominant receptors for both PVR and EGFR can make back extension become productive, which may render the border cell cluster into a tug of war situation and lead to inefficient movement (Poukkula et al. 2011).

Interestingly, disruption of the microtubule regulators Lis-1 and NudE severely affected the formation of the prominent structure of forward extension, which can explain the observed severe migration defect. If Lis-1, NudE and Dynein were required to produce load-bearing movement of the front cell nucleus or cell content, the expectation is that the microtubule cytoskeleton would be required as well. However, front extensions were not severely affected by border cell autonomous or tissue-level reduction of microtubules, implying that the microtubule cytoskeleton as such might not be essential for this structure. We cannot formally rule out microtubule independent roles of Lis-1 and NudE, however, with the observed overlapping phenotypes in border cell migration and the well known regulatory roles of Lis-1 and NudE in Dynein motor function, this is highly unlikely and we did observe mis-organization of microtubules in *Lis-1* RNAi clusters. Therefore the stronger effect caused by the disruption of Lis-1 and NudE may be caused by the mis-organized microtubule cytoskeleton, which might be more disruptive for polarized migratory cells than the simple loss of microtubules altogether.

Microtubules also play roles in regulating the back extensions. Autonomous reduction of microtubules by over-expressing the severing protein spastin in border cells caused a significant increase in the number and size of back extensions, making back extensions bigger and maybe more stable. This indicates microtubules may preferentially destabilize back extensions in the back cell. With limited effect on front extesions, microtubule depletion reduces the difference between front and back cells, making them more similar to each other. In addition, loss of function of the microtubule-depolymerization factor Stathmin in the tissue but not in the border cells causes a similar effect in promoting back extensions, suggesting a non-autonomous requirement in the nurse cells, possible due to an effect in stabilizing microtubules.

Interestingly, the apparent large effect on back extensions upon microtubule depletion did not affect clusters' movement, indicating these stabilized back extensions appear to still be non-productive. This implies that microtubules either negatively regulate back extensions independently of the guidance signaling, or microtubules themselves are not the downstream effecters of the guidance cues. Instead, microtubules might regulate adhesions that are essential for border cells' invasiveness when they invade the germline nurse cells.

3.6 Common features of Lis-1/NudE/Dynein and microtubules in cell-on-cell migration

The mammalian Lis-1, Ndel1 (one of the two NudE-related proteins in mammals) and Dynein complex has well known roles in neuronal migration in the cerebral cortex. It is interesting to compare neuronal migration in the brain to border cell migration as both represent cells migrating in a crowded three-dimensional environment upon other cells. They also both require the evolutionally conserved Lis-1/NudE/Dynein complex. In neuronal cell migration, depletion of Lis-1 and Dynein specifically in the neurons (Tsai et al. 2005) or the entire animal (Youn et al. 2009) had a prominent effect on cell and nuclear movement as well as an effect on axonal extensions, which was also observed in culture (Grabham et al. 2007), but not on all extensions. In border cell migration, Lis-1/NudE/Dynein complex is strongly required and disruption of Lis-1 and NudE had strong effects on the front extensions. In addition, neuronal progenitors undergo changes to switch from one differentiated cell state and shape to another (multipolar to bipolar migratory state), just as border cells re-organize to become migratory (epithelial to cluster transition); and *Lis-1* RNAi retained neuronal progenitors' multipolar morphology (Hippenmeyer et al. 2010). Therefore, it is interesting to speculate the transition to a migratory state is a Lis-1-dependent step.

Recent advance in genetic mosaic techniques have allowed the appreciation of extensive cell-cell interactions among migrating neurons and revealed an unexpected degree of non-cell autonomy of phenotypic effects for both Lis-1 and Ndel1. It was speculated that the

non-autonomous functions may be due to community effects (piggy-backing) that can be observed for collective cell migration (Rorth 2009) or cell-cell signaling effects. Given the effects of microtubules in border cell migration, it is also interesting to speculate that the non-cell autonomous requirements for Lis-1/Ndel1 might be liked to cell-cell adhesion: effects in both the migrating cell and the substrate cells. There are obviously significant differences between neuronal and border cell migration. For example, migrating neurons have a prominent centrosomes and microtubules are aligned parallel to the long axis with plus end predominantly outwards (Rakic et al. 1996; Tsai et al. 2007), but the common features of cell-on-cell migration by different cell types may be informative and are clearly worth further investigation.

4. Material and Methods

4.1 *Drosophila* genetics

4.1.1 Fly stocks and husbandry

All flies were grown on standard corn meal and crosses were set up at 25 ºC except for the cross between *slboGal4, slbo*^{1310} and *nudE* RNAi flies that was carried out at 29 ºC. PolyUbiqutin promoter driven EB1-GFP flies were obtained from Ohkura (Shimada et al. 2006). *Tubulin-GFP* (Grieder et al. 2000) and *UAS-spastin-EGFP* (Trotta et al. 2004) flies were obtained from Damian Brunner. 10xGFP (Poukkula et al, 2011) was used as a marker for the movie analysis. Slbo^{LacZ} was used for scoring border cell migration delay by X-Gal. Neur^{A101} was used to mark polar cells.

4.1.2 RNAi mediated knockdown

For the RNAi-mediated knockdown screen, fly stocks were obtained from the Bloomington (including Trip lines generated at the Harvard Medical School) and Vienna *Drosophila* RNAi Center (details included in supplementary table). All RNAi expressions were driven by either a border cell specific driver SlboGal4 or the actin-flip-out Gal4 driver (AFG) for robust expression in all somatic cells. For the slboGal4 driven RNAi screen, *slbo*^{1310} was introduced as a sensitized background. For AFG, to obtain expression in all border cells, female flies were heat shocked at 37ºC for 30min at larval stage and ovaries

from 1-2 day old female were dissected, except for a few lines that early expression resulted in lethality (Msps, Ssp4, Spastin, Tektin-C, Sw, Unc-104, Ctp and Klp64D, Lis-1, Dhc64C). To bypass the early lethality upon expression by those RNAi lines, adult female flies were heat shocked at 37ºC for 30min and ovaries were dissected 3-4 days later. For AFG driving expression, *w1118* were crossed as a control. For *slboGal4*^{1310}, egg chambers of w1118/+; slboGal4^{1310}/+ often displayed strong migration delay and *yw and Canton-S* were used as additional controls. Border cell migration was scored by comparing the position of border cells with follicle cells at mid-late stage 9 or at stage 10. Generally, border cells lagging behind the anterior end of retracting follicle cells by at least one nurse cell is scored as a migration delay.

4.1.3 Generation of mosaic clones

4.1.3.1 MACRM clones

For generation of *stai*^{KO} mutant border cell clones for live imaging analysis, *stai*^{KO} mutants were recombined with *FRT40,42* on the second chromosome and mitotic clones were generated and positively marked by GFP using the MARCM (Mosaic Analysis of a Repressive Marker) system (Lee and Luo 1999). Mitotic *stai*^{KO} clones were induced by heat shocking larvae of the genotype *hsFLP/+; FRT40,42,stai*^{KO}*/FRT40,Gal80*; *slboGal4,UAS-10xGFP/+* and border cell cluster expressing GFP in all outer border cells were scored as full

mutant clones for analysis. *FRT40,42* was used to induce empty clones as control.

4.1.3.2 Regular clones

Regular mitotic clones (GFP negatively marked) were generated according to Xu and Rubin (Xu and Rubin 1993). For *chb* clones, chb^{1} (BL24502) was recombined with *FRT80* and mitotic clones were induced by heat shocking larvae of the genotype *hsFLP/+; chb^{1},FRT80/ubiqutinGFP,FRT80* and border cells with loss of GFP expression were scored as mutant clones for analysis. For $stai^{KO}$, mitotic clones were induced by heat shocking larvae of the genotype *hsFLP/+; $stai^{KO}$,FRT40,42/ubiqutinGFP,FRT40*. For *Lis-1* clones, FRT^{G13},$Lis\text{-}1^{G10.14}$ (BL8773) was used and adult flies with genotype *hsFLP/+; FRT^{G13} ,$Lis\text{-}1^{G10.14}$ /FRT^{G13},ubiquitinGFP* were heat shocked at 37ºC for 30 minutes and ovaries were dissected 3–4 days later. For *Dhc64C* clones, $Dhc64C^{4\text{-}19}$,FRT^{2A} (BL23863) was used. *Dynein* mutant clones were initially induced as the same way as for *Lis-1*, whereby $Dhc64C^{4\text{-}19}$,FRT^{2A} was crossed with *hsFLP; FRT2A,ubiqutinGFP* and adult flies with genotype *hsFLP/+;*$Dhc64C^{4\text{-}19}$,FRT^{2A}/FRT^{2A},*ubiquitnGFP* were heat shocked. *Dynein* mutant clones were also generated according to Van de Bor et al, whereby $Dhc64C^{4\text{-}19}$,FRT^{2A} were crossed to *e22cgal4, UAS-FLP/CyO;* FRT^{2A}*, UbiGFP* and *e22cgal4, UAS-FLP/+;* $Dhc^{4\text{-}19}$*,* FRT^{2A}*/UbiGFP,* FRT^{2A} females were kept at 30°C before dissection. There was not obvious difference in clonal induction efficiency as well as border cell migration phenotype

between the two methods. The clonal analysis of *Dhc64C* results included mutant clones induced by both methods.

4.2 Cloning and generating of *stai*^{KO} mutant and stai rescue flies

4.2.1 Generating *stai*^{KO} mutant flies

4.2.1.1 Cloning of *stai*^{KO} knock-out vector

The *stai*^{KO} knock-out vector was constructed to carried two homology arms with about 3.5kb sequence homology to nucleotides flanking upstream and downstream the targeted knock out region (starts from nucleotide sequence encoding exon 6 and finishes at exon 8). The two homology arms were amplified from genomic DNA extracted from *w1118* flies using two sets of primer pairs:

- 5’ Upstream flanking homology region:

  Forward: 5’-TTGCGGCCGCTCTATTATGGCGGGTTATGC-3’

  Reverse: 5’-TTGCGGCCGCAGGAGGAAGGAAAGCAAAGG-3’

- 3’ Downstream flanking homology region:

  Forward: 5’- TTGGCGCGCCGCATGGCCAAAAGTTTTCAT-3’

  Reverse: 5’-TTGGCGCGCCCTACGAGAACGCAGTGGTCA -3’

The PRC amplified upstream homology arm was cloned into *pW25* vector using *Not1* and downstream homology arm was cloned using

AscI. Clones with the two homology arms inserted in the correct orientation (with respect to each other) was selected and used for generating transgenic donor flies for the knock out.

4.2.1.2 Creating *stai*^{KO} knock-out donor flies

Transgenic flies were made by *P*-element mediated germ-line transformation (Rubin and Spradling 1982; Spradling and Rubin 1982) and mapped to inserted chromosomes. 4 transformants with *stai*^{KO} construct inserted at the third chromosome were used as “donors flies” for the subsequent homologous recombination.

4.2.1.3 Generating *stai*^{KO} knock out flies

stai^{KO} mutant was generated using homologous recombination-based ends-out gene targeting (Rong and Golic 2001). 200 crosses were set for each *stai*^{KO} knock-out donor lines with *hsFlp, hs-I-SceI*. F1 progeny were heat shocked at 37ºC three times for 1 hour each with about 12 hours interval since 2nd instar larval. F1 progenies were screened and mapped for the loss of *w*+ from the third chromosome. 21 candidates were obtained. 19 had been tested and14 were verified to have eliminated sequences from the knock-out targeted region checked by PRC amplified using one primer set:

- Knock out region Forward: 5’-AAGAACGTTAGCGTCGAGGA-3’
- Knock out region Reverse: 5’-CTCCTTTAGGCGATCCAACA-3’

Initially 5 *stai*^{KO} lines had been tried to verify by position mapping for the two homology arms insertions using two sets of primers:

- 5' Upstream homology arm
    - Forward: 5'-CAAATGCGAACATTTTAACTCG-3' (upstream sequence from the 5' Upstream homology arm)
    - Reverse: 5'-CGACGAAGCGCCTCTATTTA-3' (sequence from the white gene, reverse complemented)
- 3' Downstream homology Arm:
    - Forward: 5'-TCGCTGCATGAATTAGCTTG-3' (sequence from the white gene)
    - Reverse: 5'-TTAAACGGAACGGAAACGAC-3' (downstream sequences from the 3' downstream homology arm, reverse complemented)

Only 1 *stai*^{KO} line had been successfully verified to have correct insertions of both homology arms. This line was lethal however when crossed with the small deficiency of *stathmin*^{L27} and with other *stai*^{KO} lines (most of the *stai*^{KO} lines were lethal, few were viable however with very much reduced viability), transheterozygous flies were viable and used for the subsequent phenotypic analysis. This *stai*^{KO} line was recombined with *FRT40,42* on the second chromosome for generating mitotic *stai*^{KO} border cell clones for border cell migration. Rescue

experiments were always performed concurrently to confirm the phenotypes were indeed due to loss of Stathmin, but not due to any background mutations that might have occured from the homologous recombination process.

4.2.2 Generating of *stai* rescue flies

4.2.2.1 Cloning of *stai* rescue construct

For the *pCasper-attB-tubulin-stathmin* rescue construct, *pCasper-attB-tubulin* was first generated by subcloning the *tubulin* promotor from *pCasper-tubulin* into *pattB* (Bischof et al. 2007) by *Xho1* and *EcoR1*. The cDNA of *staithmin A* was subcloned from *pBS-stai* (Borghese et al. 2006) into *pCasper-attB-tubulin* using *Not1* and *Xho1*.

For the *pUAST-attB-stathmin* rescue constructs, it was subcloned from *pCasper-attB-tubulin-stathmin* into *pUAST-attb* (Konrad Basler and Francois Karch) using *Not1* and *Xho1*.

4.2.2.2 Making stai rescue flies

Transgenic flies were made by PhiC31 integrase-mediated transgenesis systems at targeted insertion site 86Fb.

4.3 Calculation of percentage of viability

5 to 10 male and females of *stai*^{KO} mutant with heterozygous balancer chromosomes (*CyO*) were crossed and the number of each F1 progenies was counted. The fraction of viable homozygous *stai*^{KO} mutant flies ($F_{experiment}$) was calculated as the number of hatched *stai*^{KO} mutant flies divided by the total number of F1 adult flies. The ultimate viability percentage was calculated by dividing the fraction of viable homozygous *stai*^{KO} mutant flies ($Viability_{experiment}$) by the expected fraction of viability ($Viability_{expected}$). The expected fraction of viability ($Viability_{expected}$) was calculated according to Mendelian inheritance pattern, which has the Mendelian rate to be 33.3%.

4.4 Fertility assay

Each 1 to 2 days old male flies with assayed genotypes were crossed individually to 3 to 4 virgins of flies with genotype of *w1118*. More than 10 crosses were set up. The ability of the parental cross to generate F1 progenies was checked. The percentage of fertile males with individual genotypes was calculated.

4.5 Climbing assay

Each five-days old male with assayed genotypes was transferred to individual empty vials and left for thirty minutes. Each vial had an outer circle marked at the 5cm position from its bottom. After thirty minutes' recovery from anesthesia, each fly was gently tapped to the bottom of the vial. The time taken for individual fly to reach from the bottom of the

vial to the circle mark was recorded up to 2 minutes. Each assay was repeated three times and average time was calculated. Although with variation, generally the three measurements gave consistent results, i.e, the single male either succeed in all the three climbing assays within two minutes or fail in all the three climbing assays within two minutes. However, there were few cases in which heterogeneity occurred. Those heterogeneous events all consisted of one failure and two successes. In such situation, the average was calculated from the two success events.

4.6 Live imaging and analysis

4.6.1 Imaging condition

Egg chambers were dissected and cultured as described previously (Bianco et al. 2007). Briefly, yeast-fed females were dissected in Schneider's media plus 5 mg/ml insulin, and imaged in dissection media supplemented with 2.5% fetal calf serum (FCS), 2 mg/ml trehalose, 5 mM methoprene, 1 mg/ml 20-hydroxyecdysone, 50 ng/ml adenosine deaminase (ADA) and 9 mM FM 4-64. Dissection time did not exceed 15 min. Images were acquired by the inverted confocal microscopy (SP5, Leica) with a 63X, 1.2 NA Plan Apochromat water immersion objective calibrated to the coverslip thickness of the imaging chambers. Fluorescence was excited with the 488-nm line of an argon ion laser, and the emitted fluorescence was acquired simultaneously for GFP (500–550 nm) and red (600–700 nm) for either the membrane

dye FM 4–64 or red fluorescence protein (RFP) in addition to the transmission image. Egg chambers were aligned by rotating the scan field with the anterior tip of the egg chamber aligned to the left and the image x-axis going from this point through the middle of the oocyte (far right).

Damaged egg chambers due to bad dissection were exluded from on set of imaging, as judged by the visualization from FM 4-64. Imaging was carried out up for two hours to ensure healthy development of the egg chamber.

For imaging the border cell clusters marked with 10xGFP, the images were zoomed in 1.3X and pinhole of 1 airy unit was used. Z sections 2.98 μm apart covering the entire border cell cluster were captured at between 30sec–120sec intervals.

4.6.2 Imaging analysis and statistics

All images were processed with ImageJ and its customized macros. Processed movies were first checked for quality control. Only growing egg chambers with nurse cell nuclei showing rotations were included for further analysis.

All statistic analysis was done by a two-tailed student t test except for the comparisons of percentage of phenotype in which the Fisher's

exact test were used

(http://www.graphpad.com/quickcalcs/contingency1.cfm)

4.6.2.1 Calculation of net cluster speed

For the analysis of behaviors of border cell clusters marked with 10xGFP, projected images from GFP channel were used. For the migrating cluster, analysis was done from videos covering up to 50% migration path, and the minimum length of videos used was 20 min. Net cluster speed was calculated from the displacement of the border cell cluster from initial and final position.

4.6.2.2 Nuclei tracking and calculation of apparent single cell speed

10xGFP was excluded from the nucleus due to its large size, and thus tracking was done on identifying the center of the GFP negative region. Single cell nuclei were tracked manually per frame and average of all the instantaneous speed were calculated for each cluster per movie. Extensions were identified and analyzed as described in (Poukkula et al. 2011).

4.6.2.3 Analysis of initiation of migraiton

For the analysis of behaviors of border cells prior to migration, only videos with starting frames in which the border cell clusters had not yet

detached from epithelium were included for the quantification. All visible extensions from the border cell cluster were manually identified until the frame when the cluster detached from epithelium. The maximum lengths of all extensions were measured from the projections of the GFP channel using Image J.

4.7 Drug treatments

To disrupt microtubules, nocodazole (Sigma) and taxol (Sigma) were used and DMSO (Sigma) was for control. For nocodazole, various concentrations had been tested in egg chambers and 2*μ*M was shown not to disrupt the overall development of the egg chamber. For taxol, a final concentration of 2*μ*M taxol was used.

4.7.1 Assaying drugs' effect on microtubules

To assess whether the drugs affect microtubules, egg chambers from outcrossed flies with genotype of *tubulinGFP/w1118* were first loaded into three wells of an imaging chamber and each image covering the entire border cell cluster were taken at zoom in 4X with Z stack at 2.98μm interval. Nocodazol, taxol and DMSO were subsequently added to the egg chambers. Images were taken immediately with about less than 2 minutes lag time. Images from GFP channels were compared between before and after drug treatment. Images for each egg chambers were variable as the signal depended on the depth of the border cell cluster inside the tissue. We observed no effect of

DMSO after treatment from GFP image. Nocodazol and taxol both had an effect (shown in results section) after treatment. Egg chambers with similar amount of GFP signals initially (before treatment) were selected and images for those egg chambers post drug treatment were shown in Figure 2.6.

4.7.2 Assaying drugs' effect on behavior of border cell clusters

For the analysis of the immediate effects of the drug treatment on the behaviors of border cell clusters, same concentrations of drugs were added to egg chambers with genotype of *slboGal4,10xGFP/+* flies and live imaging were set up immediately afterwards with an average lag period about 10 minutes.

4.8 High-resolution imaging and analysis of EB1-GFP tracks

For imaging the EB1-GFP, most of the images were zoomed in 4X and pinhole of 1 airy unit was used. For some samples that had relative weak signals due to their deep position inside the tissue, the pinhole was opened to 2 airy unit to increase the detection and line average up to 4 was used to increase the signal to noise ratio. At least 10 frames were taken for each sample at each section with time interval between 0.6 second up to 2.4 seconds. Z sections 2 μm apart covering the entire border cell cluster were also captured to provide the view of the overall organization of the cluster.

4.8.2 Analysis of EB1-GFP track directions

For EB1-GFP dot tracking in both border cells and follicle cells, visible moving EB1-GFP dots from GFP channel were manually tracked using the Image J plugin MTrackJ (http://www.imagescience.org/meijering/software/mtrackj/)

For each individual EB1-GFP track, its net movement was defined as the vector displacement between its initial and final position.

4.8.1 EB1-GFP in border cells

For border cells, the angle of this vector relative to the x-axis can be calculated by its arc-tan value. For each track, based on its angle, its direction was assigned into one of the three categories: front (0–45° and 315– 360°), back (135–225°) and side (>255 to <315° + >45 to<135°). A Perl script (designed by Dr. ZhangRui) was used to automatically calculate the total number of tracks in each of the three directions for individual cell analyzed.

4.8.2 EB1-GFP in follicle cells

For follicle cells that had well defined apical to basal polarity, EB1-GFP track directions were assigned into towards apical, basal and lateral respectively.

4.9 Immunostaining and analysis

Ovaries were dissected in Schedium medium (Gibco) with 0.5μM insulin (Sigma) and fixed in 4% para-formaldehyde (Electron Microscopy Sciences) for 20 minutes. Subsequent washes were done in 1xPBS containing 1% Triton X-100 (PT). The samples were blocked with 5% Natural Goat Serum for 1 hour and then incubated with primary antibodies at 4 degree over-night. Samples were washed several times in PT then incubated with 2nd antibodies for 2 hours. Samples were washed several times for 2 hours before mounting in the mounting medium (5% n-propyl gallate dissolved in PBS and 80% glycerol). The following primary antibodies were used: mouse anti-alpha-Tubulin (1:5000; DM1A, Sigma); mouse anti-actylated-Tubulin (1/1000; T7451**,** Sigma); rat anti-Slbo (1/500); mouse anti-FasII (1/100; 1D4, Developmental Studies Hybridoma Bank (DSHB); mouse anti-FasIII (1/100; 7G10, DSHB); rat anti-DE-cadherin (1:100, DCAD2, DHSB), rabbit anti-aPKC (1/2000, sc-216, Santa CRuz), rabbit anti-βGal (1/1000, Cappel). Secondary antibodies used were Rhodamine (TRITC), Cy5 or Dylight-649 conjugated (Jackson ImmunoResearch). Alexa Fluor 546-Phallodin (Molecular Probes) was used for visualized F-actin and DAPI was used to visualize nuclei.

Images were taken by the upright confocal microscope (Zeiss,LSM700) with 40X oil-immersion objective at 0.5X zoom in. Pinhole of airy 1 unit was used. Z-sections of 2 μm were taken to cover the entire border cell clusters. For high magnification images, 2X zoom in was used.

The 405-nm and 543-nm Diode lasers were co-excited for the simultaneous detection of emitted fluorescence from two PMTs: DAPI (SP490 filter) and Rhodamine (BP505-600 filter). The 488-nm and 633-nm lasers were co-excited for the simultaneous detection of emitted fluorescence from GFP (SP555 filter) and Cy5 or Dylight-649 (LP640 filter).

Bibliography

Adams, R. H. and K. Alitalo (2007). "Molecular regulation of angiogenesis and lymphangiogenesis." Nat Rev Mol Cell Biol **8**(6): 464-78.

Affolter, M. and E. Caussinus (2008). "Tracheal branching morphogenesis in Drosophila: new insights into cell behaviour and organ architecture." Development **135**(12): 2055-64.

Akhmanova, A. and M. O. Steinmetz (2010). "Microtubule +TIPs at a glance." J Cell Sci **123**(Pt 20): 3415-9.

Bai, J., Y. Uehara and D. J. Montell (2000). "Regulation of invasive cell behavior by taiman, a Drosophila protein related to AIB1, a steroid receptor coactivator amplified in breast cancer." Cell **103**(7): 1047-58.

Beccari, S., L. Teixeira and P. Rorth (2002). "The JAK/STAT pathway is required for border cell migration during Drosophila oogenesis." Mech Dev **111**(1-2): 115-23.

Bershadsky, A., A. Chausovsky, E. Becker, et al. (1996). "Involvement of microtubules in the control of adhesion-dependent signal transduction." Curr Biol **6**(10): 1279-89.

Bershadsky, A. D., E. A. Vaisberg and J. M. Vasiliev (1991). "Pseudopodial activity at the active edge of migrating fibroblast is decreased after drug-induced microtubule depolymerization." Cell Motil Cytoskeleton **19**(3): 152-8.

Bianco, A., M. Poukkula, A. Cliffe, et al. (2007). "Two distinct modes of guidance signalling during collective migration of border cells." Nature **448**(7151): 362-5.

Bischof, J., R. K. Maeda, M. Hediger, et al. (2007). "An optimized transgenesis system for Drosophila using germ-line-specific phiC31 integrases." Proc Natl Acad Sci U S A **104**(9): 3312-7.

Borghese, L., G. Fletcher, J. Mathieu, et al. (2006). "Systematic analysis of the transcriptional switch inducing migration of border cells." Dev Cell **10**(4): 497-508.

Borghese, L., G. Fletcher, J. Mathieu, et al. (2009). "Correction to [Systematic analysis of the transcriptional switch inducing migration of border cells]." Dev Cell **10**(4): 497-508.

Bratman, S. V. and F. Chang (2008). "Mechanisms for maintaining microtubule bundles." Trends Cell Biol **18**(12): 580-6.

Chausovsky, A., A. D. Bershadsky and G. G. Borisy (2000). "Cadherin-mediated regulation of microtubule dynamics." Nat Cell Biol **2**(11): 797-804.

Chrzanowska-Wodnicka, M. and K. Burridge (1996). "Rho-stimulated contractility drives the formation of stress fibers and focal adhesions." J Cell Biol **133**(6): 1403-15.

Crowley, E. and A. F. Horwitz (1995). "Tyrosine phosphorylation and cytoskeletal tension regulate the release of fibroblast adhesions." J Cell Biol **131**(2): 525-37.

Danowski, B. A. (1989). "Fibroblast contractility and actin organization are stimulated by microtubule inhibitors." J Cell Sci **93 (Pt 2)**: 255-66.
Derycke, L. D. and M. E. Bracke (2004). "N-cadherin in the spotlight of cell-cell adhesion, differentiation, embryogenesis, invasion and signalling." Int J Dev Biol **48**(5-6): 463-76.
Desai, A. and T. J. Mitchison (1997). "Microtubule polymerization dynamics." Annu Rev Cell Dev Biol **13**: 83-117.
Duchek, P. and P. Rorth (2001). "Guidance of cell migration by EGF receptor signaling during Drosophila oogenesis." Science **291**(5501): 131-3.
Duchek, P., K. Somogyi, G. Jekely, et al. (2001). "Guidance of cell migration by the Drosophila PDGF/VEGF receptor." Cell **107**(1): 17-26.
Dujardin, D. L., L. E. Barnhart, S. A. Stehman, et al. (2003). "A role for cytoplasmic dynein and LIS1 in directed cell movement." J Cell Biol **163**(6): 1205-11.
Dujardin, D. L. and R. B. Vallee (2002). "Dynein at the cortex." Curr Opin Cell Biol **14**(1): 44-9.
Edwards, K. A. and D. P. Kiehart (1996). "Drosophila nonmuscle myosin II has multiple essential roles in imaginal disc and egg chamber morphogenesis." Development **122**(5): 1499-511.
Euteneuer, U. and M. Schliwa (1984). "Persistent, directional motility of cells and cytoplasmic fragments in the absence of microtubules." Nature **310**(5972): 58-61.
Ezratty, E. J., M. A. Partridge and G. G. Gundersen (2005). "Microtubule-induced focal adhesion disassembly is mediated by dynamin and focal adhesion kinase." Nat Cell Biol **7**(6): 581-90.
Faulkner, N. E., D. L. Dujardin, C. Y. Tai, et al. (2000). "A role for the lissencephaly gene LIS1 in mitosis and cytoplasmic dynein function." Nat Cell Biol **2**(11): 784-91.
Fulga, T. A. and P. Rorth (2002). "Invasive cell migration is initiated by guided growth of long cellular extensions." Nat Cell Biol **4**(9): 715-9.
Geisbrecht, E. R. and D. J. Montell (2002). "Myosin VI is required for E-cadherin-mediated border cell migration." Nat Cell Biol **4**(8): 616-20.
Ghiglione, C., O. Devergne, E. Georgenthum, et al. (2002). "The Drosophila cytokine receptor Domeless controls border cell migration and epithelial polarization during oogenesis." Development **129**(23): 5437-47.
Gigant, B., P. A. Curmi, C. Martin-Barbey, et al. (2000). "The 4 A X-ray structure of a tubulin:stathmin-like domain complex." Cell **102**(6): 809-16.
Goldman, R. D. (1971). "The role of three cytoplasmic fibers in BHK-21 cell motility. I. Microtubules and the effects of colchicine." J Cell Biol **51**(3): 752-62.
Gomes, E. R., S. Jani and G. G. Gundersen (2005). "Nuclear movement regulated by Cdc42, MRCK, myosin, and actin flow

establishes MTOC polarization in migrating cells." Cell **121**(3): 451-63.
Gonzalez-Reyes, A. and D. St Johnston (1998). "Patterning of the follicle cell epithelium along the anterior-posterior axis during Drosophila oogenesis." Development **125**(15): 2837-46.
Grabham, P. W., G. E. Seale, M. Bennecib, et al. (2007). "Cytoplasmic dynein and LIS1 are required for microtubule advance during growth cone remodeling and fast axonal outgrowth." J Neurosci **27**(21): 5823-34.
Grenningloh, G., E. J. Rehm and C. S. Goodman (1991). "Genetic analysis of growth cone guidance in Drosophila: fasciclin II functions as a neuronal recognition molecule." Cell **67**(1): 45-57.
Grieder, N. C., M. de Cuevas and A. C. Spradling (2000). "The fusome organizes the microtubule network during oocyte differentiation in Drosophila." Development **127**(19): 4253-64.
Gundersen, G. G. and J. C. Bulinski (1988). "Selective stabilization of microtubules oriented toward the direction of cell migration." Proc Natl Acad Sci U S A **85**(16): 5946-50.
Harris, T. J. and M. Peifer (2005). "The positioning and segregation of apical cues during epithelial polarity establishment in Drosophila." J Cell Biol **170**(5): 813-23.
Hippenmeyer, S., Y. H. Youn, H. M. Moon, et al. (2010). "Genetic mosaic dissection of Lis1 and Ndel1 in neuronal migration." Neuron **68**(4): 695-709.
Horne-Badovinac, S. and D. Bilder (2008). "Dynein regulates epithelial polarity and the apical localization of stardust A mRNA." PLoS Genet **4**(1): e8.
Inaki, M., S. Vishnu, A. Cliffe, et al. (2012). "Effective guidance of collective migration based on differences in cell states." Proc Natl Acad Sci U S A **109**(6): 2027-32.
Insall, R. H. and L. M. Machesky (2009). "Actin dynamics at the leading edge: from simple machinery to complex networks." Dev Cell **17**(3): 310-22.
Jankovics, F. and D. Brunner (2006). "Transiently reorganized microtubules are essential for zippering during dorsal closure in Drosophila melanogaster." Dev Cell **11**(3): 375-85.
Juliano, R. L. (2002). "Signal transduction by cell adhesion receptors and the cytoskeleton: functions of integrins, cadherins, selectins, and immunoglobulin-superfamily members." Annu Rev Pharmacol Toxicol **42**: 283-323.
Kaverina, I., O. Krylyshkina and J. V. Small (1999). "Microtubule targeting of substrate contacts promotes their relaxation and dissociation." J Cell Biol **146**(5): 1033-44.
Kaverina, I., K. Rottner and J. V. Small (1998). "Targeting, capture, and stabilization of microtubules at early focal adhesions." J Cell Biol **142**(1): 181-90.
Keating, T. J. and G. G. Borisy (1999). "Centrosomal and non-centrosomal microtubules." Biol Cell **91**(4-5): 321-9.
Keller, H. U., A. Naef and A. Zimmermann (1984). "Effects of colchicine, vinblastine and nocodazole on polarity, motility, chemotaxis and

cAMP levels of human polymorphonuclear leukocytes." Exp Cell Res **153**(1): 173-85.
Kupfer, A., G. Dennert and S. J. Singer (1983). "Polarization of the Golgi apparatus and the microtubule-organizing center within cloned natural killer cells bound to their targets." Proc Natl Acad Sci U S A **80**(23): 7224-8.
Kupfer, A., D. Louvard and S. J. Singer (1982). "Polarization of the Golgi apparatus and the microtubule-organizing center in cultured fibroblasts at the edge of an experimental wound." Proc Natl Acad Sci U S A **79**(8): 2603-7.
Lauffenburger, D. A. and A. F. Horwitz (1996). "Cell migration: a physically integrated molecular process." Cell **84**(3): 359-69.
Lee, T. and L. Luo (1999). "Mosaic analysis with a repressible cell marker for studies of gene function in neuronal morphogenesis." Neuron **22**(3): 451-61.
Lemos, C. L., P. Sampaio, H. Maiato, et al. (2000). "Mast, a conserved microtubule-associated protein required for bipolar mitotic spindle organization." EMBO J **19**(14): 3668-82.
Levy, J. R. and E. L. Holzbaur (2008). "Dynein drives nuclear rotation during forward progression of motile fibroblasts." J Cell Sci **121**(Pt 19): 3187-95.
Liao, G., T. Nagasaki and G. G. Gundersen (1995). "Low concentrations of nocodazole interfere with fibroblast locomotion without significantly affecting microtubule level: implications for the role of dynamic microtubules in cell locomotion." J Cell Sci **108 (Pt 11)**: 3473-83.
Liedtke, W., E. E. Leman, R. E. Fyffe, et al. (2002). "Stathmin-deficient mice develop an age-dependent axonopathy of the central and peripheral nervous systems." Am J Pathol **160**(2): 469-80.
Lin, D. M., R. D. Fetter, C. Kopczynski, et al. (1994). "Genetic analysis of Fasciclin II in Drosophila: defasciculation, refasciculation, and altered fasciculation." Neuron **13**(5): 1055-69.
Lu, R. (2011). "Arp2/3 complex in border cell migration." NUS DBS THESIS.
Mandelkow, E. and E. M. Mandelkow (1995). "Microtubules and microtubule-associated proteins." Curr Opin Cell Biol **7**(1): 72-81.
Mathieu, J., H. H. Sung, C. Pugieux, et al. (2007). "A sensitized PiggyBac-based screen for regulators of border cell migration in Drosophila." Genetics **176**(3): 1579-90.
Mattila, P. K. and P. Lappalainen (2008). "Filopodia: molecular architecture and cellular functions." Nat Rev Mol Cell Biol **9**(6): 446-54.
McKenney, R. J., M. Vershinin, A. Kunwar, et al. (2010). "LIS1 and NudE induce a persistent dynein force-producing state." Cell **141**(2): 304-14.
Mitchison, T. and M. Kirschner (1984). "Dynamic instability of microtubule growth." Nature **312**(5991): 237-42.
Montell, D. J. (2003). "Border-cell migration: the race is on." Nat Rev Mol Cell Biol **4**(1): 13-24.

Montell, D. J., P. Rorth and A. C. Spradling (1992). "slow border cells, a locus required for a developmentally regulated cell migration during oogenesis, encodes Drosophila C/EBP." Cell **71**(1): 51-62.

Niewiadomska, P., D. Godt and U. Tepass (1999). "DE-Cadherin is required for intercellular motility during Drosophila oogenesis." J Cell Biol **144**(3): 533-47.

Niewiadomska, P., D. Godt and U. Tepass (1999). "DE-Cadherin is required for intercellular motility during *Drosophila* oogenesis." J. Cell Biol. **144**: 533-547.

Nogales, E. (2000). "Structural insights into microtubule function." Annu Rev Biochem **69**: 277-302.

Ozon, S., A. Guichet, O. Gavet, et al. (2002). "Drosophila stathmin: a microtubule-destabilizing factor involved in nervous system formation." Mol Biol Cell **13**(2): 698-710.

Pacquelet, A., L. Lin and P. Rorth (2003). "Binding site for p120/delta-catenin is not required for Drosophila E-cadherin function in vivo." J Cell Biol **160**(3): 313-9.

Pacquelet, A. and P. Rorth (2005). "Regulatory mechanisms required for DE-cadherin function in cell migration and other types of adhesion." J Cell Biol **170**(5): 803-12.

Palazzo, A. F., H. L. Joseph, Y. J. Chen, et al. (2001). "Cdc42, dynein, and dynactin regulate MTOC reorientation independent of Rho-regulated microtubule stabilization." Curr Biol **11**(19): 1536-41.

Pinheiro, E. M. and D. J. Montell (2004). "Requirement for Par-6 and Bazooka in Drosophila border cell migration." Development **131**(21): 5243-51.

Piperno, G., M. LeDizet and X. J. Chang (1987). "Microtubules containing acetylated alpha-tubulin in mammalian cells in culture." J Cell Biol **104**(2): 289-302.

Porter, J. R. (1976). "Antony van Leeuwenhoek: tercentenary of his discovery of bacteria." Bacteriol Rev **40**(2): 260-9.

Poukkula, M., A. Cliffe, R. Changede, et al. (2011). "Cell behaviors regulated by guidance cues in collective migration of border cells." J Cell Biol **192**(3): 513-24.

Prasad, M. and D. J. Montell (2007). "Cellular and molecular mechanisms of border cell migration analyzed using time-lapse live-cell imaging." Dev Cell **12**(6): 997-1005.

Quintyne, N. J., S. R. Gill, D. M. Eckley, et al. (1999). "Dynactin is required for microtubule anchoring at centrosomes." J Cell Biol **147**(2): 321-34.

Rakic, P., E. Knyihar-Csillik and B. Csillik (1996). "Polarity of microtubule assemblies during neuronal cell migration." Proc Natl Acad Sci U S A **93**(17): 9218-22.

Redeker, V., S. Lachkar, S. Siavoshian, et al. (2000). "Probing the native structure of stathmin and its interaction domains with tubulin. Combined use of limited proteolysis, size exclusion chromatography, and mass spectrometry." J Biol Chem **275**(10): 6841-9.

Reiner, O., R. Carrozzo, Y. Shen, et al. (1993). "Isolation of a Miller-Dieker lissencephaly gene containing G protein beta-subunit-like repeats." Nature **364**(6439): 717-21.
Reinsch, S. (2001). "Movement of nuclei." Curr Protoc Cell Biol **Chapter 13**: Unit 13 4.
Ridley, A. J., M. A. Schwartz, K. Burridge, et al. (2003). "Cell migration: integrating signals from front to back." Science **302**(5651): 1704-9.
Rinnerthaler, G., B. Geiger and J. V. Small (1988). "Contact formation during fibroblast locomotion: involvement of membrane ruffles and microtubules." J Cell Biol **106**(3): 747-60.
Roll-Mecak, A. and R. D. Vale (2008). "Structural basis of microtubule severing by the hereditary spastic paraplegia protein spastin." Nature **451**(7176): 363-7.
Rong, Y. S. and K. G. Golic (2001). "A targeted gene knockout in Drosophila." Genetics **157**(3): 1307-12.
Rorth, P. (2002). "Initiating and guiding migration: lessons from border cells." Trends Cell Biol **12**(7): 325-31.
Rorth, P. (2003). "Communication by touch: role of cellular extensions in complex animals." Cell **112**(5): 595-8.
Rorth, P. (2009). "Collective cell migration." Annu Rev Cell Dev Biol **25**: 407-29.
Rorth, P. (2011). "Whence directionality: guidance mechanisms in solitary and collective cell migration." Dev Cell **20**(1): 9-18.
Rorth, P., K. Szabo, A. Bailey, et al. (1998). "Systematic gain-of-function genetics in Drosophila." Development **125**(6): 1049-57.
Rubin, G. M. and A. C. Spradling (1982). "Genetic transformation of Drosophila with transposable element vectors." Science **218**(4570): 348-53.
Ruoslahti, E. (1996). "RGD and other recognition sequences for integrins." Annu Rev Cell Dev Biol **12**: 697-715.
Schober, M., I. Rebay and N. Perrimon (2005). "Function of the ETS transcription factor Yan in border cell migration." Development **132**(15): 3493-504.
Schubart, U. K., J. Yu, J. A. Amat, et al. (1996). "Normal development of mice lacking metablastin (P19), a phosphoprotein implicated in cell cycle regulation." J Biol Chem **271**(24): 14062-6.
Sheetz, M. P., D. Felsenfeld, C. G. Galbraith, et al. (1999). "Cell migration as a five-step cycle." Biochem Soc Symp **65**: 233-43.
Shimada, Y., S. Yonemura, H. Ohkura, et al. (2006). "Polarized transport of Frizzled along the planar microtubule arrays in Drosophila wing epithelium." Dev Cell **10**(2): 209-22.
Shumyatsky, G. P., G. Malleret, R. M. Shin, et al. (2005). "stathmin, a gene enriched in the amygdala, controls both learned and innate fear." Cell **123**(4): 697-709.
Silies, M. and C. Klambt (2010). "APC/C(Fzr/Cdh1)-dependent regulation of cell adhesion controls glial migration in the Drosophila PNS." Nat Neurosci **13**(11): 1357-64.
Small, J. V., T. Stradal, E. Vignal, et al. (2002). "The lamellipodium: where motility begins." Trends Cell Biol **12**(3): 112-20.

Sobel, A. (1991). "Stathmin: a relay phosphoprotein for multiple signal transduction?" Trends Biochem Sci **16**(8): 301-5.

Spradling, A. C. and G. M. Rubin (1982). "Transposition of cloned P elements into Drosophila germ line chromosomes." Science **218**(4570): 341-7.

Stehbens, S. J., A. D. Paterson, M. S. Crampton, et al. (2006). "Dynamic microtubules regulate the local concentration of E-cadherin at cell-cell contacts." J Cell Sci **119**(Pt 9): 1801-11.

Stramer, B., S. Moreira, T. Millard, et al. (2010). "Clasp-mediated microtubule bundling regulates persistent motility and contact repulsion in Drosophila macrophages in vivo." J Cell Biol **189**(4): 681-9.

Svitkina, T. M., A. B. Verkhovsky, K. M. McQuade, et al. (1997). "Analysis of the actin-myosin II system in fish epidermal keratocytes: mechanism of cell body translocation." J Cell Biol **139**(2): 397-415.

Szafranski, P. and S. Goode (2004). "A Fasciclin 2 morphogenetic switch organizes epithelial cell cluster polarity and motility." Development **131**(9): 2023-36.

Tanentzapf, G., C. Smith, J. McGlade, et al. (2000). "Apical, lateral, and basal polarization cues contribute to the development of the follicular epithelium during Drosophila oogenesis." J Cell Biol **151**(4): 891-904.

Tekotte, H., D. Tollervey and I. Davis (2007). "Imaging the migrating border cell cluster in living Drosophila egg chambers." Dev Dyn **236**(10): 2818-24.

Thiery, J. P., H. Acloque, R. Y. Huang, et al. (2009). "Epithelial-mesenchymal transitions in development and disease." Cell **139**(5): 871-90.

Trotta, N., G. Orso, M. G. Rossetto, et al. (2004). "The hereditary spastic paraplegia gene, spastin, regulates microtubule stability to modulate synaptic structure and function." Curr Biol **14**(13): 1135-47.

Tsai, J. W., K. H. Bremner and R. B. Vallee (2007). "Dual subcellular roles for LIS1 and dynein in radial neuronal migration in live brain tissue." Nat Neurosci **10**(8): 970-9.

Tsai, J. W., Y. Chen, A. R. Kriegstein, et al. (2005). "LIS1 RNA interference blocks neural stem cell division, morphogenesis, and motility at multiple stages." J Cell Biol **170**(6): 935-45.

Ueda, M., R. Graf, H. K. MacWilliams, et al. (1997). "Centrosome positioning and directionality of cell movements." Proc Natl Acad Sci U S A **94**(18): 9674-8.

Vale, R. D. (2003). "The molecular motor toolbox for intracellular transport." Cell **112**(4): 467-80.

Vallee, R. B., R. J. McKenney and K. M. Ori-McKenney (2012). "Multiple modes of cytoplasmic dynein regulation." Nat Cell Biol **14**(3): 224-30.

Vallee, R. B. and J. W. Tsai (2006). "The cellular roles of the lissencephaly gene LIS1, and what they tell us about brain development." Genes Dev **20**(11): 1384-93.

Van de Bor, V., G. Zimniak, D. Cerezo, et al. (2011). "Asymmetric localisation of cytokine mRNA is essential for JAK/STAT activation during cell invasiveness." Development **138**(7): 1383-93.

Vasiliev, J. M., I. M. Gelfand, L. V. Domnina, et al. (1970). "Effect of colcemid on the locomotory behaviour of fibroblasts." J Embryol Exp Morphol **24**(3): 625-40.

Vorobjev, I., V. Malikov and V. Rodionov (2001). "Self-organization of a radial microtubule array by dynein-dependent nucleation of microtubules." Proc Natl Acad Sci U S A **98**(18): 10160-5.

Wang, X., J. Bo, T. Bridges, et al. (2006). "Analysis of cell migration using whole-genome expression profiling of migratory cells in the Drosophila ovary." Dev Cell **10**(4): 483-95.

Waterman-Storer, C. M., R. A. Worthylake, B. P. Liu, et al. (1999). "Microtubule growth activates Rac1 to promote lamellipodial protrusion in fibroblasts." Nat Cell Biol **1**(1): 45-50.

Wittmann, T. and C. M. Waterman-Storer (2001). "Cell motility: can Rho GTPases and microtubules point the way?" J Cell Sci **114**(Pt 21): 3795-803.

Xu, T. and G. M. Rubin (1993). "Analysis of genetic mosaics in developing and adult Drosophila tissues." Development **117**(4): 1223-37.

Youn, Y. H., T. Pramparo, S. Hirotsune, et al. (2009). "Distinct dose-dependent cortical neuronal migration and neurite extension defects in Lis1 and Ndel1 mutant mice." J Neurosci **29**(49): 15520-30.

Publication

Yang N, Inaki M, Cliffe A, Rørth P (2012) Microtubules and Lis-1/NudE/Dynein Regulate Invasive Cell-on-Cell Migration in Drosophila. PLoS ONE 7(7): e40632. doi:10.1371/journal.pone.0040632